Biophysical Investigations on the Interaction of the Major Bovine Seminal Plasma Protein, PDC-109 with Model Membranes

A thesis submitted for the degree of
DOCTOR OF PHILOSOPHY

By
V. Anbazhagan

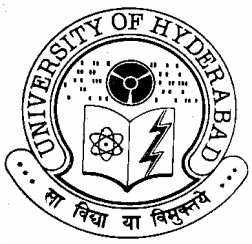

School of Chemistry
University of Hyderabad
Hyderabad – 500 046
INDIA

July 2005

Dedicated to
my beloved parents

CONTENTS

School of Chemistry
University of Hyderabad
Hyderabad – 500 046

STATEMENT

I hereby declare that the matter embodied in this thesis is the result of investigations carried out by me in the School of Chemistry, University of Hyderabad, Hyderabad, under the supervision of **Prof. Musti J. Swamy**.

In keeping with the general practice of reporting scientific observations, due acknowledgements have been made whenever the work described is based on the finding of other investigators. Any omission which might have occurred by oversight or error is regretted.

Hyderabad

July 2005 **V. Anbazhagan**

School of Chemistry
University of Hyderabad
Hyderabad – 500 046

CERTIFICATE

Certified that the work embodied in this thesis entitled **"Biophysical Investigations on the Interaction of the Bovine Seminal Plasma Protein, PDC-109 with Model Membranes"** has been carried out by **Mr. V. Anbazhagan**, under my supervision and the same has not been submitted elsewhere for any degree.

Hyderabad

July 2005

Prof. Musti J. Swamy
(Thesis Supervisor)

Dean

ACKNOWLEDGEMENT

A journey is easier when you travel together. Interdependence is certainly more valuable than independence. This thesis is the result of five years of work in which I have been accompanied and supported by many people. I am very happy that I now have the opportunity to express my gratitude for all of them.

The first person I would like to thank is my supervisor Professor Musti J. Swamy. During these years I have known Prof. Swamy as a sympathetic and principle-centered person. His undying enthusiasm and integral view on research and his emphasis on doing high-quality science has made a deep impression on me. I owe him enormously for showing me this way of research. Besides being an excellent mentor, Prof. Swamy is as close as a relative and a good friend. I am really glad that I have come to know Prof. Swamy in my life.

I would like to thank Prof. Periasamy, Dean, School of Chemistry and the former Deans, Prof. Jemmis and Prof. Desiraju for making my research feasible with the excellent infrastructure and laboratory facilities.

I am indebted to Prof. Basaviah for his invaluable support and care shown when needs. I am really thankful to all the faculty members, who welcomed me in the School. I am grateful to Prof. Samanta and his students, for allowing me to use their picosecond time-resolved fluorescence spectrophotometer. I am thankful to Dr. Lalitha Guruprasad for introducing me to the basics of protein modeling and software. I express my sincere gratitude to Prof. Surolia for help in carrying out the experiment reported in Chapter 3 and Prof. Marsh for the fruitful collaboration, the results of which are reported in Chapter 2. I am also grateful to the Central Instrumental Laboratory, University of Hyderabad for providing an excellent work environment and Dr. K.V. Ready, Mr. Murthy, Mr. Suresh and other staff for their cheerful assistance. I record my sincere thanks to all the non-teaching staff of the School, NRS hostel and Administrative office for their cooperation.

I am grateful to Dr. K. Babu Rao of the Lam Farm, Guntur, ANGR University of Agricultural Science; Dr. Sadasiva Rao, Dr. Salomon Raju of the Department of Gynecology & Animal Reproduction, ANGR University of Agricultural Science, Hyderabad for providing samples of bovine semen used in this thesis.

I also thank all great people who lay the foundation of science and make me to think in a global way: Mr. Periyanayagasamy, Dr. Thanikachalam, Prof. Surya Prakash Rao.

My special thanks are to the faculties of KMCPGS, Pondicherry, St Joseph College, Cuddalore, Tamil Nadu, NKC, Ilango Adigal and Fathima Higher Secondary School, Pondicherry.

I am extremely grateful to my colleagues: Ramakrishnan, Roopa, Nabil, Ravi, Rajini, Kavitha, Hari and Pradip for maintaining a cheerful atmosphere in the lab. I express my gratitude to all COSIST lab members and NRS A-wing, where my stay was filled with wonderful experiences and helping me to come out of my bad moods.

This acknowledgement would be definitely incomplete if I forget to thank my friends: Britto, Jegan, Lebel, Karthik, Sankar, Sridhar, Girija, Kumar, Geetha, Praneeth, Kalpana, Sezhian, Chandran, Mari, Philip, Perumal, Senthil's, Siva's, Jaya kumar, Guruparan, Mangai, Suresh, Desigan, Mani, Sundaram, Vairam, Padma, Venki, Madhu, Selam, Prakash, Bal, Arumugan, Bharati, Sathish, Dhamu, Francy, Chandu, Vijyan, Sekar, Badugu, Srinivas's, Narsi, Suresh, Shyam, Mala, Gupta, Balu, Pavan, Sharath, Suni, Manap, Binoy, Dinu, Tamal, Aparna, Param, Usha, Nagendar…

It gives me immense pleasure to thank Kannayan periyappa for inculcating motivation and encouragement in me towards academics from my childhood days. I am thankful to Chinna appa, Kasthuri amma, Karuna, Aravind, Nadu appa, Muthu amma and appa, V.P.K. Velmurugan and Siva amma, Kasthuri, wonderful human beings who took part in all ups and downs in my life.

Last, but not least, I thank my family: my parents, Veerappan and Govindammal, for giving me life in the first place, for educating me with aspects from both arts and sciences, for unconditional support and encouragement to pursue my interests even when interests went beyond boundaries. Words cannot be expressed in thanking my brother Ganapathy, sister Sathya and uncle Natraj, Nisha and Haritha kuti for their Himalayan support and immense love showered on me.

I finally thank Council for Scientific and Industrial research, India for the financial support.

If you cannot find your name here, it does not mean I do not appreciate you, simply I do not have enough space here (if you know me well, you know there are too many people whom I owe something).

V. Anbazhagan

ABBREVIATIONS

Apo A1	-	apolipoprotein A1
AR	-	acrosome reaction
ASL	-	androstanol spin label; 17β-hydroxy-4',4'-dimethyl-spiro[5α-androstane-3,2'-oxazolidin]-3'-yloxyl
BSA	-	bovine serum albumin
BSP	-	bovine seminal plasma
C	-	carbon
Ca^{2+}	-	calcium ion
cAMP	-	cyclic adenosine mono phosphate
CD	-	circular dichorism
Chol.	-	cholesterol
CSL	-	cholestane spin label; 4',4'-dimethylspiro[5α-cholestane-3,2'-oxazolidin]-3'-yloxyl)
DMPA	-	1,2-dimyristoyl-*sn*-glycero-3-phosphatidic acid
DMPC	-	1,2-dimyristoyl -*sn*-glycero-3-phosphocholine
DMPE	-	1,2-dimyristoyl -*sn*-glycero-3-phosphoethanolamine
DMPG	-	1,2-dimyristoyl -*sn*-glycero-3-phosphoglycerol
DNA	-	deoxyribonucleic acid
DOPC	-	1,2-dioleyl -*sn*-glycero-3-phosphocholine
DPPC	-	1,2-dipalmitoyl -*sn*-glycero-3-phosphocholine
EDTA	-	ethylenediaminetetraacetic acid

ESR	-	electron spin resonance
Fn	-	fibronectin
FTIR	-	Fourier transform infra red
GAG	-	glycosaminoglycan
HBS	-	hepes buffer containing, 10 mM Hepes, 1 mM EDTA, 0.15 M NaCl, pH 7.4
HDL	-	high density lipoprotein
Hepes	-	*N*-(2-hydroxyethly)piperazine-*N´*-2-ethanesulfonic acid
ITC	-	isothermal titration calorimetry
Lyso-PC	-	lysophosphatidylcholine
MLV	-	multilamellar vesicles
NaCl	-	sodium chloride
NAPESL	-	*N*-acyl PE spin label; 1,2-dipalmitoyl- *sn*-glycero-3-(*N*-*n*-(4,-dimethyloxazolidine-*N´*-oxyl)stearoyl)phosphoethanolamine
NMR	-	nuclear magnetic resonance
PA	-	phosphatidic acid
PAF	-	platelet activating factor
PASL	-	phosphotidic acid spin label; 1-acyl-2-[*n*-(4,4-dimethyl oxazolidine-*N*-oxyl)]stearoyl-*sn*-glycero-3-phosphoacid
PC	-	phosphatidylcholine
PCSL	-	phosphotidylcholine spin label; 1-acyl-2-[*n*-(4,4-dimethyl oxazolidine-*N*-oxyl)]stearoyl-*sn*-glycero-3-phosphocholine
PDB	-	protein data bank
PE	-	phosphatidylethanolamine

PGSL	-	phosphotidylglycerol spin label; 1-acyl-2-[*n*-(4,4-dimethyl oxazolidine-*N*-oxyl)]stearoyl-*sn*-glycero-3-phosphoglycerol
PI	-	phosphatidylinositol
PPC	-	*p*-amino phenyl phosphorylcholine
PrC	-	*O*-phosphorylcholine
PS	-	phosphatidylserine
PSSL	-	phosphotidylserine spin label; 1-acyl-2-[*n*-(4,4-dimethyl oxazolidine-*N*-oxyl)]stearoyl-*sn*-glycero-3-phosphoserine
SDS	-	sodium dodecyl sulphate
SM	-	sphingomylein
SMSL	-	sphingomylein spin label
sn	-	stereo specific numbering
SPR	-	surface plasmon resonance
SUV	-	small unilamellar vesicles
TBS I	-	tris buffer containing 50 mM Tris, 0.15 M NaCl, 5 mM EDTA, 0.025% NaN_3, pH = 7.4
TBS II	-	tris buffer containing 25 mM Tris, 1 M NaCl, 0.025% NaN_3, pH = 6.4
TBS	-	tris buffer containing 50 mM Tris, 0.5 M NaCl, 5 mM EDTA,0.025 % NaN3, pH = 7.4
Thr	-	theronine
Trp (W)	-	tryptophan
Tyr (Y)	-	tyrosine

Chapter 1

Introduction

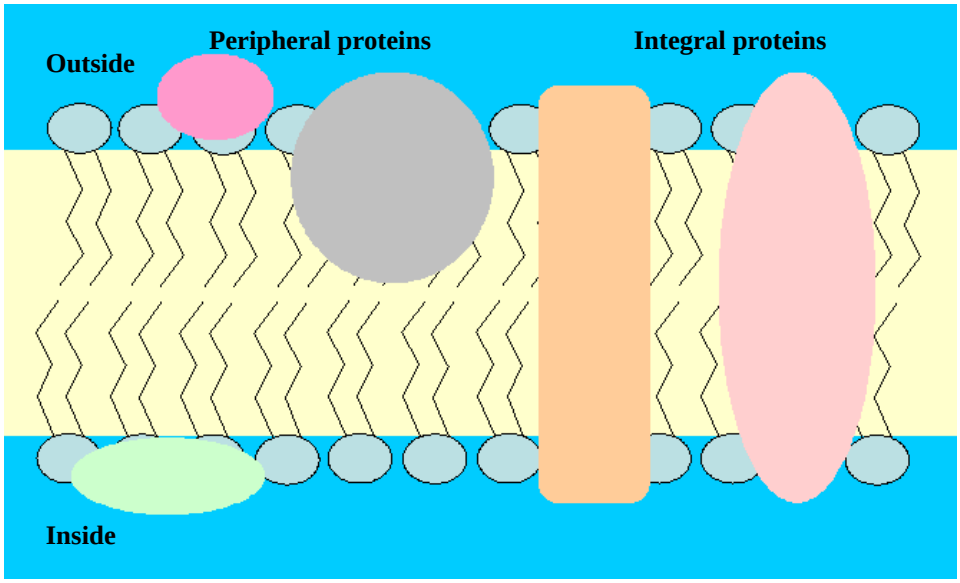

1. 1. Biomembranes

Living creatures are composed of one or more cells, which serve as chemical engines and function at constant temperature. Cells of all living organisms are made up of complex molecules, such as *lipids*, *proteins*, *carbohydrates* and *nucleic acids*. All the key constituents of the cell are separated from the rest of the universe by an external boundary called *membrane*. Likewise, different organelles within the cells are also compartmentalized by additional membranes, which ensure that such compartments can have segregated processes and compositions. Membranes, which make such compartmentalization possible, are highly selective permeability barriers rather than passive walls; they can act as 'pumps' and 'gates' for specific cellular components. Membranes are ubiquitous in living systems and have evolved over time to perform diverse tasks. Most of the fundamental biochemical functions of cells are controlled by membranes at some point; such as prokaryotic DNA replication, protein biosynthesis, protein secretion, bioenergetics and hormonal responses [Gennis, 1989]. In general, a biological membrane can be defined as ***"an extensive, self-sealing, fluid, asymmetric, selectively permeable, compartmental barrier essential for a cell or organelle for its survival and correct functioning"***.

1.2. Components of biomembranes and their functions

Biological membranes are organized assemblies consisting mainly of lipids and proteins; the small amounts of carbohydrates are present invariably in the form of glycolipids or glycoproteins. The relative proportions of lipid and protein differ in different membranes, ranging from about 20% to 80% by weight; less than 10% by weight is constituted by carbohydrates, which are covalently attached to protein and lipids (Table 1.1) [Guidotti, 1972]. Membrane density increases with increase in

protein content, i.e., it is directly proportional to the amount of protein in the membrane. The significant variation in the lipid and protein composition of membranes from different sources appears to reflect their functional specialization. For example, the plasma membrane of erythrocytes contains 49% proteins, which serve as transporters of specific solutes across the membrane. On the other hand, the myelinated neurons, which serve as a passive electrical insulator, contain as much as 79 % lipids [Lai et al., 1987]. While the plasma membrane proteins contain covalently bound carbohydrate, membranes of the intracellular components such as mitochondria and chloroplasts rarely contain covalently bound carbohydrate. The sugar moieties present on the surface glycoproteins influence protein folding, cell transport and receptor functions of these glycoproteins. Some membrane proteins are attached covalently to one or more lipids, which most likely serve as hydrophobic anchors and hold the proteins to membranes [Gennis, 1989].

Table 1.1: Protein, lipid and carbohydrate composition of some membranes.

Membrane	Percent by weight		
	Protein	Lipid	Carbohydrate
Myelin	18	79	3
Human erythrocyte plasma membrane	49	43	8
Amoeba plasma membrane	54	42	4
Mitochondria outer membrane	52	48	0
Chloroplast spinach lamellae	70	30	0
Gram-positive bacteria	75	25	0
Mitochondria inner membrane	79	24	0

1.2.1. Membrane lipids

Lipids are the major structural elements of biomembranes. The general definition of a lipid is a biological material that is insoluble or slightly soluble in water, which can be extracted from cells by organic solvents of low polarity like ether or chloroform. They are made up of diverse classes of compounds, such as long-chain fatty acids, alcohols and their derivatives, sterols, bile acids, carotenoids and terpenes [Gunstone

et al., 1986]. Lipids are generally classified into two types: *complex lipids*, which on hydrolysis yield smaller molecules such as fats and waxes and, *simple lipids*, which cannot be hydrolyzed e.g., cholesterol and other steroids. The lipids in membranes are usually made up of a non-polar portion, mostly polymethylene chains and a polar portion, such as alcohol. In aqueous environment, lipid molecules spontaneously tend to form organized structures which are the key for the structure of cell membrane and its function. Membranes contain three major kinds of lipids; they are phospholipids, glycolipids and sterol [Jain, 1988].

Phospholipids are the most abundant amphipathic lipids found in all biomembranes. Mostly they are derived from either glycerol or from sphingosine. Glycerophopholipids contain fatty acyl side chains attached to two of the three hydroxy groups of a glycerol molecule; the third hydroxyl is esterified with a polar phosphate-containing group. A schematic diagram depicting the general structure of phospholipids is shown in Fig. 1.1. Each phospholipid differs from another by the head group (X) attached to the phosphate moiety, with 'X' being a hydroxyl, ethanolamine, serine, choline, glycerol, inositol or phosphatidylgycerol. In addition, differences in the attached acyl chains (R1 and R2) also generate a large number of molecular species. The fatty acid chains may be saturated or unsaturated or one chain may be saturated and the other unsaturated. They usually contain an even number of carbon atoms, typically between 14 and 24, but most common ones are 16- and 18-carbon acyl chains.

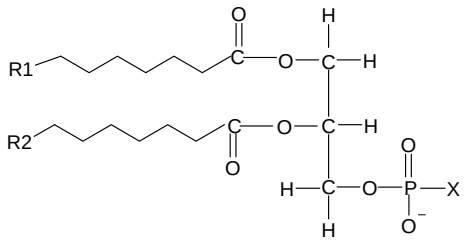

Fig. 1.1: The general structure of a glycerophospholipid linked to hydrophobic and hydrophilic moieties. Each derivative is named after the head-group alcohol (X), with prefix "phosphatidyl".

Most of the animal tissues and some unicellular organisms contain ether rich lipids. They differ from glycerophospholipids in C-1 position; which is linked with an alkyl ether or a vinyl ether, as in *plasmologens*. About half of the heart phospholipids are plasmalogens. The important hormone, platelet-activating factor (Fig. 1.2) is an example of ether-containing phospholipids.

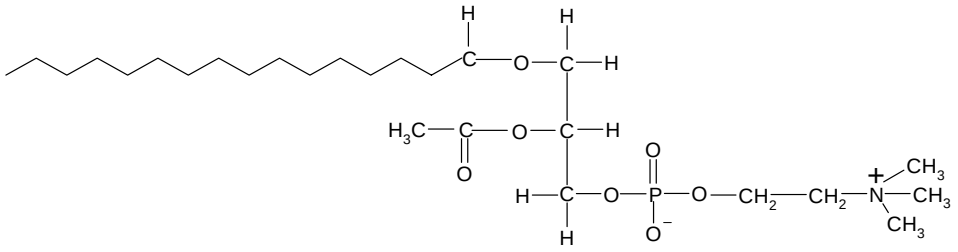

Fig. 1.2: The structure of platelet-activating factor.

Sphingolipids are nearly ubiquitous constituents of membranes in animals, plants, and some lower forms of life. Structurally, they are composed of a hydrophobic portion, which contains a mixture of fatty acids that are amide-linked to sphingosine (an amino alcohol) or other related long-chain aliphatic amine (sphingoid bases), and a polar head group made up of an alcohol and sometimes a phosphoric acid in diester linkage at the polar head group (Fig. 1.3).

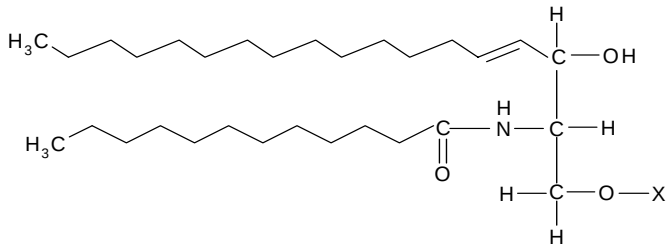

Fig. 1.3: The general structure of a sphingolipid linked to hydrophobic and hydrophilic moieties.

Glycolipids are compounds in which carbohydrate chains of variable length are covalently linked to lipids. The simplest glycolipid, glucoysylcerbroside is shown in Fig. 1.4, where the primary hydroxyl is linked with a glucose residue. *Gangliosides* are complex glycolipids, which contain one or more sugars, often *N*-acetylneuraminic

acid. The human glycolipids and glycoproteins contain important blood group antigens.

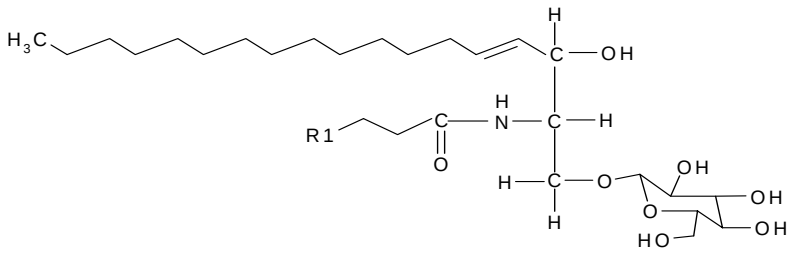

Fig. 1.4: Structure of glucosylcerebroside.

Cholesterol and its derivatives constitute another important class of membrane lipids, the steroids. The basic structure of sterols is the cyclopentanoperhydrophenanthrene (Fig. 1.5). Cholesterol is the major constituent of animal tissues, whereas other sterols such as sitosterol and stigmasterol play important roles in plant cell membranes [Jain, 1988]. Membrane cholesterol is the major determinant of membrane fluidity, but the net effect changes with lipid composition. Eukaryotic microorganisms, such as yeast contain *ergosterol*. Some sterol-like lipids, *hopanoids* are also present in bacteria and some plants [Prince, 1987]. Hopanoids are pentacyclic triterpenoid lipids and are important for bacterial membrane stability and functioning. Hopanoids predominantly occur in aerobically growing bacteria of oxic environments.

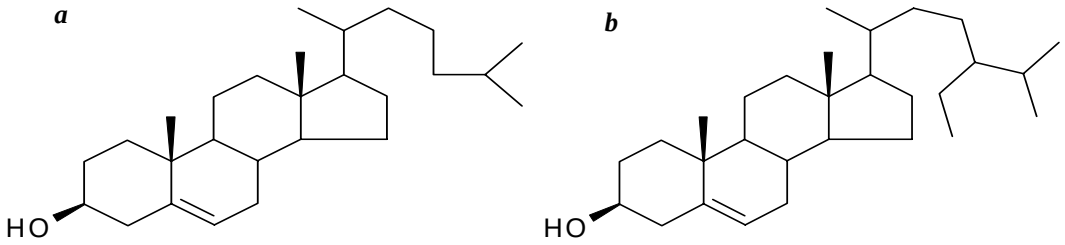

Fig. 1.5: Structure of (a) cholesterol and (b) sitosterol.

1.2.2. Membrane proteins

Proteins, which constitute about 20-80% of the weight of various cellular membranes, are responsible for a variety of functions associated with the membranes. Most of the

membrane proteins interact with the hydrophobic core of the membrane through non-covalent forces, such as the hydrophobic force or electrostatic interactions. However, some proteins are also bound to membrane covalently; for example, membrane bound form of the penicillinase from *Bacillus licheniformis* is attached to the cytoplasmic membrane by an amino terminal fatty acylated glyceride [Lai et al., 1981]. The majority of the fatty acylated proteins are localized on the cytoplasmic surface of the plasma membrane [Wilcox & Olson, 1987], whereas proteins attached to glycolipids are localized on the outer surface of the plasma membrane [Ferguson et al., 1985].

Membrane proteins are broadly classified based on the type of interaction they maintain with the membranes. Integral or *intrinsic proteins* contain amino acid residues with hydrophobic side chains that interact with fatty acyl groups of the membrane lipids (e.g., bacteriorhodopsin). These proteins can only be removed from the membrane through harsh treatment with detergents or non-polar solvents [Helenius & Simons, 1975, Tanford & Reynolds, 1976]. Peripheral or *extrinsic proteins* are bound to membranes directly by their interaction with lipid polar head groups or indirectly by interaction with integral proteins. Peripheral proteins mostly contain a large proportion of the positively charged lysine and arginine residue, are predominantly basic and exhibit specific binding to negatively charged lipids. Most of the peripheral proteins interact with specific integral proteins by ionic or other weak interactions, such that these proteins can be detached from the membrane by a solution of high ionic strength (e.g., cytochorme *c*). Unlike integral proteins most peripheral proteins are water soluble and do not require harsh treatments for their removal from the membrane.

Glycoproteins, as the name itself suggests, are proteins with covalently bound carbohydrate. The sugar moieties often contribute importantly to the folding and stability of the proteins as well as to their synthesis and positioning within a cell. The

presence of sugar increases the solubility of glycoprotein in aqueous medium. In glycoproteins, carbohydrates attached to amino acid residues either by *O*-linkage to the hydroxyl oxygen of serine or threonine or by *N*-linkage to the amide nitrogen of asparagine.

1.2.3. The fluid mosaic model

The *fluid-mosaic model*, proposed by Singer and Nicolson in 1972, describes how the components of the plasma membrane are thought to interact. It updated the earlier models of biomembranes by Gorter and Grendel [1925] and Danielle and Davison [1935], as well as Robertson's unit-membrane model [Robertson, 1957, 1959]. Fluid mosaic model describes the membrane as a fluid mosaic and suggests that the lipids form a viscous, two-dimensional solvent into which proteins are inserted and integrated more or less deeply (Fig. 1.6). The important feature of this model is that the amphipathic phospholipids, glycolipid and sterols form a lipid bilayer, with the nonpolar regions of lipids facing each other at the core of the bilayer and their polar head groups facing outward. Protein-lipid interaction is thought to be stabilized through hydrophobic (fat soluble) contact points on the surface of the proteins [Richardson et al., 1964]. Based on thermodynamic and functional considerations, it was postulated that the membrane proteins are active components of signal transduction and transport, and span the entire thickness of a lipid bilayer. The mosaic architect is fluid because of the interactions among lipids, and between lipids and proteins, are noncovalent, leaving individual lipid and protein molecules free to move laterally in the plane of the membrane.

The fluid mosaic membrane model predicts lateral and rotational freedom and random distribution of molecular components in the membrane and explains many phenomena that take place in biological membranes, but certainly not all.

Experiments that were carried out subsequent to the proposal of the fluid-mosaic model suggest that the mobility of specific lipids or proteins in the biomembrane may be restricted [Jain, 1983]. More recent experiments suggest that the biomembranes may have domains that differ in their dynamic order, leading to the proposal of a new model for the cell membrane, which is called a *dynamically structured mosaic model* [Vereb et al., 2003]. The salient features of this model are: i) mosaicism can restrict free diffusion by lipid domain structure, cytoskeletal or other cytosolic interactions or by homo and heteroassociations with other integral proteins, ii) it explains the overall mobility of molecular elements by making the membrane a heavily compartmentalized, quasi-two-dimensional structure. In this two dimensional plane, diffusion, intermolecular forces, the ever changing membrane potential, and extracelluar influences can dynamically generate and destroy supramolecular structures.

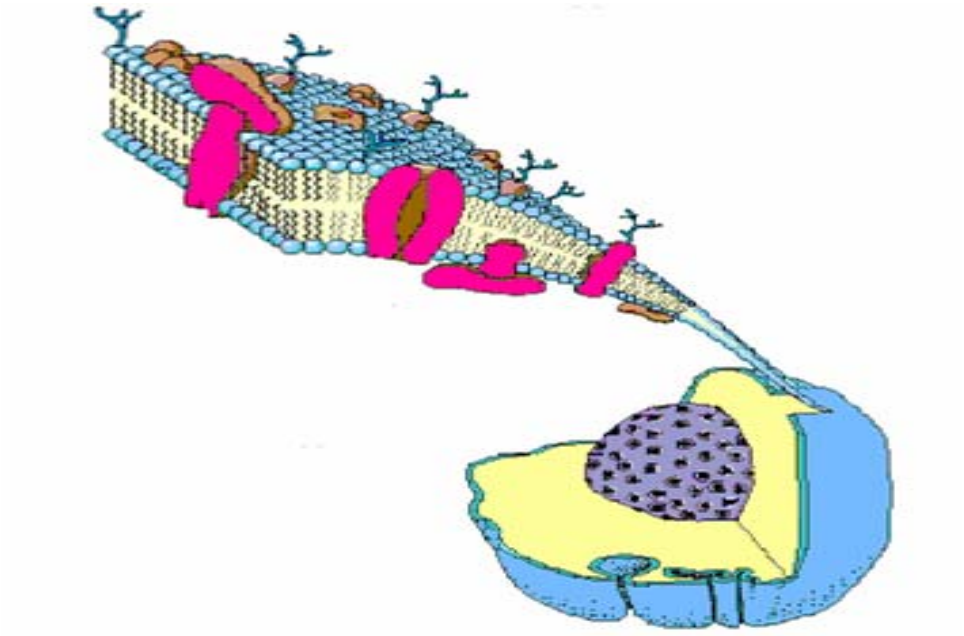

Fig. 1.6: The fluid-mosaic model proposed by Singer and Nicolson [1972].

1.3. Lipid-protein interaction

As outlined earlier in this chapter, membranes contain about 20 to 80% proteins. The nature of the cell membrane and its function can be addressed by understanding lipid-protein interactions. The organizational and motional properties of lipids are influenced by the presence of proteins; similarly, the function of membrane proteins is affected by the lipid environment.

1.3.1. Effect of lipid on protein structure

The specific folding of all intrinsic and some peripheral membrane proteins is partly determined and stabilized by the surrounding lipid. The functional properties of the proteins depend on the lipid composition and it is directly evident from the lipid-induced conformational changes in the protein and their specificity. These structural changes can be studied by physical methods which respond to changes in protein structure and dynamics, especially by circular dichorism, fluorescence spectroscopy and fourier transform infrared spectroscopy [Lux et al., 1972; Jonas & Krajnovich, 1977; Blondelle et al., 1999].

1.3.2. Effect of protein on lipid structure and mobility

Membrane proteins exert changes in the molecular order and restrict mobility of the annular lipid. The interaction of proteins with lipids can directly affect the phase transition of the lipids by inducing the formation of domains in the lipid bilayer, or by the formation of hexagonal phase or inverse hexagonal phase. The asymmetric distributions of lipid molecules between the two monolayer of biological or reconstituted membrane may be promoted and stabilized by proteins in their environment. These effects of proteins on lipid have been studied by electron-spin resonance spectroscopy [Marsh & Watts, 1982; Marsh & Páli, 2004], differential

scanning calorimetry [McElhaney, 1986], nuclear magnetic resonance spectroscopy [Knowles & Marsh, 1991; Marsh & Páli, 2004], fluorescence depolarization method [Cherry, 1981] and also by absorbance measurements.

1.3.3. Functional significance of lipid-protein interaction

Phospholipase A_2, an enzyme whose catalytic efficiency is related to the quality of the water-lipid interface and the structural organization of the lipid, instantaneously hydrolyzes diacyl phospholipids, and prefers aggregated phospholipids in the gel-to-fluid transition region. Microheterogenity of the lipid matrix plays an important role in phospholipase A_2 activation on membrane surfaces [Biltonen et al., 1990]. The interaction of integral membrane proteins in the lipid bilayer is mediated by the hydrophobic intramembranous surface residues and the fluid lipid bilayer. The stoichiometry of such interaction gives the intramembranous perimeter of the protein exposed to the lipid chains and the amino acid residues located close to the lipid polar head groups in the three-dimensional structure of the integral protein is indicated by their lipid selectivity [Marsh, 1993]. Intrinsic proteins induce lipid polymorphism, for example, the hydrophobic antibiotic peptide, gramicidin spans the lipid bilayer as a dimer and strongly destabilizes the bilayer and even induces H_{II} phase structure in phophatidylcholine systems [Jost & Griffth, 1982]. However, the major asialo-glycoprotein, glycophorin from the erythrocyte stabilizes the bilayer structure of unsaturated phophatidylethanolamines. Other studies show that signal peptides have the ability to induce non-bilayer structure, which plays an important role in protein insertion and translocation across membranes [Killian et al., 1990].

The transient association of peripheral proteins with membrane has been shown to be involved in membrane translocation processes; for example, apocytochrome *c* can be translocated from the cytoplasmic ribosome to the

intermembrane space between the outer and the inner mitochondrial membranes. The absolute requirement of acidic lipids for membrane binding of peripheral proteins may help in determining the location and orientation of these proteins. In myelin basic protein, acidic lipids bind with high specificity and make the myelin an insulator by forming a non-conducting sheath around the nerve axon. Spectrin binds to the inner surface of the erythrocyte membrane and contributes materially to the unique elastic properties required in the circulation of the red blood cells. The influence of extrinsic proteins on the polymorphic properties of lipids showed the competition between the protein and divalent cations. For example, the highly positively charged, polylysine destabilizes the bilayer structure of cardiolipin-phosphatidylethanolamine system and strongly protects against the ability of Ca^{2+} to induce complete H_{II} organization in the pure lipid system, whereas cytochrome *c* can induce non-bilayer structures in cardiolipin-conatining systems. This shows the apparent ability of cytochrome *c* to translocate rapidly across bilayers that contain cardiolipin [Jost & Griffith, 1982]. The most general membrane mediated events are membrane fusion, which occur during the process of fertilization, cell division, exo- and endocytosis, infection by membrane-bound viruses and intracellular membrane transport.

1.4. Sperm cell and plasma membrane

One of the most complex and exciting biological materials is the semen, which consists of a cellular component, the spermatozoa or male germ cells (commonly called as *sperm*) and a non-cellular component, the seminal fluid or plasma. The spermatozoa suspended in the seminal plasma pass through the female genital tract and interact with ovum through various mechanisms, and finally fertilize the egg. The first scientific evidence on seminal plasma goes back to the studies of Antonie von

Leeuwenhoek in 1677 and Vanquelin in 1791, who was the first to publish the chemical composition of semen [Shivaji et al., 1990].

1.4.1. Sperm cell and its structure

A spermatozoon is a haploid cell, which contains half of the genetic information needed to create life. Spermatozoa are produced in the seminiferous epithelium of the testis by a well organized process of cell proliferation and differentiation known as spermatogenesis [Clermont et al., 1993; de Krester & Kerr, 1994]. Mammalian spermatozoa are fundamentally similar in their basic structure, but vary tremendously in size and in details of their morphology depending upon the species. The male germ cell is made of two major parts, the head and the tail; importantly it is the only cell which knows how to "swim". The primary components of the sperm head are the nucleus and acrosome (Fig. 1.7) [Guraya, 1965; Phillips, 1975].

The acrosome contains hydrolytic enzymes which are released during acrosome reaction. The posterior portion of the acrosome is the equatorial segment, which remains intact during the acrosome reaction and is the site of initial contact between the sperm and egg at fertilization. The sperm nucleus occupies the maximum part of the spermatozoa head, which contains mostly DNA and proteins. The sperm nuclei contain the paternal genetic material (DNA), consisting of a haploid set of somatic chromosomes and in addition, one sex chromosome (X or Y).

The head is connected to the tail region by a neck, which is a short, constricted segment [Sato & Oura, 1985]. The tail consists mainly of the midpiece, the principle piece, and the end piece [Philips, 1975]. The mitochondrial sheath and the outer ring of coarse fibers constitute the midpiece of the spermatozoa, where they are arranged in the form of a helical sheath covering the longitudinal fibrous elements of the tail [Fawcett, 1975; Phillips, 1975]. Mitochondrial sheath is particularly rich in

phospholipids, most of which are bound to proteins and provide the energy required for spermatozoa motilility and are also the seat of transcriptional and translational activity in mature spermatozoa [Premkumar & Bhargava, 1972, 1973]. The axial filament complex running from one end of the tail to the other end consists of two central microtubules surrounded by a cylinder of nine evenly spaced microtubule doublets called as the *axoneme*, which in turn is surrounded by nine dense outer fibers composed of *dynein*. Interactions between the inner microtubules and the radial spokes coordinate the sliding activities of the outer doublets and produce the bending action that propels the sperm.

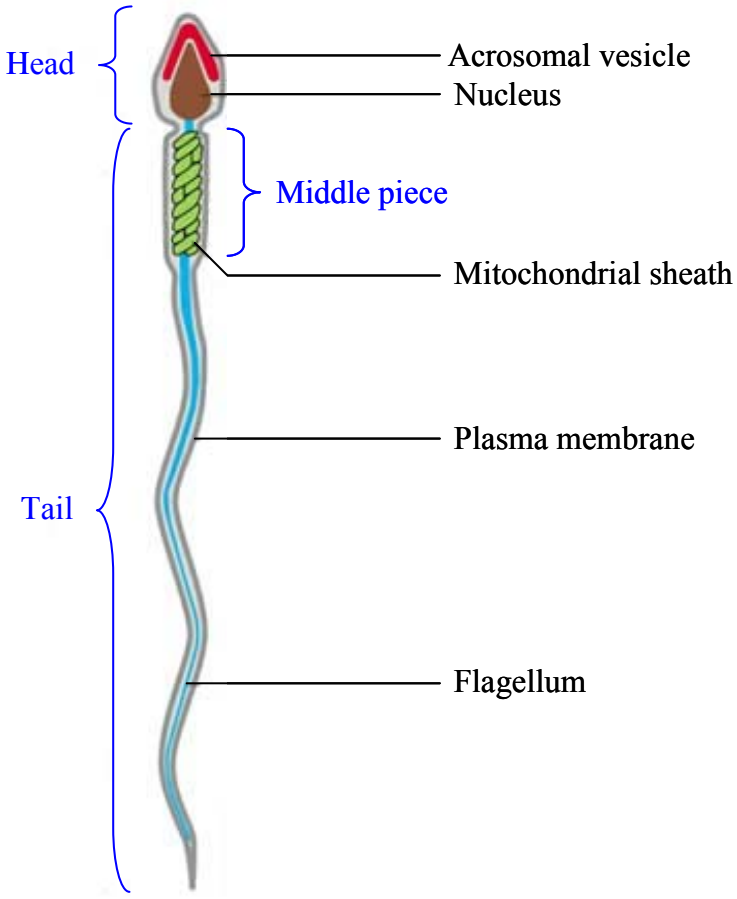

Fig. 1.7: Schematic diagram of a typical spermatozoon.

1.4.2. Capacitation and acrosome reaction

Ejaculated spermatozoa undergo capacitation in the female fallopian tube before fertilizing the oocyte by a membrane remodeling process and induce the acrosome reaction (AR). The molecular basis of sperm capacitation still remains a puzzle and it is believed to be a multistep process [Yanagimachi, 1994].

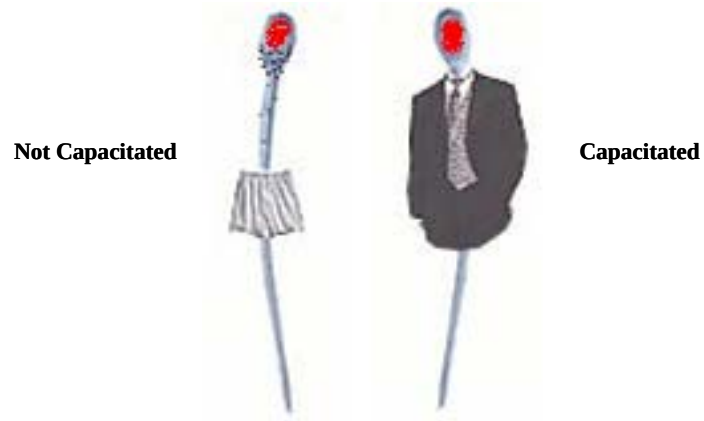

Fig. 1.8: A cartoon diagram illustrating the capacitated and incapacitated state of the spermatozoa.

Davis was the first to report that sperm capacitation involves removal of membrane cholesterol, with a consequent decrease in the cholesterol/phospholipid ratio [Davis, 1981; Hoshi et al., 1990]. Cholesterol, the major sterol in ejaculated bovine sperm [Parks et al., 1987], is known to regulate the fluidity of membrane lipid bilayers and the permeability of membrane [Yeagle, 1985, 1991] and to modulate the lateral mobility of integral proteins and functional receptors within the membrane. Thus the loss of cholesterol destabilizes the plasma membrane and allows the spermatozoa to undergo the acrosome reaction (AR) following interaction with the *zona pellucida*, the egg's extracellular matrix. Studies have shown that the influx of cholesterol inhibits capacitation in many species including the rabbit [Davis, 1982], rat [Davis et al., 1980], mouse [Go & Wolf, 1983, 1985], guinea pig [Fleming & Yanagimachi, 1981], human [Mosubasher et al., 1986] and bovine [Ehrenwald et al.,

1988a, 1988b]. On the contrary the efflux of cholesterol leads to bovine sperm capacitation and predisposes the sperm to penetrate egg at a higher rate than those sperm without reduced cholesterol levels [Ehrenwald et al., 1988a, 1988b].

Cross [1996] has shown that the human spermatozoa become non-responsive to the agonist, progesterone in the presence of seminal plasma and become responsive after their loss of the unesterified cholesterol (progesterone induces the AR in human sperm) [Zarintash & Cross, 1996]. Several studies have indicated that the components of the oviductal fluid in the female genital tract promote the efflux of cholesterol. Albumin and high-density lipoprotein (HDL) act as sterol acceptors, whereas HDL, the only class of lipoprotein present in the oviductal and follicular fluid, appears to be a more efficient acceptor of cholsterol than albumin [Thérien et al., 1997]. This was evident from the variation in the concentration of HDL in oviductal fluid during the estrous cycle, higher during the ovulation period and lower during the remainder of the cycle [Ehrenwald et al., 1990; Brantmeier et al., 1987; Langlais et al., 1988]. In vitro medium containing serum albumin depleted the sterol content to 29 – 50% in a time dependent manner [Go et al., 1983, 1985]. Ehrenwald and coworkers demonstrated that sperm cells challenged with lysophosphotidylcholine bound to bovine serum albumin (BSA) induce acrosome reaction after reducing sperm cholesterol [Ehrenwald et al., 1988a,b]. These results suggest that cholesterol efflux may be an early step in sperm capacitation and is followed by the acrosome reaction.

1.4.3. Seminal plasma and its constituents

The seminal plasma of mammals is a complex fluid, which serves as a carrier for the spermatozoa in their journey from the male testes to their target, the female uterus. It contains both organic and inorganic molecules of low as well as high molecular weight. While the low molecular weight fraction contains a wide variety of chemical

constituents such as metal ions, organic acids, sugars, lipids and amino acids, the only high molecular weight constituents found in seminal plasma are proteins; other biopolymers such as polysaccharides and nucleic acids are not present in it [Shivaji et al., 1990]. The major constituents of the plasma membrane are phospholipids, such as sphingomylein, phosphatidylcholine (lecithin), choline plasmalogen, ethanolamine, plasmologen, phosphotidylehtanolamine, phosphotidylserine, cardiolipin as well as gangliosides [Mann & Lutwalk-Mann, 1981; Martinez & Morros, 1996]. Cholesterol is the major sterol in mammalian spermatozoa (exceptions are hamster and mouse spermatozoa, which have 40% desmosterol [Awano et al., 1993; Visconti et al., 1995]) and is distributed throughout the plasma membrane with higher concentrations overlying the head region [Suzuki, 1990; James et al., 1999]. The other exotic material which is present in seminal plasma is fructose, the role of which in the seminal fluid remains an enigma [Shivaji et al., 1990].

1.4.4. Seminal plasma proteins and their role in sperm cell activation

Seminal plasma proteins are produced by the seminal vesicles, prostate glands and bulbourethral gland. Some of them bind specifically to sperm surface upon ejaculation and play an important role in capacitation – decapacitation process and also protect the spermatozoa in the female reproductive tract [Dravland & Joshi, 1981; Mukherjee et al., 1983; Shivaji et al., 1990]. The proportion of these secreted proteins differs from species to species. In bovine species, the acidic seminal plasma proteins (BSP proteins) constitute the major protein fraction of seminal plasma and modulate sperm capacitation by interacting with the various components present in follicular fluid. Several studies have shown that heparin-like glycosaminoglyans (GAG) induce capacitation and acrosome reaction of the ejaculated spermatozoa in a shorter period compared with the cauda epididymal bovine spermatozoa. In vitro, lysophosphatidylcholine (Lyso-PC) induced AR, when the spermatozoa are incubated

under capacitation conditions with heparin but had no effect under noncapacitating conditions without heparin [Thérien et al., 1995]. This evidence suggested that GAG modulate capacitation by binding to sperm surface proteins. Albumin and HDL present in uterine fluid, follicular fluid, or in-vitro medium containing serum albumin act as sterol acceptors and induce cholesterol efflux from sperm membrane.

Manjunath and co-workers have investigated the importance of bovine seminal plasma proteins (BSP proteins) in sperm capacitation [Manjunath & Thérien, 2002]. The BSP proteins accelerate the capacitation of bovine epididymal sperm induced by heparin and HDL, which mediate capacitation through different mechanisms [Lane et al., 1999]. Biophysical and biochemical studies have shown that the BSP proteins bind with high affinity to choline phospholipids [Swamy, 2004] and generate homogeneous lipid efflux particles of large size and high density on incubation with efflux medium [Moreau et al., 1999, 2000]. These efflux particles are composed of cholesterol, choline phospholipids and BSP proteins. This complex may be due to the aggregated form of BSP proteins [60,000 – 150,000], which exhibit hydrophobic cavities in which cholesterol could be trapped [Manjunath & Sairam, 1987; Gasset et al., 1997].

On the other hand, heparin-induced capacitation does not involve the efflux of sperm membrane cholesterol. The molecular basis for heparin-induced capacitation is unknown. However, Handrow et al. [1982] reported that heparin binds to bovine spermatozoa via a typical receptor-ligand interaction and recent reports indicate that BSP proteins may induce membrane reorganization which could result in the appearance of a new receptor for the heparin like GAG or HDL on the sperm surface [Lee et al., 1985; Chandonnet et al., 1990; Miller et al., 1990; Thérien et al., 1995]. Heparin-stimulated capacitation induces a series of intracellular events such as the

modification of lipid composition, increased permeability to Ca^{2+}, redistribution of surface components, changes in intramembranous particle distribution and an increase in the cAMP-dependent protein phosphorylation, whereas HDL stimulated capacitation shows no effect on tyrosine phosphorylation.

Recent studies have shown that in bull, cattle, pig, rabbit, mouse and hamster, spermatozoa bind to the surface of mucosal epithelium, mediated by sperm surface proteins. This results in the formation of oviductal sperm reservoir, which prevents polyspermic fertilization, assists hyperactivated motility and ensures sperm capacitation at the appropriate time [Harper, 1994; Suarez, 1998]. In bovine system, sperm surface binding protein PDC-109 is involved in the formation of sperm reservoir by interacting with Le^a trisaccharide present on the surface of the oviductal epithelium [Revah et al., 2000; Ignotz et al., 2001]. Liberda et al. [2001] showed that the low molecular weight components such as monosaccharide D-fructose, present in the seminal plasma inhibit the heparin binding activity of BSP proteins. Since BSP proteins stimulate heparin-induced capacitation, D-fructose can play an important role in GAG interaction and participate in fertilization process.

1.5. Acidic bovine seminal plasma proteins

The major heparin-binding proteins of bovine seminal plasma – BSP-A1, BSP-A2, BSP-A3 and BSP-30kDa, collectively termed as BSP proteins, are the secretory products of the seminal vesicle epithelium. The apparent molecular masses of the single chain polypeptides, BSP-A1, A2 and A3 are in the range 15 to 16.5 kDa as judged by SDS-PAGE. Two dimensional electrophoresis shows that all four are acidic proteins with pI 3.6 – 5.2. The amino acid sequence of BSP-A1 is identical to that of BSP-A2 but the former is *O*-glycosylated at Thr-11 with a single

oligosaccharide [Neu5*N*Ac(α2-3)Gal(β1-3)Gal*N*Ac-], whereas BSP-A2 contains one disaccharide [Gal-Gal*N*Ac-] [Calvete et al., 1994; Gerwig et al., 1996]. The mixture of BSP-A1 and BSP-A2 is also referred to as PDC-109. BSP-A3 is not glycoslated, while BSP-30kDa protein contains six trisaccharides [Neu5*N*Ac(α2-3)Gal(β1-3)Gal*N*Ac-] linked through *O*-glycoslation to threonine residues. All BSP proteins belong to the same protein family, display a mosaic architecture, which consists of an N-terminal portion of variable length that is distinctly *O*-glycosylated, followed by two tandemly arranged and highly conserved fibronectin type II (Fn2) domains [Manjunath & Thérien, 2002]. Complementary deoxyribonucleic acid cloning (cDNA) and sequencing of all three BSP proteins are reported [Kemme et al., 1988; Salois et al., 1999]. BSP-A3 is homologous to PDC-109, with ca. 70% sequence identity; both are also homologous to collagen-binding domain of bovine fibronectin (type II sequence) [Seidah et al., 1987].

Immunofluorescence studies on the epidiymal spermatozoa have shown that BSP proteins are localized on the acrosome, postacrosome and mid-piece region [Manjunath et al., 1994]. Anti-BSP cross-reacting proteins have been detected in the seminal fluids of the human, porcine, hamster, mouse, and rat using the *p*-aminophenyl phosphorylcholine-Agarose (PPC-Agarose) affinity matrix [Leblond et al., 1993]. Proteins homologous to the BSP proteins are found in other mammalian seminal plasma fluids such as stallion (HSP-1 and HSP-2), porcine (pB1) [Calvete et al., 1995, 1997], goat (GSP-14 kDa, GSP-15 kDa, GSP-20 kDa and GSP-22 kDa) [Villemure et al., 2003], bison (BiSV-16kDa, BiSV-17kDa, BiSV-18kDa and BiSV-28kDa) [Boisvert et al., 2004] and ram (RSP-15 kDa and RSP-16 kDa) [Bergeron et al., 2005]. These observations show that the BSP family of proteins are ubiquitous in mammalian seminal plasma, exist in several forms in each species and may play a common biological role.

1.5.1. Major bovine seminal plasma protein, PDC-109

The major protein of bovine seminal plasma is a **P**rotein containing N-terminal asparatic acid (**D**) and C-terminal cystine (**C**)] and contains **109** residues. Therefore it is given the trivial name, PDC-109. It is present at a concentration of 15-25mg/ml in bovine seminal plasma. Upon ejaculation approximately 9.3×10^6 molecules of PDC-109 bind to the surface of each sperm cell [Scheit et al., 1988; Calvete et al., 1994]. The polypeptide chain of 109 amino acids is made up of two tandemly repeating fibronectin type II domains, preceded by a 23-residue N-terminal segment (Fig. 1.8). Modification of the lysine side chain amino groups of PDC-109 by citraconic anhydride, followed by tryptic digestion under controlled conditions, yielded the intact second fibronectin type II domain, which was referred to as PDC-109 domain b (PDC-109/b) [Banyai et al., 1990; Constantine et al., 1991, 1992]. The structure of this domain has been determined in solution by ^{1}H-NMR spectroscopy.

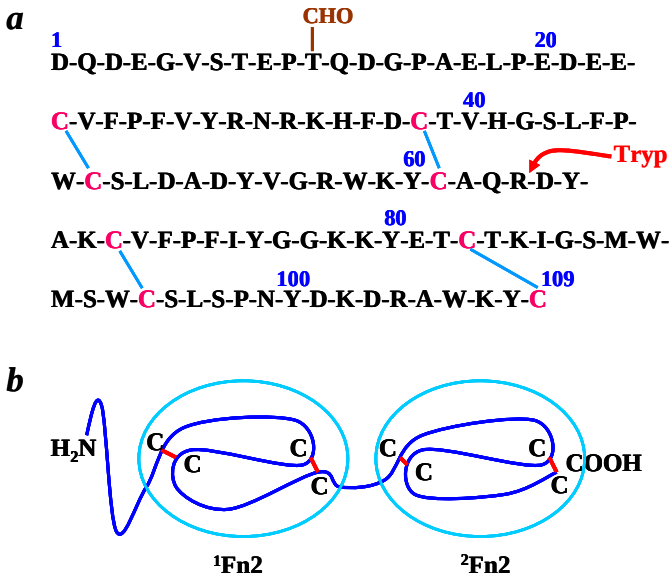

Fig. 1.9: Amino acid sequence of PDC-109 (a) and a schematic diagram of its domain structure (b). Taken from Swamy [2004].

The binding sites for PDC-109 on spermatozoa were found to be resistant to protease treatment (trypsin, pronase and proteinase K) or acid treatment and heat-stable, but could be extracted with organic solvents, indicating that the receptor for the protein on spermatozoa is lipid rather than a protein [Desnoyers & Manjunath, 1992]. The sperm plasma membrane is composed of a variety of lipids [Parks et al., 1987] and studies aimed at characterizing the lipid specificity of BSP proteins showed that PDC-109 (BSP-A1/A2) and BSP-A3 proteins specifically recognize phospholipids containing the phosphorylcholine head group, such as phosphatidycholine (PC), sphingomyelin (SM), lyso-PC, PC plasmalogen, platelet activating factor (PAF), and lyso-PAF. On the other hand, BSP-30 kDa displays broader binding specificity. It recognizes phosphorylcholine-containing lipids with greater affinity, but also interacts with phosphatidylethanolamine (PE), phosphatidylserine (PS), phosphatidylinositol (PI), phosphatidic acid (PA) and cardiolipin [Desnoyers & Manjunath, 1992]. Lipid binding by these proteins is calcium-independent in nature. The specificity is further supported by the purification of BSP proteins through affinity chromatography on *p*-amino-phenyl phosphorylcholine coupled to sepharose, or quaternary methylamine coupled to silica particles, or DEAE-Sephadex and elution by the specific ligand, phosphorylcholine [Desnoyers & Manjunath, 1993].

BSP proteins also interact with different type of collagens (types I, II, IV, V), fibrinogen, apolipoprotein A-1 (ApoA-1), ApoA-1 associated with high-density lipoproteins [Manjunath et al., 1989, 1993] and low-density lipoprotein fraction [Manjunath et al., 2002]. They also bind to calmodulin in the presence and absence of Ca^{2+} and it is also shown that upon limited proteolysis with trypsin, peptides of BSP-A1/-A2 and BSP-30 kDa exhibited higher calmodulin-binding activity than the intact BSP proteins. Considering the important role of Ca^{2+} in triggering the acrosome reaction and the role of calmodulin in intracellular transport of calcium, it is suggested

that BSP proteins are involved in sperm capacitation and the acrosome reaction [Manjunath et al., 1993]. BSP proteins also bind to heparin-like glycosaminoglycans (GAGs) present in the female reproductive tract, which appear to participate in the process of capacitation [Miller et al., 1990; Lane et al., 1999]. In mammals, the spermatozoa are trapped in a reservoir in the caudal isthmus of the oviduct until the time of ovulation through a specific interaction with sperm surface molecule overlying the acrosome and the specific carbohydrate moiety on the surface of the mucosal epithelium [Lefebvre et al., 1995; Suarez, 2001]. In bovine system, it was found that PDC-109 mediates the interaction between sperm cells and oviductal mucosa, by interacting with fucosylated molecules present in oviducatal epithelium, which contain the Le^a trisaccharide (α-L-Fuc[1,4]-β-D-Gal[1,3]-D-GlcNAc) [Revah et al., 2000; Ignotz et al., 2001]. It has been shown that D-fructose inhibits heparin-binding activity of bovine seminal plasma proteins and epididymal sperm [Liberda et al., 2001], indicating that D-fructose present in seminal plasma not only serves as energy source [Parrish et al., 1989]. Although the role of PDC-109 and other BSP proteins in capacitation and their interaction with various components are studied, the molecular mechanism underlying capacitation remains unclear.

1.5.2. Biophysical study on the interaction of PDC-109 with lipids

In order to understand molecular details of lipid binding by the BSP proteins and to investigate their role in sperm capacitation and fertilization process, biophysical and spectroscopic studies have been carried out on the interaction of PDC-109 with lipid membranes. Equilibrium dialysis studies performed at 4^oC to investigate the binding of choline yielded a stoichiometry of 1.8 binding sites per PDC-109 monomer with a binding constant of 0.95mM [Desnoyers & Manjunath, 1993]. Gel filtration experiments showed the polydisperse nature of PDC-109, which dissociates into dimers upon binding to *O*-phosphorylcholine (PrC). Differential scanning

calorimetric studies demonstrated that binding of phosphorylcholine increases the thermal unfolding temperature of the protein by ca. 13 degrees, suggesting that the protein structure is stabilized by ligand binding. Fourier-transform infrared spectral studies on native PDC-109 and on its complex with PrC revealed that binding of the soluble PrC molecule results in a small increase in the turn content, with a proportional decrease in the unordered structure, which is consistent with the calorimetric studies [Gasset et al., 1997].

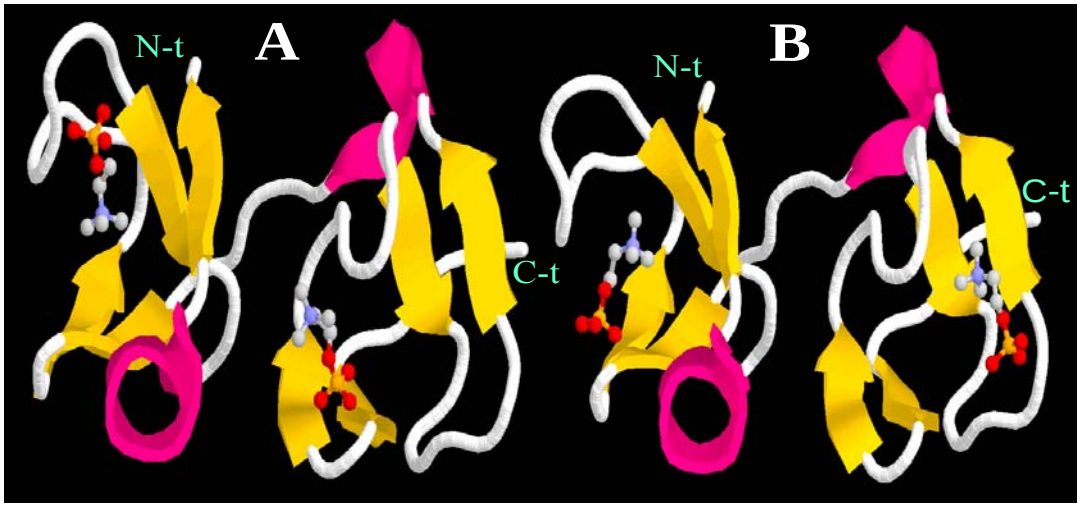

Fig. 1.10: Structure of the PDC-109 dimer with bound phosphorylcholine molecule. The structure was generated using Rasmol software from the coordinates in pdb (id = 1h8p). Each PDC-109 monomer, labeled A and B, comprises two Fn2 domains. The structure elements are shown as ribbon (yellow arrows, β strand; pink cylinders, α helix) and the bound phosphorylcholine molecules are rendered in ball and stick model.

The most direct evidence for the specificity of PDC-109 towards the phosphorylcholine moiety came from the single crystal X-ray diffraction studies [Wah et al., 2002]. These studies showed that each of the two Fn2 domains bind one phosphorylcholine molecule with both the binding sites located on the same face of the molecule. Binding of phosphorylcholine to the Fn2 domains involves a cation–π interaction between the quaternary ammonium group of the ligand and a core tryptophan ring of the polypeptide (Fig. 1.10). Additional stabilization comes from

hydrogen bonding interaction of the hydroxy groups of tyrosine side chains or main chain amide groups with the phosphate groups. The loop comprising residues 41–44 of the 1Fn2 domain, which is extended away from the core of the protein in the unbound structure [Constantine et al., 1992], packs closer to the binding site and interacts with the ligand (Fig. 1.11). This conformational change most likely triggers the dissociation of the polydisperse aggregate form of PDC-109, resulting in the formation of dimers in which all the four choline-binding sites lie on the same face of the protein. Such an orientation in which the four choline-binding sites of the PDC-109 dimer are all on the same face of the protein is consistent with the binding and optimal interaction of this protein with choline lipid-rich membranes [Swamy, 2004]. Since choline phospholipids comprise 60–70% of the total phospholipids of bull sperm plasma membrane [Watson, 1981; Parks et al., 1987], the specific interaction of PDC-109 with the phosphorylcholine moiety of these lipids seems to be an effective means of coating the sperm plasma membrane with this protein, which leads to the efflux of cholesterol and choline phospholipids.

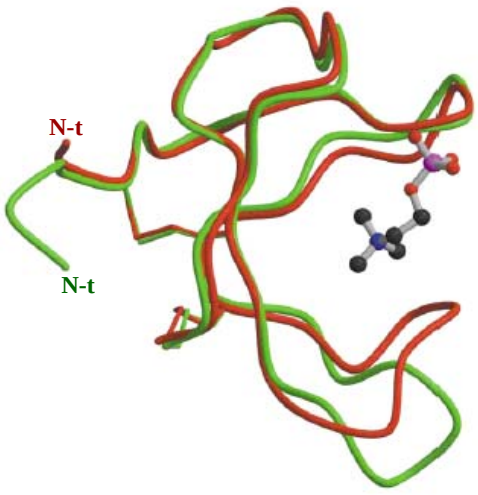

Fig. 1.11: Backbone diagram of PDC-109 1Fn2 domain with bound ligand phosphorylcholine (red) and without ligand (green). Note that in the phosphorylcholine-bound structure the loop at the lower right corner has moved closer to the ligand (shown as a ball and stick model). Taken from Wah et al. [2002].

Although ultrastructural and biochemical studies have suggested that spermatozoa undergoing capacitation exhibit a membrane remodeling process, the molecular events of this process are not well understood [Manjunath et al., 1988; Aumüller et al., 1988; Desonyers & Manjunath, 1992]. Biophysical studies were carried out on the interaction of sperm surface lipids with the seminal plasma proteins in order to understand the mechanism involved in sperm capacitation. The intrinsic fluorescence emission spectrum of PDC-109 was blue shifted upon binding to small unilamellar vesicles of phosphatidylcholine and its intensity increased, which indicates that the environment of tryptophan residues becomes more hydrophobic [Müller et al., 1998]. Monitoring these fluorescence changes, it was found that saturation binding with SUV occurred at a lipid/protein ratio of 10-11 PC molecules/PDC-109 molecule. Incorporation of PE or PS into PC vesicles decreased binding, indicating that density of phosphorylcholine groups is an important factor for the binding to take place. Stopped-flow fluorescence studies have shown that binding of PDC-109 to PC vesicles (SUV) is a very rapid, biphasic process with half times of less than one second [Muller et al., 1998]. In additional experiments these authors have incorporated 1-palmitoyl 2-(4-doxylpentanoyl)-PC and -PE into PC vesicles and obtained ESR spectra in the absence and in the presence of PDC-109. Spectra obtained at 4°C in the presence of the protein consisted of two components – a rigid component and a fluid component, which could be resolved by spectral subtraction. On the other hand, spectra obtained from PC vesicles alone contained only the fluid component, demonstrating that binding of PDC-109 to phosphatidylcholine vesicles led to a rigidification of the membrane. FTIR studies on PDC-109 bound to phosphatidylcholine membranes showed that the solvent exposed loop content increases by 5–6% upon membrane binding [Gasset et al., 2000].

1.6. Objectives and scope of the present study

Fertilization is a complex process, in which morphologically different gametes, the spermatozoa from male and ovum from female interact to form zygote. Chang [1951] and Austin [1952] proposed the role of seminal plasma proteins in sperm capacitation, but the mechanism underlying the process remains an enigma. In bovine system, PDC-109, the major seminal plasma protein binds to the sperm surface on ejaculation and interacts with specific phospholipids and primes the spermatozoa for fertilization by inducing cholesterol efflux, which appears to be an important step in the capacitation process [Thérien et al., 1998; Moreau et al., 1999; Manjunath & Thérien, 2002].

The molecular events involved in the capacitation process can be understood in detail by studying the interaction of the molecules present in the seminal plasma and sperm surface. Since the receptor for the BSP proteins is found to be choline phospholipids, which are present on the sperm surface, biophysical studies on the interaction of this lipid with BSP proteins may shed more light on the mechanism of sperm capaciation and acrosome reaction. Further, due to the ubiquitous nature of phophatidylcholines (or sphingomyelin) in mammalian cell membranes, the identification of proteins that specifically interact with these particular phospholipids is of great interest and potential importance. This is not solely from a structural and functional standpoint, but also with regard to the possibility that pathologies might occur arising from specific protein or peptide interactions with this major membrane constituent. Finally the understanding of the molecular interaction involved in various steps of animal reproduction is of practical importance in veterinary and human medicine, for eg. in birth control and in vitro fertilization. Moreover, BSP proteins are shown to interact rapidly with the low-density lipoprotein fraction of egg yolk, the

major component of extenders used in sperm storage [Manjunath et al., 2002]. It is known that BSP proteins destabilize the sperm membrane by removing cholesterol and phospholipids and induce capacitation [Manjunath & Thérien, 2002]. In view of the above, it is important to study the interaction of this protein with various molecules. Such studies will be useful in developing improved methods of sperm cryopreservation for commercial application and also for preserving wild animals and endangered species.

The main focus of the studies reported in this thesis is to investigate the interaction of the major protein form bovine seminal plasma, PDC-109 with phospholipid membranes and soluble ligands, namely phosphorylcholine and choline. The major objectives of this study are the following: i) to understand the lipid specificity of PDC-109 in greater detail, ii) to characterize the effect of PDC-109 binding on the phase properties of phospholipid membranes, iii) to investigate the kinetics and mechanism of PDC-109 binding to phospholipid membranes, and iv) to determine the thermodynamic forces that characterize the interaction between PDC-109 and various ligands. In order to achieve the above objectives, the following studies were carried out.

- Spin label electron spin resonance (ESR) studies were carried out to investigate the influence of PDC-109 on the lipid chain mobility and on the membrane chain-melting transition. The penetration of the protein into the membrane and its direct interaction with the lipid chains as well as the specificity of its interaction with different lipid species were also studied by ESR spectroscopy using spin-labeled lipids with different polar headgroups.
- The effect of cholesterol on the interaction of PDC-109 with phosphotidylcholine membranes was also studied by spin label ESR spectroscopy.

- The kinetics of interaction of PDC-109 with different phospholipids membranes containing cholesterol were investigated by the surface plasmon resonance (SPR) technique.
- Thermodynamic forces that govern the binding of soluble ligand, *O*-phosphorylcholine and Lyso-PC were investigated by absorption spectroscopy.
- The exposure and accessibility of tryptophan residues in the native PDC-109 and membrane bound state were studied by fluorescence quenching technique.
- The energetics of phospholipid interaction with PDC-109, were investigated by isothermal titration calorimetry (ITC).

Chapter 2

Spin-Label Electron Spin Resonance Spectroscopic Studies on the Interaction of PDC-109 with Phospholipid Membranes

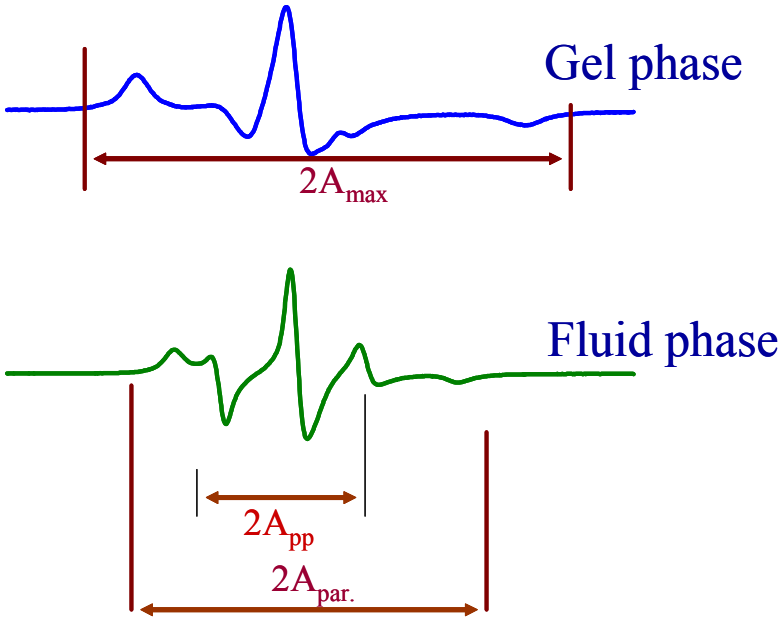

Ramakrishan, M., ***Anbazhagan, V.***, *Pratap, T.V., Marsh, D. and Swamy, M.J.* (2001) *Membrane insertion and lipid-protein interactions of bovine seminal plasma protein PDC-109 investigated by spin-label electron spin resonance spectroscopy.* ***Biophys. J.*** *81: 2215-2225.*

Swamy, M.J., Marsh, D., ***Anbazhagan, V.*** *and Ramakrishnan, M.* (2002) *Effect of cholesterol on the interaction of seminal plasma protein, PDC-109 with phosphatidylcholine membranes.* ***FEBS Lett.*** *538: 230-234.*

2.1. Summary

The interaction of the major acidic bovine seminal plasma protein, PDC-109, with dimyristoylphosphatidylcholine (DMPC) membranes has been investigated by spin-label electron spin resonance spectroscopy. Studies employing phosphatidylcholine spin labels, bearing the spin labels at different positions along the *sn*-2 acyl chain indicate that the protein penetrates into the hydrophobic interior of the membrane and interacts with the lipid acyl chains up to the 14^{th} C-atom. Binding of PDC-109 at high protein/lipid ratios (PDC-109:DMPC = 1:2, w/w) results in a considerable decrease in the chain segmental mobility of the lipid as seen by spin-label electron spin resonance spectroscopy. A further interesting new observation is that, at high concentrations, PDC-109 is capable of (partially) solubilizing DMPC bilayers. The selectivity of PDC-109 in its interaction with membrane lipids was investigated by using different spin-labeled phospholipid and steroid probes in the DMPC host membrane. These studies indicate that the protein exhibits highest selectivity for the choline phospholipids phosphatidylcholine and sphingomyelin under physiological conditions of pH and ionic strength. The selectivity for different lipids is in the following order: phosphatidylcholine ≈ sphingomyelin ≥ phosphatidic acid (pH 6.0) > phosphatidylglycerol ≈ phosphatidylserine ≈ androstanol > phosphatidylethanolamine ≥ *N*-acyl phosphatidylethanolamine >> cholestane. Thus, lipids bearing the phosphocholine moiety in the headgroup are clearly the lipids most strongly recognized by PDC-109. However, these studies demonstrate that this protein also recognizes other lipids such as phosphatidylglycerol and the sterol androstanol, albeit with somewhat reduced affinity. In addition, the presence of cholesterol leads to an increased association of different phospholipid as well as sterol probes, thus modulating the interaction of PDC-109 with phospholipid membranes.

2.2. Introduction

As mentioned in Chapter 1 (Section 1.4.4) BSP proteins bind to sperm cell membranes by their specific interaction with the choline containing phospholipids, namely phosphatidylcholine (PC) and sphingomyelin (SM) [Desnoyers & Manjunath, 1992]. This binding results in an efflux of choline phospholipids and cholesterol, referred to collectively as *cholesterol efflux*. Cholesterol efflux results in a decrease of the cholesterol/phospholipid ratio and promotes capacitation, which is a necessary event before the sperm can undergo acrosome reaction and finally fertilize the egg [Thérien et al., 1997;1998]. Each Fn2 domain of PDC-109 binds to one choline phospholipid molecule and both binding sites are necessary for inducing cholesterol efflux [Moreau et al., 1998]. In order to understand at the molecular level how cholesterol efflux is induced by this protein, it is important to investigate its interaction with phospholipid membranes with and without cholesterol.

Such studies are expected not only to shed light on the molecular events involved in the capacitation process but can potentially lead to the development of novel anti-fertility drugs. Not only from the biological point of view, but also from a biophysical perspective, the BSP proteins are of great interest. Phosphatidylcholines (or the sphingolipid analog, sphingomyelin) are the major phospholipid component of mammalian cell membranes. It is generally assumed that these zwitterionic phospholipids play a passive structural role as the major building blocks in biological membranes, without any specific interactions. Results on lipid-protein interactions with both integral and peripheral membrane proteins also generally indicate a lack of specific interactions with PC [reviewed in Marsh & Horváth, 1998]. In view of the ubiquitous nature of PC in mammalian membranes, the identification of proteins that specifically interact with it is of great interest and potential significance. In addition

to the structural and functional significance, studies on these proteins are expected to throw light on the possibility that pathologies might occur due to their specific interactions with PC or with sphingomyelin, another phospholipid containing a choline headgroup.

In the studies reported in this chapter, the interaction of PDC-109 with membranes made up of phosphatidylcholine and phosphatidylcholine/cholesterol mixtures bearing probe amounts of different spin-labeled phospholipids and steroid probes (see Fig. 2.1) was investigated by electron spin resonance (ESR) spectroscopy. Particularly, by using spin-labeled phospholipids bearing the nitroxide probe at different positions of the *sn*-2 acyl chain of phophatidylcholine as well as spin labeled phospholipids with different head groups the following aspects of the interaction were studied: i) the influence of the protein on the lipid chain mobility and on the membrane chain-melting phase transition, ii) the penetration of the protein into the membrane and its direct interaction with the lipid chains, and iii) the specificity of interaction of PDC-109 with phospholipids having different polar head groups. These studies showed that in addition to spin-labeled phosphatidylcholine and sphingomyelin, PDC-109 also recognizes phosphatidylserine and phosphatidyl-glycerol spin labels as well as a cholesterol analogue, androstanol spin label with considerable affinity, whereas very weak interaction was observed with spin-labeled phosphatidylethanolamine. It has also been demonstrated that, upon binding PDC-109 penetrates into the hydrophobic interior of the membrane. The effect of cholesterol on the interaction of PDC-109 with model membranes made up of dimyristoylphosphatidylcholine was also investigated by spin-label ESR spectroscopy. The results obtained indicate that the interaction of PDC-109 with different phospholipids is increased considerably by the presence of cholesterol.

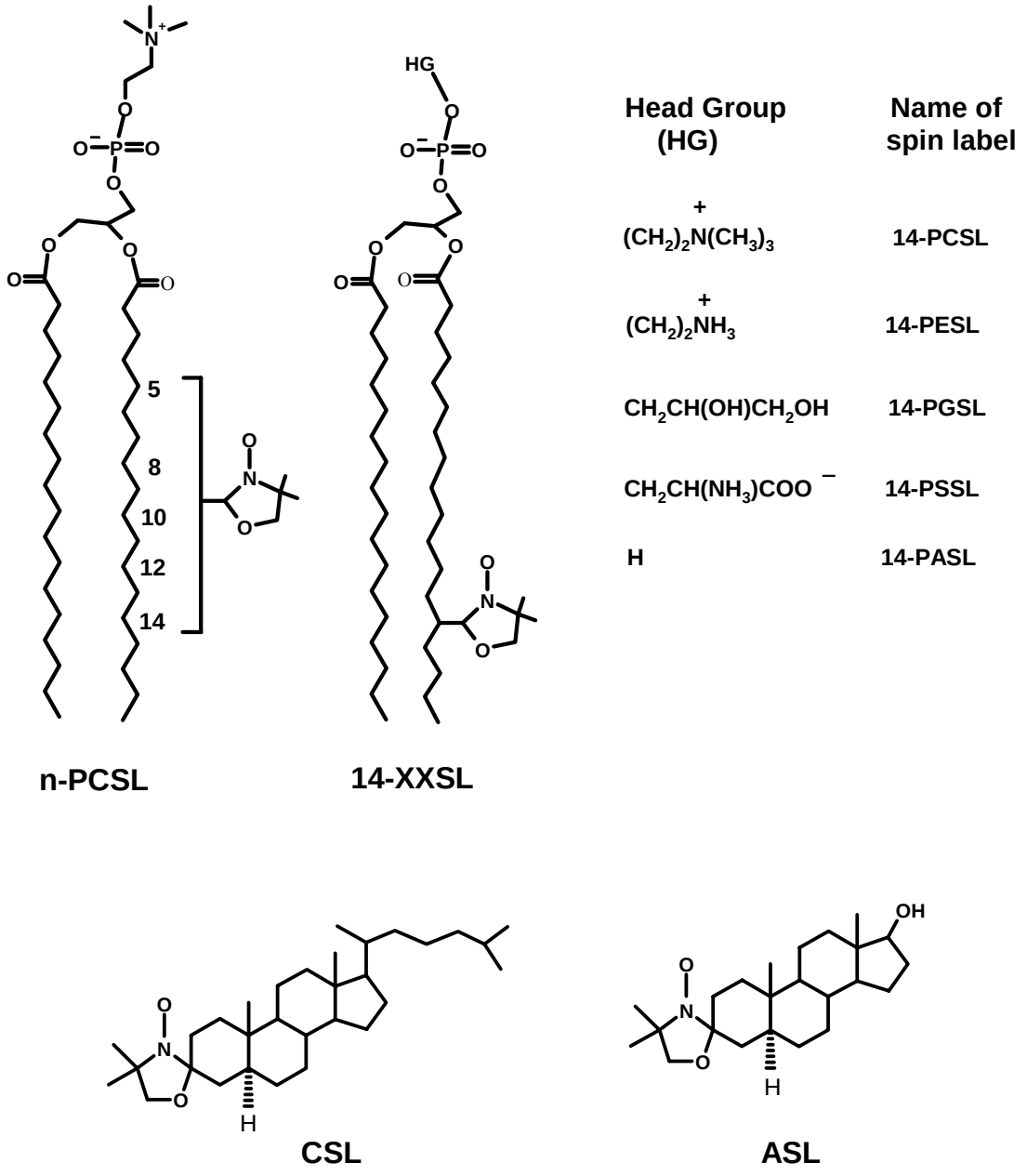

Fig. 2.1: **Structures** of the spin label probes investigated in the present study. n-PCSL are phosphatidylcholine spin labels bearing the nitroxide moiety at on of the various positions on the sn-2 acyl chain as indicated, 14-XXSL are different phospholipids bearing the nitroxide moiety on the 14th C-atom of the sn-2 acyl chain, CSL is the cholestane spin label, ASL is the androstanol spin label.

2.3. Experimental Section

2.3.1. Materials

Phosphorylcholine chloride (Ca^{2+} salt), choline chloride and Tris base were from Sigma (St. Louis, MO). Sephadex G-50 (superfine) and DEAE Sephadex A-25 were obtained from Pharmacia Biotech (Uppsala, Sweden). Dimyristoylphosphatidyl-choline (DMPC), and cholesterol were obtained from Avanti Polar Lipids (Alabaster, AL). Stearic acid spin-labeled on the 14^{th} C-atom and phosphatidylcholine, spin-labeled on the 14^{th} C-atom of the *sn*-2 acyl chain (14-PCSL; 1-acyl-2-[*n*-(4,4-dimethyloxazolidine-*N*-oxyl)]stearoyl-s*n*-glycero-3-phosphocholine) were synthesized according to procedures outlined in Marsh and Watts [1982]. Spin-labeled phospholipids with different polar head groups (14-PESL, phosphatidylethanolamine; 14-PSSL, phosphatidylserine; 14-PGSL, phosphatidyl-glycerol and 14-PASL, phosphatidic acid) were prepared from 14-PCSL by phospholipase D-catalyzed head group exchange, as described in the same reference. Spin-labeled *N*-acyl phosphatidylethanolamine, 14-NAPESL, with the spin label in the *N*-acyl chain was synthesized as described by Swamy et al. [2000]. Spin-labeled sphingomyelin (14-SMSL) was prepared as described by Hofmann et al. [2000]. Cholestane spin label (CSL) (4',4'-dimethylspiro[5α-cholestane-3,2'-oxazolidin]-3'-yloxyl) and androstanol (ASL) spin label (17β-hydroxy-4',4'-dimethyl-spiro[5α-androstane-3,2'-oxazolidin]-3'-yloxyl) were obtained from Syva (Palo Alto, CA).

2.3.2. Extraction of BSP Proteins

Samples of bovine semen, freshly collected from Ongole bulls with the aid of an artificial vagina, were kindly provided by the Department of Animal Reproduction, Acharya N. G. Ranga University of Agricultural Sciences, Hyderabad and Lam Farm,

Department of Animal Breeding of the same university at Guntur, Andhra Pradesh, India. The samples were stored on ice for a maximum of 9 h (until they were brought to the laboratory), and then centrifuged at 3000 rpm in a refrigerated centrifuge to separate the sperm cells and the seminal plasma. Total proteins from the seminal plasma were precipitated by adding eight volumes of cold ethanol, and the precipitated proteins were dissolved in distilled water and lyophilized. The lyophilized protein fraction was delipidated by extraction with a mixture of n-butanol/diisopropylether (40/60, v/v) as described by Desnoyers and Manjunath [1993].

2.3.3. Purification of PDC-109

PDC-109 was purified by a modification of the procedure reported by Calvete et al. [1996]. In the modified procedure, delipidated BSP protein fraction obtained according to the procedure of Desnoyers and Manjunath [1992, 1993] was used instead of the bovine seminal plasma, used by Calvete and co-workers [Calvete et al., 1996]. The delipidated BSP protein fraction was dissolved in 50mM Tris buffer, 0.15M NaCl, 5 mM ethylenediaminetetraacetic acid (EDTA), pH 7.4 (TBS-I) and subjected to gel filtration on a column of Sephadex G-50 superfine (2.5 × 170 cm), pre-equilibrated with the same buffer (Fig. 2.2A). Under these conditions PDC-109 elutes in the void volume, as it exists as a polydisperse aggregate with an average molecular weight of ~ 70 kDa [Gasset et al., 1997]. The fractions corresponding to this peak (major peak) were collected, dialyzed against 25 mM Tris, 1.0 M NaCl, pH 6.4 (TBS-II) and loaded onto a column of DEAE Sephadex A-25 (or A-50), pre-equilibrated with the same buffer. After washing the column with the same buffer until no protein was found in the washings, the bound protein was eluted with 100 mM choline chloride in the same buffer (Fig. 2.2B). The eluted protein was dialyzed extensively against TBS-I to remove the choline chloride, concentrated by lyophilization, and then dialyzed again against the same buffer and stored at 4^{o}C.

Alternatively, the protein was lyophilized to a powder and stored at -20^{o}C. Both types of samples were found to bind to phosphatidylcholine membranes or to DEAE Sephadex A-25 without any noticeable decrease in the activity over several months of storage. Purity of PDC-109 was assessed by SDS-PAGE [Laemmli, 1970], where the protein moved as a single band (Fig. 2.2C). In some experiments two closely spaced bands of Mr ~ 13 kDa, corresponding to the glycosylated and unglycosylated forms, could be seen.

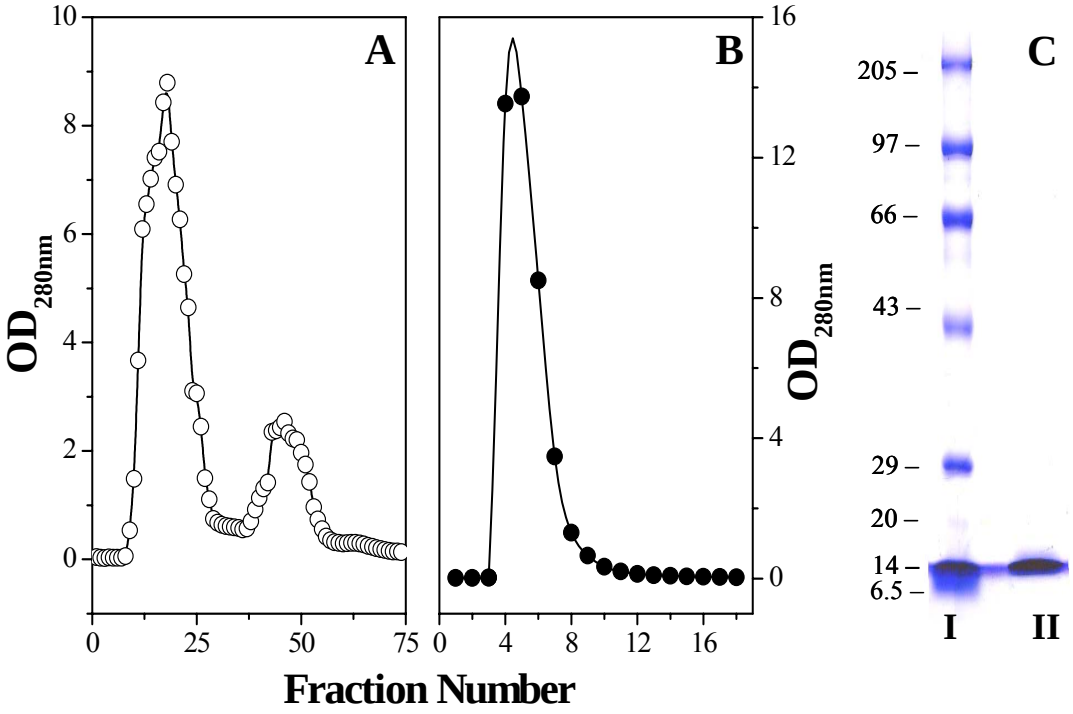

Fig. 2.2: Purification of PDC-109. (A) **Sephadex G-50** gel filtration elution profile. (B) **DEAE Sephadex A-25** affinity chromatography elution profile, PDC-109 was eluted with 100 mM Choline chloride. (C) **10 % SDS-PAGE**: Lane I: Molecular weight markers (kDa); lane II: PDC-109.

2.3.4. Protein assay

Protein concentrations were determined by the method of Lowry et al., [1951] using bovine serum albumin as the standard. The concentration of purified PDC-109 was

estimated coefficient at 280 nm of 2.5 for a 1 mg/ml sample concentration [Calvete et al., 1996].

2.3.5. Binding of PDC-109 to DMPC and DMPC/cholesterol mixtures

The binding of PDC-109 to DMPC multilamellar vesicles (MLVs) and to DMPC MLVs containing 25 mol% cholesterol was investigated by turbidimetry. The lipid or lipid mixture was dissolved in CH_2Cl_2, and aliquots corresponding to 1.0 mg of DMPC were transferred to glass test tubes and the solvent was removed in a nitrogen gas stream. After removing the traces of solvent by vacuum desiccation for over 3 h, the lipid film was hydrated with 1.0 ml of 10 mM Hepes, 1 mM EDTA, 0.15 M NaCl, pH 7.4 buffer (HBS), or with different amounts of protein solution in the same buffer. An appropriate volume of buffer was added in the latter case to make up the volume to 1.0 ml. The samples were warmed to ~ 30°C and were mildly vortexed several times and then subjected to 10 freeze-thaw cycles to get a homogenous suspension. Alternately, samples were prepared by first hydrating the lipid film with HBS, followed by the addition of PDC-109 and 10 freeze-thaw cycles. Turbidity of the samples was measured at 330 nm in a Shimadzu UV-3101PC UV-Vis-NIR double beam spectrophotometer using 1-cm-path-length cells. Essentially similar results were obtained with both methods of sample preparation.

The PDC-109/DMPC recombinants of high protein/lipid ratio (P/L > 2.0 w/w) were further analyzed by gel filtration on Sepharose CL6B [cf. Moreau and Manjunath, 1999]. The gel filtration column (1.7 × 50 cm) was equilibrated with HBS and calibrated with standards with M_r values in the range of 60,000 to 2×10^6 Da. Fractions were monitored by checking absorption at 280 nm for protein and 330 nm for turbidity.

2.3.6. Sample preparation

Samples for ESR spectroscopy were prepared as follows. The lipid and 1 mol% of the spin label were co-dissolved in CH_2Cl_2, and a thin film of the lipid was produced by evaporating the solvent with dry nitrogen gas. Final traces of solvent were removed by subjecting the sample to vacuum desiccation for at least 3 h. The sample was then hydrated with 100 µl of HBS buffer and vortexed. The lipid suspension thus obtained was transferred into a 100-µl glass capillary and pelleted in a tabletop centrifuge. Excess supernatant was removed and the capillary was flame-sealed. Samples containing protein-lipid complex were prepared in a similar manner except that the lipid film was hydrated directly with the protein solution in HBS and subjected to at least five freeze-thaw cycles before transferring to the glass capillaries. It was found that the samples containing protein could no longer be pelleted, and therefore the sample was used as such for ESR studies. In view of this limitation, the volume of protein solution added was minimized by using a high concentration protein solution (> 30 mg/ml), such that the amount of sample in the ESR cavity was maximized.

2.3.7. Electron spin resonance spectroscopy

ESR spectra were recorded on a Varian E-12 Century Line 9-GHz ESR spectrometer. Samples in 100-µl sealed glass capillaries were placed in a standard 4-mm quartz sample tube containing light silicone oil for thermal stability. The temperature of the sample was maintained constant by blowing thermostatted nitrogen gas through a quartz dewar. Spectra were recorded using the following instrumental settings: scan width, 100 G; scan time, 4 min; time constant, 0.25 s; modulation amplitude, 1.25 G; incident power, 10 mW. Values of the outer hyperfine splitting, $2A_{max}$, were determined by measuring the difference between the low-field maximum and the high-field minimum. The error in measuring the position of the maximum and minimum is ~ 0.1– 0.3 G depending on the degree of motional line broadening; therefore the

overall error in the estimation of $2A_{max}$ is ~ 0.2 – 0.6 G. Spectral subtractions were performed essentially as described by Marsh [1982], using a program written by Dr. Jörg H. Kleinschmidt. Reference spectra for the motionally restricted components were selected from a library of spectra of 14-PCSL bound to the proteolipid protein from bovine myelin, recorded at different temperatures. Reference spectra for the fluid components were taken either from spectra of the same spin-labelled lipid in the lipid mixture alone recorded at a slightly lower (by ca.2-4 degrees) temperature or from a library of spectra of 14-PCSL in lipid extracts from the (Na^+,K^+)-ATPase membranes of *Squalus acanthias* [Esmann et al., 1985]. Reference spectra for the fluid components obtained from DMPC membranes in the presence of PDC-109 were taken from a library of spectra of 14-PCSL in egg yolk PC, recorded at different temperatures. Subtraction end points were established by overlaying the difference spectrum with the matching fluid reference spectrum. To improve precision, the spectra were expanded vertically in the outer wings. Uncertainty in the determination of the end point is in the region of ±0.02– 0.05, and this corresponds also to the repeatability of determinations of the subtraction factor, *f*. This estimate does not include the systematic error associated with imperfections in the match with the reference spectra.

2.4. Results

2.4.1. Turbidimetric studies on the binding of PDC-109 to DMPC and DMPC/cholesterol membranes

Preliminary experiments on the binding of PDC-109 to multilamellar vesicles of DMPC indicated that binding results in a partial solubilization of the vesicles as could be observed by a decrease of the sample turbidity. Therefore, binding and

solubilization were monitored by measuring turbidity of the samples at a wavelength of 330 nm.

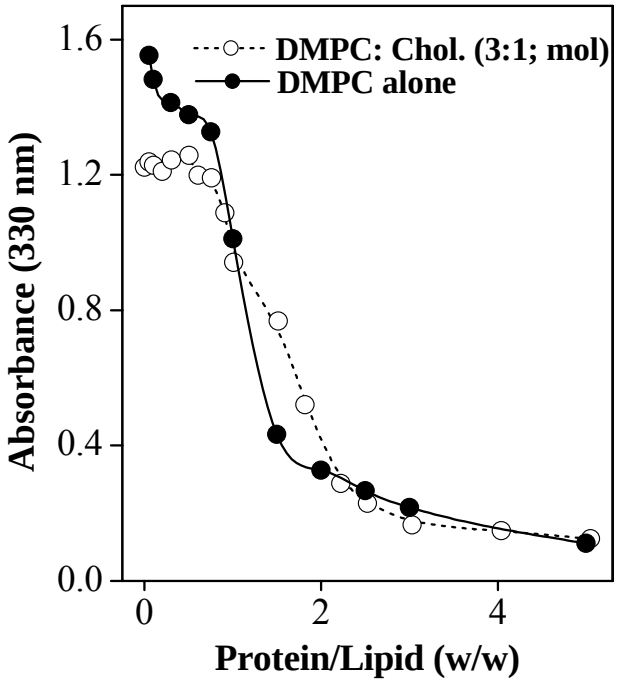

Fig. 2.3: Binding of PDC-109 to DMPC multilamellar vesicles and DMPC:cholesterol mixture, monitored by turbidimetry. The samples were prepared by directly hydrating 1.0 mg of the lipid, with an appropriate amount of the protein and making up the volume to 1.0 ml. The samples were then subjected to 10 freeze-thaw cycles, and the turbidity was measured spectrophotometically at 330 nm. Temperature = 30^{o}C.

Fig. 2.3 gives the results of binding experiments where the turbidity of MLVs of DMPC as well as DMPC:cholesterol (3:1; mol/mol) was monitored as a function of the protein/lipid (P/L) ratio. From this figure it is seen that the sample turbidity decreases very little at low P/L ratios (up to ~ 0.75 P/L weight ratio), both for DMPC as well as for DMPC: cholesterol (3:1; mol/mol). However, as the P/L ratio is increased further, the sample turbidity decreases steeply up to a P/L weight ratio of ~ 1.5 and then decreases more gradually as the P/L ratio is increased further. The results obtained were qualitatively very similar irrespective of whether the lipid film was directly hydrated with the protein solution or protein solution was added to the

prehydrated lipid dispersion. Very similar results were obtained with DMPC membranes containing 25 mol% cholesterol, except that the decrease in absorbance was less steep and achieved a limiting low value at rather higher protein content (~ 2:1 w/w) (see Fig. 2.3). In view of these observations, a 2:1 P/L weight ratio was chosen for the ESR spectral studies. Furthermore, to investigate the effect of protein binding on the lipid chain-melting phase transition, membranes made up of DMPC alone were used, as this lipid gives a well defined gel-fluid phase transition. The results of these experiments are described below.

2.4.2. Effect of binding of PDC-109 on phase transition and acyl chain dynamics of DMPC membranes

ESR spectra of phophatidylcholine spin-labeled at the C-5 position of the *sn*-2 chain (5-PCSL) in DMPC membranes, in the absence and in the presence of 2:1 (w/w) ratio of added PDC-109, are shown in Fig. 2.4A. The spectra recorded in the absence of protein (dashed lines) exhibit an abrupt change in the line shapes and outer hyperfine splittings ($2A_{max}$) at ~ 24°C, resulting from the increase in lipid chain mobility at the chain-melting phase transition. Those recorded in the presence of PDC-109 (solid lines) do not show any such abrupt changes; the changes observed in the ESR spectra of the PDC-109-bound sample with increasing temperature are more gradual. ESR spectra of 5-PCSL in DMPC membranes at 28°C show a progressive increase in outer hyperfine splitting with increasing PDC-109/DMPC ratios up to ~ 2:1 (w/w) and then remain essentially constant (data not shown). This behavior is consistent with the binding stoichiometry extrapolated from the steep change in turbidity that is shown in Fig. 2.3.

Temperature dependences of the outer hyperfine splitting, $2A_{max}$, for 5-PCSL in DMPC membranes, in the presence and in the absence of a 2:1 (w/w) ratio of PDC-

109, are given in Fig. 2.4B. It is clearly seen from this figure that the chain-melting phase transition, which is indicated for DMPC membranes alone by an abrupt decrease in the value of $2A_{max}$ at ~ 23°C, is strongly perturbed by the binding of PDC-109. At any given temperature, the outer hyperfine splitting is consistently higher in the presence than in the absence of PDC-109. This indicates that the protein interacts with DMPC membranes in both the gel and fluid phases.

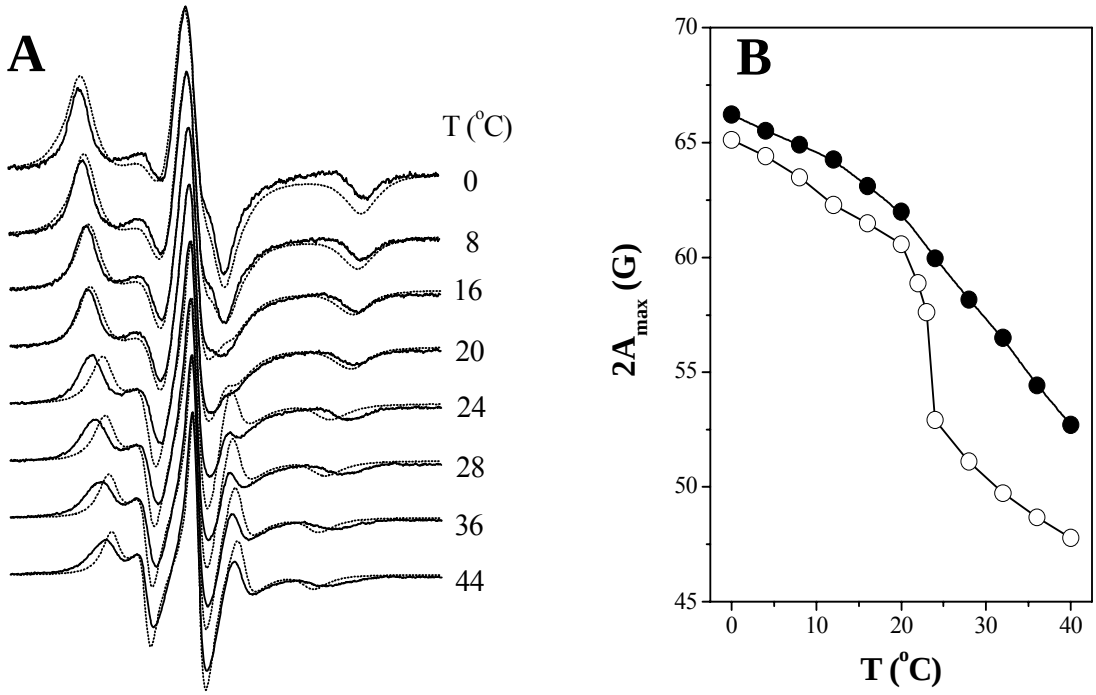

Fig. 2.4: (A) ESR spectra of the phosphatidylcholine spin label, 5-PCSL, bearing the nitroxide moiety at the C-5 position of the *sn*-2 acyl chain, in DMPC membranes in the presence (solid line) and absence of PDC-109 (dashed line) (lipid:protein, 1:2 w/w). **(B) Temperature dependence of the outer hyperfine splitting, $2A_{max}$**, for the 5-PCSL spin label in DMPC membranes (O) and in DMPC/PDC-109 recombinants (●).

2.4.3. Positional dependence of lipid chain perturbation by PDC-109

To investigate whether the binding of PDC-109 to DMPC membranes is accompanied by the interaction of the protein with the hydrophobic interior of the lipid membrane,

that is, to investigate whether the protein or a part of it inserts into the interior of the lipid bilayer, ESR studies were performed with spin-labeled phosphatidylcholines, *n*-PCSL, bearing the nitroxide spin label at different positions down the *sn*-2 acyl chain of the lipid. The ESR spectra of different positional isomers of phosphatidylcholine, in DMPC membranes and in samples containing 2:1 (w/w) ratio of added PDC-109, recorded at 0°C in the gel phase region of hydrated DMPC, are given in Fig. 2.5A. From these spectra it is evident that in the gel phase, protein binding decreases the mobility of the lipid chains of DMPC at all positions up to the 14th C-atom.

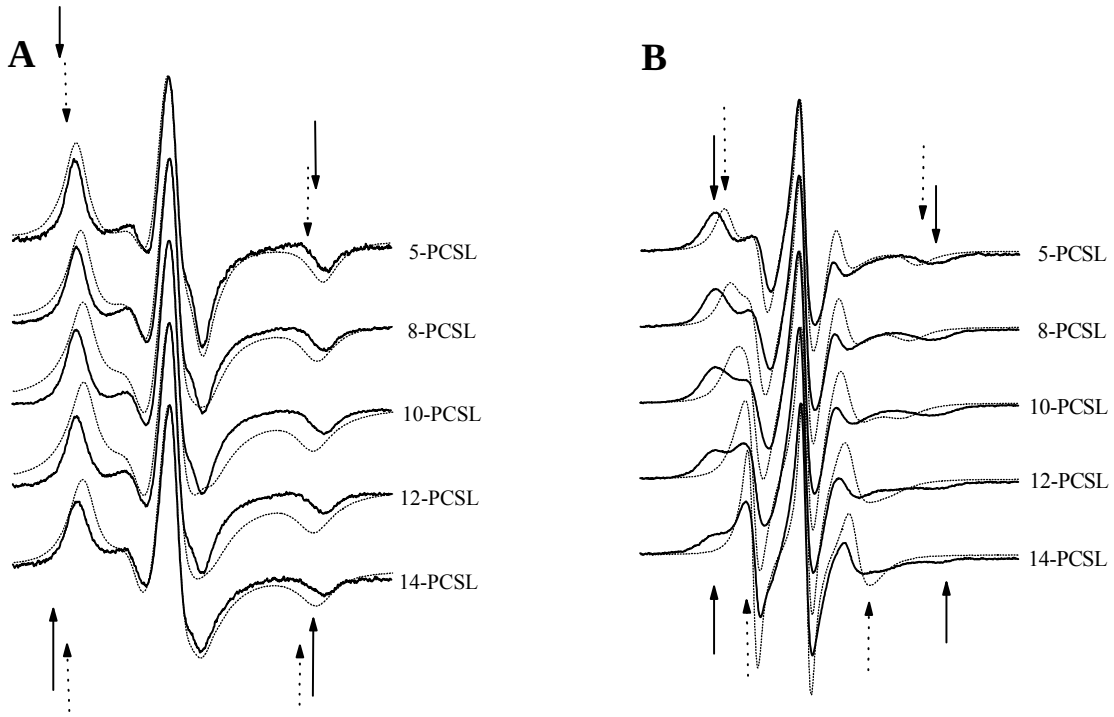

Fig. 2.5: ESR spectra of phosphatidylcholine spin labels, n-PCSL in DMPC membranes in the presence (solid lines) and absence (dotted lines) of PDC-109 (lipid:protein, 1:2 w/w). Arrows indicate the outer hyperfine splitting, $2A_{max}$. The spectral width is 100 G. (A) at 0^{o}C, gel phase and (B) at 28^{o}C, fluid phase.

ESR spectra of *n*-PCSL in dispersions of DMPC alone and in samples containing PDC-109, recorded at 28°C, corresponding to the liquid-crystalline phase

of the host lipid, are given in Fig. 2.5B. Whereas the ESR spectra of the spin-labels at positions close to the headgroup (n = 5 and 8) are broadened by protein binding, possibly indicating the presence of overlapping components, those that are closer to the methyl end of the chain (n = 12 and 14) clearly consist of two components. Notably, the spectrum of 14-PCSL closely resembles the spectra obtained with integral transmembrane proteins that have been reconstituted into lipid membranes [see, e.g., Marsh and Horváth, 1998]. One component in this spectrum is similar to the fluid lipid spectrum (shown by the dashed line). The second component (resolved in the outer wings of the spectrum) has a much larger outer hyperfine splitting, $2A_{max}$, and represents a lipid population whose acyl chains are in direct contact with the protein.

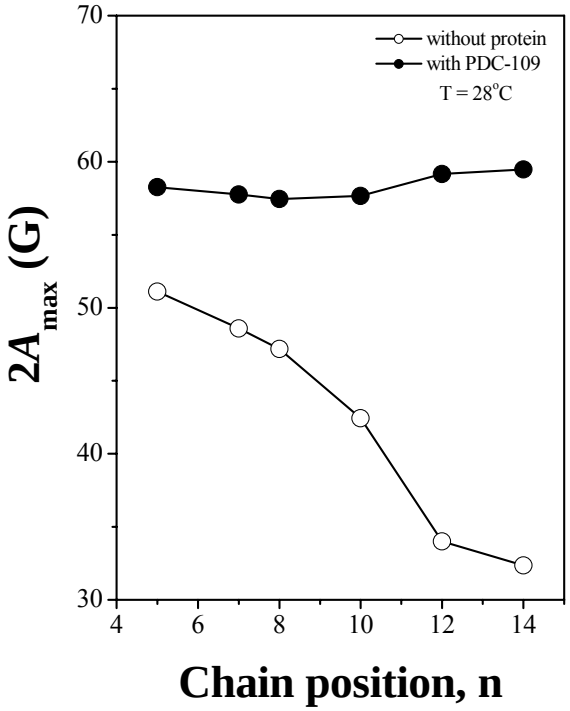

Fig. 2.6: Positional dependence of the outer hyperfine splitting, $2A_{max}$, for phosphatidylcholine spin labels, n-PCSL, in DMPC membranes (O) and in DMPC/PDC-109 (lipid:protein, 1:2 w/w) recombinants (●), at 28°C in the fluid phase. The data given for n = 12 and 14 in DMPC/PDC-109 recombinants correspond to the motionally restricted component of the two-component spectra.

A plot of the values of $2A_{max}$ as a function of chain labeling position, obtained for the phosphatidylcholine spin labels, *n*-PCSL, in membranes of DMPC alone and in DMPC/PDC-109 recombinants (corresponding to the motionally restricted component, where the lines could be resolved) at 28°C, is given in Fig. 2.6. Whereas the values of $2A_{max}$ obtained for the lipid membranes alone decrease as the spin-label position is moved down the *sn*-2 chain of the lipid, thus displaying the chain flexibility gradient characteristic of fluid lipid membranes, the values of $2A_{max}$ for the motionally restricted component remain approximately constant, and are consistently larger, throughout the chain. These observations further substantiate the interpretation given above that PDC-109 penetrates into the hydrophobic interior of the lipid membrane and interacts directly with the acyl chains.

2.4.4. Binding of PDC-109 to DMPC/cholesterol membranes

The results of turbidimetric studies presented in Section 2.4.1 clearly indicated that PDC-109 interacts both with DMPC membranes as well as DMPC/cholesterol mixtures. In order to further characterize the effect of cholesterol on the interaction of PDC-109 with PC membranes by ESR spectroscopy, the initial experiments were carried out with fluid DMPC membranes containing different amounts of cholesterol (0-20 wt%) and 1 mol% of spin-labelled PC, 14-PCSL. EPR spectra were obtained in the presence as well as in the absence of PDC-109 at a protein/lipid ratio of 2.5 (w/w). In each case the spectrum obtained in the presence of protein is made up of two components. These two components have been resolved by spectral subtraction. Spectra obtained in the presence of PDC-109 and the subtraction results are shown in Fig. 2.7. In each set of four spectra the top pair correspond to the composite spectrum obtained in the presence of PDC-109 at 30^{o}C (solid line) and a matching spectrum for the motionally restricted component alone (dotted line). The lower pair of spectra corresponds to the fluid component obtained by subtracting the rigid component

spectrum from the composite spectrum (solid line) and a matching fluid reference spectrum (dotted line). The fraction, *f*, of immobilized component obtained from spectral subtraction is also shown in the figure. The results indicate that presence of cholesterol has a significant effect on the size of the motionally restricted lipid component, the motionally restricted population being higher in the presence of cholesterol. This suggests that cholesterol potentiates the binding of PDC-109 to PC membranes. However, over the range of 5-20 wt% cholesterol, the motionally restricted fraction remains constant, or increases only slightly, within the range of error expected in the subtractions. Evidently, only relatively low concentrations of cholesterol are necessary to potentiate the binding of PDC-109.

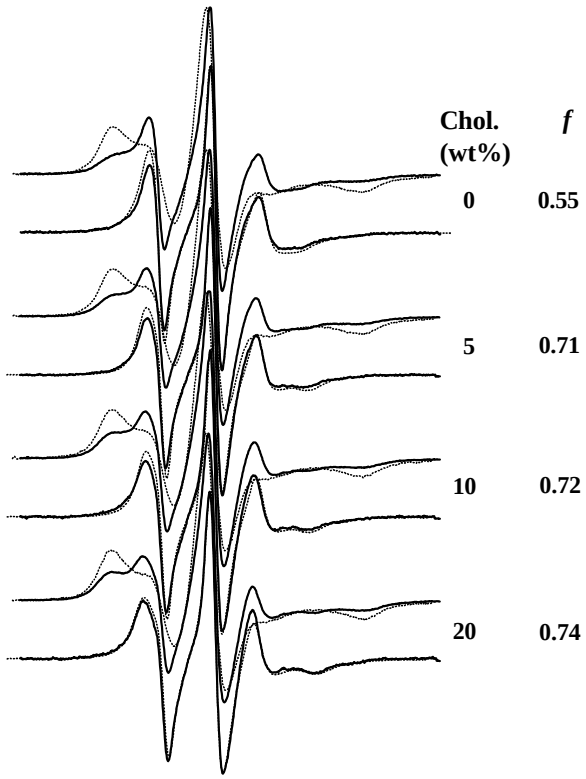

Fig. 2.7: Effect of cholesterol on the motionally restricted component of ESR spectra of 14-PCSL in membranes of DMPC and DMPC/cholesterol mixtures.

2.4.5. Lipid selectivity of PDC-109

The selectivity of PDC-109 for different lipids was investigated in DMPC membranes alone as well as in DMPC host matrix containing 20% (w/w) cholesterol. For this purpose, DMPC vesicles (or DMPC/cholesterol vesicles) containing 1 mol% of different phospholipids spin label species bearing the nitroxide moiety in the *sn*-2 acyl chain at the 14th C atom were prepared. In addition, samples were also prepared with probe amounts of two steroid-based spin labels, the cholestane spin label and the androstanol spin label. ESR spectra of the membrane samples in the presence and in the absence of the protein were recorded in the fluid-phase region of the lipid.

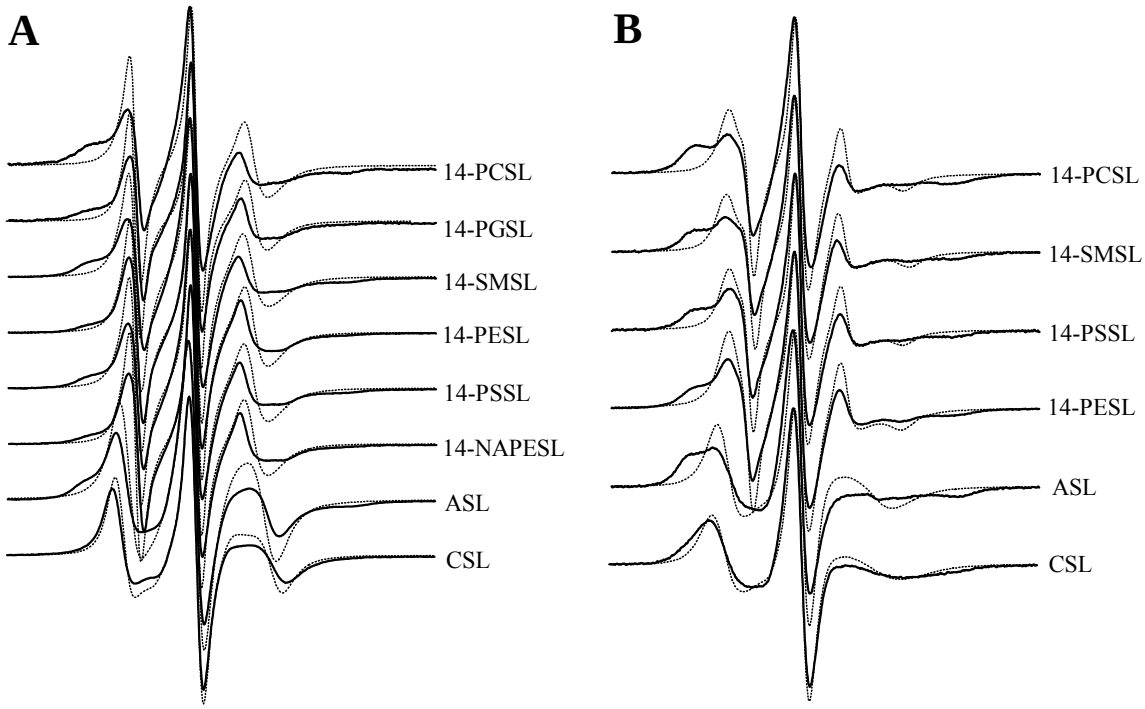

Fig. 2.8: ESR spectra of different phospholipids spin labels, 14-XXSL, as well as CSL and ASL, in the fluid phase of DMPC membranes (dotted line) and of DMPC/PDC-109 (lipid:protein, 1:2 w/w) recombinants (solid line). Phospholipid spin labels are: 14-PCSL (phosphatidylcholine), 14-PGSL (phosphatidylglycerol), 14-SMSL (sphingomyelin), 14-PESL (phosphatidylethanolamine), 14-PSSL (phosphatidylserine), and 14-NAPESL (N-acyl phosphatidyl-ethnolamine). (A) DMPC host matrix and (B) DMPC membranes containing 20 wt% cholesterol. Spectra were recorded at 28^{o}C. The spectral width is 100G.

A comparison of the spectra obtained in the presence of PDC- 109 and in its absence, recorded at 28°C, is given in Figs. 2.8A and 2.8B, respectively, for DMPC membranes and DMPC/cholesterol membranes. From this figure it is seen that, in both cases, as for 14-PCSL, all the spectra obtained in the presence of PDC-109 are composed of two components. There is a fluid-like component, which is similar to that of the spin label in lipid membranes alone, and another component that corresponds to a more motionally restricted spin-label population. The relative amounts of these two components differ between the different lipid species, reflecting the selectivity of interaction with the PDC-109 protein.

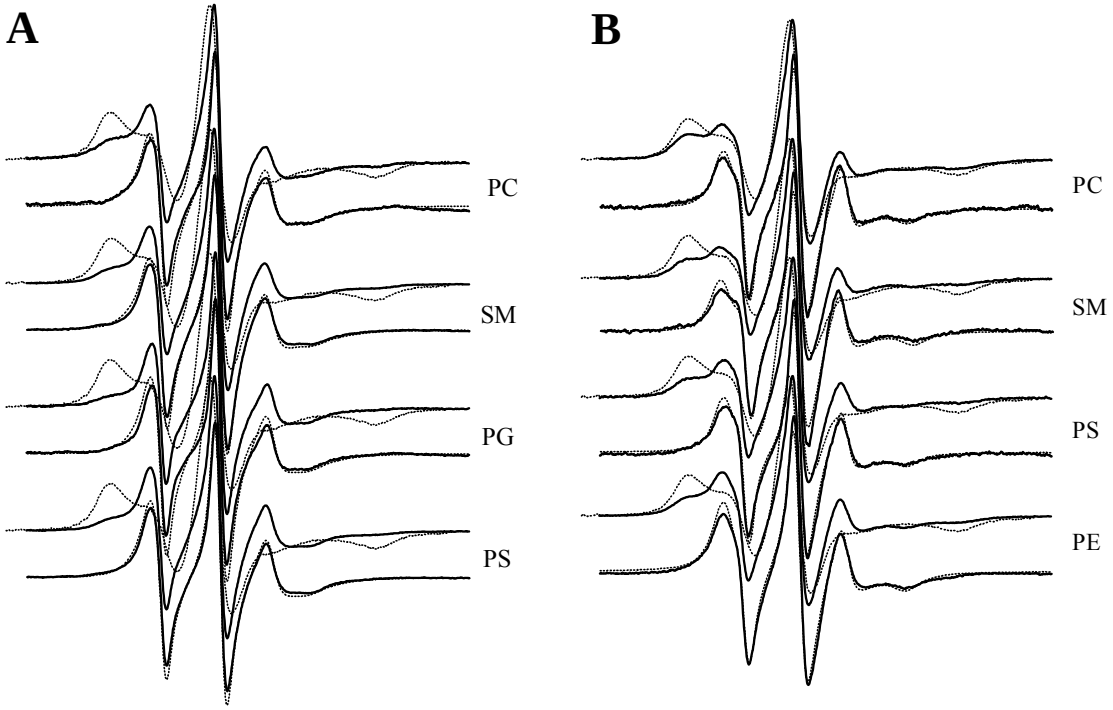

Fig. 2.9: Representative spectral subtractions for the 14th-position spin labels. Spectra of 14-XXSL in (A) DMPC/PDC-109 complexes (B) DMPC/cholesterol (80:20 w/w) host matrix in the presence of PDC-109 are shown. Spectra are all (including difference spectra) displayed normalized to the same maximum central line height.

The two components in the ESR spectra of different spin labels obtained in the presence of PDC-109 can be resolved by spectral subtraction and the contribution of

each component to the overall spectrum quantified. This is shown in Fig. 2.9A for several of the spin labels in a DMPC host matrix, in the presence of a 2:1 weight ratio of added PDC-109. The spin label in each set of spectra is indicated on the right. Similar spectral and subtraction data obtained with DMPC/cholesterol membranes are presented in Fig. 2.9B. In each set of four spectra the top pair corresponds to the composite spectrum from the lipid-protein complex (solid line) and an ESR spectrum matching the motionally restricted component alone (dotted line). The lower pair of spectra in each set of spectra corresponds to the fluid component obtained from subtraction (solid line) and a matching fluid spectrum (dotted line). The relative amounts of the motionally restricted components (fraction, *f*) for the different spin-labeled lipids in DMPC and DMPC/cholesterol host matrices in the presence of PDC-109 are given in Table 2.1. These values correspond to the fraction of the total double

Table 2.1: Fraction (*f*) of motionally restricted spin-labeled lipid and relative association constants, K_r, normalized to that for phosphatidylcholine (K_r^{PC}). The data were obtained from spectral subtractions with the ESR spectra of different spin labels in DMPC/PDC-109 complexes. The protein/lipid ratio for all the samples was 2 (w/w).

Spin label	Motionally restricted fraction (f)[a]		K_r/K_r^{PC}		$(N_t/N_b)/(n^o_t/N^o_b)$
	- Chol.	+ Chol.	- Chol.	- Chol.	
14-PASL (pH 8.5)	0.55	---	1.38	---	---
14-PCSL	0.47	0.74	1.00	1.00	0.64
14-SMSL	0.47	0.70	1.00	0.82	0.67
14-PASL (pH 6.0)	0.46	---	0.96	---	---
14-PSSL	0.35	0.64	0.61	0.63	0.63
14-PESL	0.23	0.58	034	0.49	0.59
ASL	0.35	0.59	0.61	0.51	0.67
CSL	---	0.42	---	0.25	---

[a]The *f* values are subject to an error of ~ ± 0.02 - 0.05 due to uncertainties in the spectral subtractions. For CSL, the motionally restricted spectral component was too small to quantify reliably.

integrated intensity that must be subtracted from the composite first derivative spectrum of the PDC-109/lipid complex to obtain the fluid-component end point. Note that the spectra in Fig. 2.9 are all normalized to the same maximum line height, and therefore the difference spectra do not reflect their true relative intensities.

2.5. Discussion

Considering the fact that PDC-109 induces efflux of choline phospholipids and cholesterol from spermatozoa by binding to them upon ejaculation, the molecular mechanism of this process is of great interest. Especially, because this lipid efflux from spermatozoa promotes capacitation, a clear understanding of the efflux of phosphatidylcholine and cholesterol mediated by PDC-109 could potentially lead to the development of new anti-fertility drugs. In view of this, in the present study we have characterized the interaction of PDC-109 with phosphatidylcholine and PC/cholesterol membranes by using turbidity measurements and spin-label ESR spectroscopy. Further, the lipid selectivity of this protein has been investigated in some detail by using spin-labeled analogs of different phospholipids and steroid derivatives.

2.5.1. Solubilization of DMPC membranes by PDC-109

As seen from Fig. 2.3, binding of PDC-109 to DMPC MLVs resulted in a decrease in the sample turbidity, indicating that the size of the lipid assemblies is decreased upon protein binding. Gel filtration on Sepharose CL6B gave an apparent mass of ~ 1.3×10^6 Da for the particles obtained upon binding of PDC-109 to DMPC MLVs. Recent experiments by Manjunath and co-workers [Thérien et al., 1997, 1998] indicate that PDC-109 and other BSP proteins promote sperm capacitation by removal of cholesterol and choline phospholipids from sperm plasma membrane. The lipid efflux

particles resulting from binding of PDC-109 to human fibroblasts (a cell model used to study the lipid efflux) were shown to be made up of BSP proteins, cholesterol, and choline-containing phospholipids, with a size of ~ 80 nm [Moreau & Manjunath, 1999]. Our observations indicate that most probably the binding of PDC-109 to DMPC MLVs also leads to the formation of such particles. Efflux of choline phospholipids and cholesterol would then be linked to the ability of BSP proteins to partially solubilize PC-containing lipid membranes.

The results presented in Fig. 2.3 show that, in addition to MLVs of DMPC alone, DMPC MLVs containing 25 mol % cholesterol are also solubilized by PDC-109 at high P/L ratios. The threshold required for complete solubilization, however, is higher. Calvete and co-workers [Gasset et al., 2000] have shown that the leakage of internal contents from DOPC unilamellar vesicles that is induced by PDC-109 becomes considerably reduced in the presence of cholesterol. Whereas there are certain parallels between these two sets of results, they refer to very different types of experiments. The work here concerns the fragmentation of very large MLVs into smaller particles. That of Gasset et al. [2000] involves the permeability/leakage of small, 90 nm diameter, unilamellar vesicles.

2.5.2. Stoichiometry of PDC-109/DMPC interaction

Fig. 2.3 represents the titration of DMPC dispersions with PDC-109. Because DMPC was hydrated with the protein containing solution, all lipid is available for interaction with PDC-109. Extrapolating the steeply changing part of the turbidity to the quasi-saturation level yields a protein/lipid stoichiometry of ~ 1.7 w/w, i.e., a mole ratio of ~ 11 DMPCs per PDC-109. For comparison, fluorescence titration of PDC-109 with small unilamellar DMPC vesicles yielded a stoichiometry of ~ 12 DMPC molecules per PDC-109 molecule [Gasset et al., 2000]. A corresponding fluorescence titration

with PC, also in 2:1 mixtures with phosphatidylethanolamine or phosphatidylserine, yielded a stoichiometry of ~ 10 PCs/PDC-109 [Müller et al., 1998]. Note that in both these latter cases, the PDC-109/PC ratios used in the titration were beyond that at which a drastic decrease of particle size is indicated in Fig. 2.3. The ESR spectra of PC with a short (five C atoms) *sn*-2 chain bearing the nitroxide on the 4th C-atom were found to contain a motionally restricted component with a stoichiometry of ~ 11 PCs/PDC-109 [Müller et al., 1998]. Evidently, in this study, the spin labels of all the PCs with short *sn*-2 chain with which PDC-109 interacts contact the protein more or less directly.

Simple volumetric estimates show that a compact globular protein of molecular weight 13 kDa and partial specific volume ~ 0.7 cm^3/g has a cross-sectional area in the range of ~ 6–7.5 nm^2. A protein of this size would therefore interact with ~ 10–12 DMPC molecules (cross-sectional area ~ 0.6 nm^2) at the membrane surface. These estimates therefore suggest that the PDC-109/PC binding stoichiometries found experimentally correspond approximately to complete coverage of the membrane surface by the protein.

2.5.3. Membrane penetration by PDC-109

The spectra given in Figs. 2.5A and 2.5B show that binding of PDC-109 to DMPC membranes affects the mobility of the acyl chains up to the 14th C-atom in the gel phase as well as in the fluid phase, although the changes observed in the fluid phase are certainly more marked. In particular, the spectra of the spin labels bearing the nitroxide moiety at positions close to the chain methyl terminus (12-PCSL and 14-PCSL) show two components in the fluid phase, indicating a direct interaction between the protein and the spin-labeled chain segment. Also, the outer peaks in the spectra of 5-PCSL at 36°C and 44°C in Fig. 2.4A are asymmetric. This suggests that

the spectra are two-component even up to this position of chain labeling. The spectral resolution is not so good for 5-PCSL, however, because of the larger outer hyperfine splitting of the fluid component, relative to that for 12-PCSL or 14-PCSL. All these results indicate that the protein, or a part of it, inserts into the membrane interior upon binding and comes into direct contact with the lipid chains. The reduction in cooperativity of the lipid packing that is associated with abolition of the chain-melting phase transition (see Fig. 2.4B) is also consistent with this conclusion.

The extent of motional restriction of the lipid chains by PDC-109 is also a significant indicator of the nature of the protein-lipid interaction. The value of the outer hyperfine splitting for 14-PCSL at 28°C is relatively large: $2A_{max}$ = 59.5 G (see Fig. 2.6). This can be compared with corresponding values obtained previously for 14-position labels interacting with membrane-penetrant sections of different peripheral and integral proteins [Marsh & Horváth, 1998]. The value of $2A_{max}$ for PDC-109 is considerably greater than those for the peripheral membrane proteins apocytochrome *c* ($2A_{max}$ = 49.5 G) and myelin basic protein ($2A_{max}$ = 53.0 G). It is closer to those for the integral proteins, myelin proteolipid protein ($2A_{max}$ = 62.8 G) and cytochrome *c* oxidase [$2A_{max}$ = 60.9 G; Knowles et al., 1979]. A rather intimate association of the lipid chains with PDC-109 is therefore implied. This is rather unusual for a soluble protein that recognizes the lipid headgroup in a specific manner [cf. Swamy & Marsh, 1997], and PDC-109 could be unique in this respect. Because PDC-109 undergoes a conformational change upon binding to DMPC membranes [Gasset et al., 1997], it appears likely that the initial step in the membrane binding by PDC-109 is the recognition of the phosphorylcholine headgroup of choline phospholipids by the protein, resulting in a conformational change, ultimately leading to the penetration of the protein segments into the hydrophobic interior of the

membrane. The biexponential kinetics of the binding reaction as observed by Müller et al. [1998] is consistent with this model.

At saturation binding of PDC-109 (i.e., 2:1 w/w), approximately half of the spin-labeled phosphatidylcholines are motionally restricted directly by PDC-109 (see Table 2.1). This corresponds to a rather low lipid/protein stoichiometry of ~ 5–6 mol/mol. Evidently, only part of the PDC-109 protein penetrates the membrane. Approximately 26 lipids could be accommodated around the perimeter of the protein in a compact globular form, if it is transmembrane [see Marsh, 1997], but half this number if it penetrates the membrane only partially. Additionally, it is possible that the protein is partially aggregated at saturation binding, which would further reduce the intramembrane perimeter accessible to lipid. The stoichiometry of ~ 11 motionally restricted lipids found by Müller et al. [1998] at high lipid/protein ratio that was mentioned already is possibly relevant in this connection.

2.5.4. Relation to protein structure

In this section we attempt to identify those parts of the protein sequence that are most likely to penetrate the membrane. This is done by standard hydropathy analysis, but using two separate scales corresponding to the interfacial region and hydrophobic core of the membrane, respectively [see White & Wimley, 1999].

Fig. 2.10 gives the free energy, averaged over a sliding window of seven residues, for transfer of PDC-109 to the interfacial region of the membrane (solid line). Individual residue transfer free energies are those determined by White and Wimley [1999]. Regions of this length whose transfer is energetically favorable are indicated by the horizontal solid lines in Fig. 2.10. These regions are contained within the two FnII domains and constitute a considerable part of the protein. The corresponding hydropathy profile for transfer from the interfacial region of the

membrane to the hydrophobic core is indicated by the dashed lines. Even for relatively short seven-residue regions, a substantially smaller portion of the protein is predicted to penetrate the hydrophobic regions of the membrane than partitions to the membrane interface. This is in agreement with the relatively low stoichiometry of motionally restricted lipids that is detected by spin-label ESR.

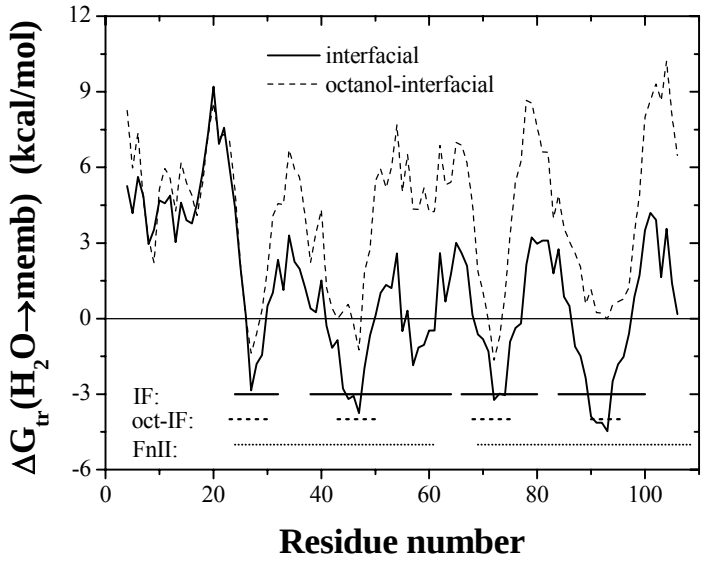

Fig. 2.10: Hydropathy profile for PDC-109 [Bräuer & Scheit, 1991], calculated with the interfacial (——) and octanol minus interfacial (— — —) hydrophobicity scales of White and Wimley [1999]. Plotted is the free energy of transfer from water to the membrane interface (——) and from the interface to the hydrophobic core of the membrane (— — —), by using a seven-residue window. Solid and dashed horizontal lines represent energetically favorable regions for transfer to the membrane interface (IF) and to the hydrophobic core (oct-IF), respectively. Dotted horizontal lines designate the two FnII domains.

When the size of the window is increased to nine residues or more, no sections of the protein with this length are predicted to have transfer free energies that favor a location in the hydrophobic core of the membrane. A similar situation was found for the myelin basic protein [Sankaram et al., 1989]. No very extended hydrophobic stretches are present in the sequence of this latter protein, although a motionally restricted lipid population was detected on binding to negatively charged lipids. As might be expected from the above, no transmembrane sections are predicted for PDC-

109 with a window length of 19 residues. However, energetically favorable transfer is still predicted to the membrane interface: for the sections of the protein consisting of residues 43–76 and 82–100. This relatively strong propensity of the protein to partition to the membrane interface will certainly potentiate penetration of the hydrophobic core by shorter sections of the protein within these regions (see Fig. 2.10). Of course, Fn2 domains could not be situated in the interfacial region of the membrane in their entirety if PDC-109 maintains its solution conformation on binding to lipid. However, solution NMR studies of the second Fn2 domain of PDC-109 and the homologous first Fn2 domain of fibronectin [Constantine et al., 1992; Pickford et al., 1997] have shown that five of the highly conserved clusters of aromatic amino acid residues in these domains form a solvent-exposed hydrophobic surface. It is therefore likely that this surface, which constitutes the binding site for collagen, is also that which binds to lipid membranes. Penetration of these hydrophobic side chains into the membrane may also, at least in part, be responsible for the direct immobilization of the lipid chains that we observe by ESR spectroscopy.

To summarize, candidate regions of the sequence for which penetration of the hydrophobic core of the membrane is energetically favorable are restricted to the Fn2 domains, because the N-terminal region outside these domains bears the acidic residues. Candidate penetrant sequences are short, seven residues or less, and are indicated by the horizontal dashed bars in Fig. 2.10. The net transfer free energies are favorable but relatively small and therefore are probably insufficient to ensure tight binding of the protein. The latter is presumably determined by interfacial interactions and the specific interaction with the headgroups of choline-containing phospholipids. The situation is somewhat analogous to that of the myelin basic protein [Sankaram et al., 1989] and apocytochrome *c* [Görrissen et al., 1986; Marsh, 2001]. Both these

proteins partially penetrate negatively charged lipid membranes but are displaced from the membrane at high ionic strength.

2.5.5. Lipid selectivity

A clear pattern of selectivity in the interaction of PDC-109 with different lipid species is evident from Table 2.1. The lipid affinity can be expressed thermodynamically in terms of the association constants, K_r, for interaction of the different spin-labeled lipids with PDC-109, relative to the background DMPC host lipid. The experimentally determined fractions, f, of motionally restricted lipid depend directly on these relative association constants. Normalized relative to the value, K_r^{PC}, for spin-labeled phosphatidylcholine, the relative association constants are given by [Marsh, 1985]:

$$K_r/K_r^{PC} = (1/f_{PC} - 1)/(1/f - 1) \qquad (1)$$

where f_{PC} (= 0.47) is the fraction of the motionally restricted 14-PCSL. The values of K_r/K_r^{PC}, evaluated using eq. 1 are also listed in Table 2.1. Equation 1 is derived from the equation for equilibrium lipid-protein association, taking into account the fact that the lipid/protein ratio is the same for all samples. Based on the data given in Fig. 2.8A and Table 2.1, the lipid selectivity of PDC-109 is in the following order: phosphatidylcholine ≈ sphingomyelin ≥ phosphatidic acid (pH 6.0) > phosphatidyl-glycerol ≈ phosphatidylserine ≈ androstanol > phosphatidylethanolamine ≥ N-acyl phosphatidylethanolamine >> cholestane. Though the highest selectivity is seen for phosphatidic acid dianion, the physiologically irrelevant pH of 8.5 where it is seen coupled with the fact that phosphatidic acid is normally present only at very low concentrations in normal membranes makes this observation less important. The selectivity observed for the phosphocholine-containing lipids, phosphatidylcholine and sphingomyelin, is the highest among other lipids for their interaction with PDC-109. This is a highly unusual situation compared with spin-label results obtained on

the selectivity of lipid interactions with integral membrane proteins [Marsh & Horváth, 1998]. In the latter case, although the selectivity of interaction is not solely electrostatic in origin, the highest selectivities are obtained for anionic lipids. Neither phosphatidylcholine nor sphingomyelin display a preferential interaction with any of the integral proteins studied. Also, peripheral membrane proteins do not interact preferentially with phosphatidylcholine [Sankaram & Marsh, 1993]. A similar trend is observed with the lipid selectivity order for PDC-109 interacting with different lipid spin labels in a DMPC host matrix with 20 wt% cholesterol (Fig. 2.8B & Table 2.1).

The selectivity pattern that emerges from Table 2.1 is consistent with the findings of Desnoyers and Manjunath [1992], who investigated the selectivity with a more limited range of lipid species. Their studies involved the binding to lipids coated on plastic plates, as opposed to the lipid probes in bilayer membranes used in the present study. Also, the selectivity for phosphatidylcholine over phosphatidylserine and phosphatidylethanolamine found here is consistent with the attenuation of binding to PC vesicles containing admixtures of these latter two lipids that was observed by Müller et al. [1998]. The results obtained with the steroid probes, ASL and CSL, deserve comment in view of the involvement of BSP proteins in cholesterol efflux [Thérien et al., 1998, 1999]. We find that PDC-109 exhibits considerable selectivity for the ASL. This is a sterol analog that contains the 17β-OH group attached to the steroid nucleus. On the other hand, the CSL in which the 3β-OH group of the cholesterol structure is replaced by the nitroxide doxyl moiety is very poorly recognized by the protein. This suggests that the hydroxyl group of cholesterol is important for the recognition by the protein, whereas the alkyl tail at the 17-position is not particularly relevant for this interaction. In this connection, it should be noted that spin-labeled androstanol displays an affinity for the nicotinic acetylcholine receptor like that of cholesterol [Ellena et al., 1983] and interacts with the polyene

antibiotic amphotericin in a manner similar to that of cholesterol [Aracava et al., 1981].

2.5.6. Effect of cholesterol on lipid stoichiometry

The data presented in Table 2.1 show that, with the exception of PE, the absolute values of selectivity of PDC-109 towards different spin labeled lipid probes, relative to PC, i.e. K_r/K_r^{PC}, are comparable for PDC-109 bound to DMPC membranes with and without cholesterol. Thus, if it is assumed that the relative association constant, K_r, in the presence of cholesterol is equal to that in its absence, K^o_r, and further that $K^o_r = 1$ for spin-labelled PC, then:

$$(n_t/N_b)/(n^o_t/N^o_b) = f_o^{PC} + (1 - f_o^{PC})\,(1/f - 1)/(1/f_o - 1) \qquad (2)$$

where n_t is the ratio of lipid to bound protein, N_b is the number of lipid association sites on the protein, f_o and f_o^{PC} are the fractions of a given spin-labelled lipid and PC, respectively, that are motionally restricted in the absence of cholesterol. The left-hand side of eq.2 is the ratio of the lipid-binding stoichiometry to the intramembrane lipid/protein interaction stoichiometry, i.e. the value of n_t/N_b, relative to that in the absence of cholesterol. For spin-labelled PC, Eq.3 reduces to:

$$(n_t/N_b)/(n^o_t/N^o_b) = f_o^{PC}/f^{PC} \qquad (3)$$

If the unlabelled host lipid is PC, then eq.3 is the most direct means of determining the effect of cholesterol on the lipid/protein stoichiometries.

Values of $(n_t/N_b)/(n^o_t/N^o_b)$ calculated from eq.2 given in the Table 2.1. With the exception of PE, the values are comparable for the different spin labels, consistent with the assumption that cholesterol does not have a large effect on lipid selectivity for PDC-109. As mentioned above, the value of $(n_t/N_b)/(n^o_t/N^o_b)$ for PC then most directly reflects cholesterol-induced changes in the lipid-binding stoichiometry. In principle, the decrease in the ratio n_t/N_b with cholesterol could be caused either by an increase in the number of lipid association sites, N_b, on PDC-109, or by an increase in

binding stoichiometry, $1/n_t$, of PDC-109 to the membranes, in either case by approximately 50%. Most likely cholesterol potentiates the interaction between PC membranes and PDC-109 predominantly by the former mechanism, because fluorescence titrations have indicated no changes in binding stoichiometry at saturation by cholesterol addition [Gasset et al., 2000].

In summary, the ESR results presented in this chapter demonstrate that PDC-109 binds to phospholipid membranes by specific interaction with choline phospholipids. The binding results in an immobilization of the lipid acyl chains and also solubilizes multilamellar liposomes made up of PC and of PC/cholesterol, suggesting that PC probably mediates the interaction between PDC-109 and cholesterol. Although PDC-109 exhibits the highest selectivity for the choline phospholipids (PC and SM), it also shows considerable selectivity for other phospholipids such as phosphatidylglycerol and phosphatidylserine. The distinctly higher selectivity observed for the ASL as opposed to the CSL shows that the hydroxyl group of the sterol plays a crucial role in the interaction of the steroid with PDC-109 and hence could be important in the process of cholesterol efflux. The specific recognition of PC and SM by PDC-109 is a significant result because the zwitterionic lipids PC, phosphatidylethanolamine, and SM have long been considered to play a passive structural role in biological membranes. The present results demonstrate that the phosphorylcholine moiety of PC (or the sphingolipid analog SM) can be specifically recognized by proteins, and such recognition can mediate biologically important processes such as cholesterol efflux from the sperm cell membranes. Further, it has shown that the presence of cholesterol potentiates the association of PDC-109 with lipids. It would be interesting to see whether there are other choline-binding proteins in nature that recognize PC/SM in their interaction with biological membranes.

Chapter 3

Surface Plasmon Resonance Studies on the Mechanism of Membrane Binding by PDC-109

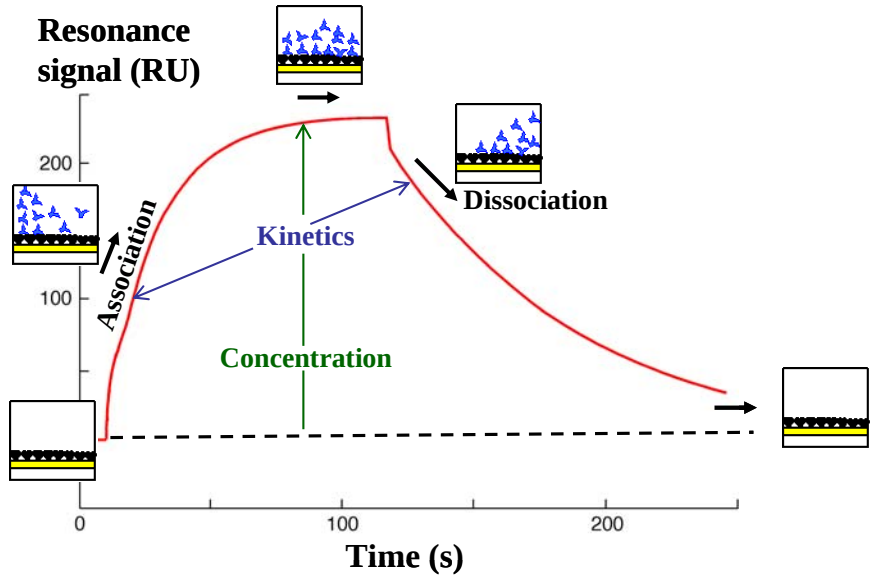

*Thomas, C.J., **Anbazhagan, V.,** Ramakrishnan, M., Sultan, N., Surolia, I. and Swamy, M.J.* (2003) *Mechanism of membrane binding by the bovine seminal plasma protein, PDC-109 : A surface plasmon resonance study. **Biophys. J.** 84: 3037-3044.*

3.1. Summary

Binding of PDC-109 to sperm plasma membranes is mediated primarily by its specific interaction of PDC-109 with choline-containing phospholipids. In the present study the kinetics and mechanism of the interaction of PDC-109 with phospholipid membranes were investigated by the surface plasmon resonance technique. Binding of PDC-109 to different phospholipid membranes containing 20% cholesterol (wt/wt) indicated that binding occurs by a single step mechanism. The association rate constant (k_1) for the binding of PDC-109 to DMPC membranes containing cholesterol was estimated to be 5.7×10^5 M^{-1} s^{-1} at 20°C, while the values of k_1 estimated at the same temperature for the binding to membranes of negatively charged phospholipids such as dimyristoylphosphatidylglycerol (DMPG) and dimyristoylphosphatidic acid (DMPA) containing 20% cholesterol (wt/wt) were at least three orders of magnitude lower. The dissociation rate constant (k_{-1}) for the DMPC/PDC-109 system was found to be 2.7×10^{-2} s^{-1} whereas the k_{-1} values obtained with DMPG and DMPA was about three to four times higher. From the kinetic data, the association constant for the binding of PDC-109 to DMPC was estimated as 2.1×10^7 M^{-1}. Binding of PDC-109 to dimyristoylphosphatidylethanolamine (DMPE), which is also zwitterionic, was found to be very weak, clearly indicating that the charge on the lipid headgroup is not the determining factor for the binding. The association constants for different phospholipids investigated decrease in the order: DMPC > DMPG > DMPA > DMPE. Thus the higher affinity of PDC-109 for choline phospholipids is reflected in a faster association rate constant and a slower dissociation rate constant for DMPC as compared to the other phospholipids. Analysis of the activation parameters indicates that the interaction of PDC-109 with DMPC membranes is favored by a strong entropic contribution, whereas negative entropic contribution is primarily responsible for the rather weak interaction of this protein with DMPA and DMPG.

3.2. Introduction

The interaction of BSP proteins with spermatozoa is mediated by their interaction with specific phospholipids, particularly with phosphatidylcholine (PC), which is zwitterionic [Desnoyers & Manjunath, 1992]. The interaction of PDC-109 with spermatozoa results in the efflux of PC and cholesterol (referred to as *cholesterol efflux*), which appears to be an important step in the capacitation process, a necessary event before fertilization can occur [Thérien et al., 1998; Moreau & Manjunath, 1999]. Each Fn2 domain of PDC-109 contains a choline-phospholipid binding site and both the binding sites are necessary to induce lipid efflux [Desnoyers & Manjunath, 1993; Moreau et al., 1998]. Therefore, it is important to understand the interaction of PDC-109 with sperm cell membranes, to understand the molecular events involved in the capacitation process. Most importantly, such an understanding potentially can lead to the development of novel antifertility drugs. Studies on the interaction of PDC-109 with lipid membranes can serve as useful models for its interaction with biological membranes. In the studies reported in Chapter 2, the interaction of PDC-109 with DMPC membranes was investigated by spin-label electron spin resonance (ESR) spectroscopy and the specificity of this protein for spin-labeled phospholipid and sterol probes was characterized in detail [Ramakrishnan et al., 2001; Swamy et al., 2002].

In this Chapter, the kinetics of interaction of PDC-109 with different phospholipid membranes containing cholesterol was investigated by the surface plasmon resonance (SPR) technique. The results indicate that binding of PDC-109 takes place by a single-step mechanism and that the higher affinity of this protein for PC as compared to phospholipids bearing other headgroups, such as phosphatidyl-glycerol (PG), phosphatidic acid (PA), and phosphatidylethanolamine (PE) is due to a

faster association rate constant and a slower dissociation rate constant. Analysis of the activation parameters shows that binding of this protein to PC/cholesterol membranes is favored by a positive entropic contribution.

3.3. Experimental Section

3.3.1. Materials

Phosphorylcholine chloride (Ca^{2+} salt), choline chloride and tris(hydroxymethyl) aminomethane (Tris) base were purchased from Sigma (St. Louis, MO, USA). Sephadex G-50 (superfine) and DEAE Sephadex A-25 were obtained from Pharmacia Biotech (Uppsala, Sweden). Phospholipids DMPC, DMPG, DMPE, dipalmitoylphosphatidylethanolamine (DPPE), DMPA and cholesterol were obtained from Avanti Polar Lipids (Alabaster, AL, USA). PDC-109 was purified from the seminal plasma of healthy and reproductively active bulls as reported in Chapter 2.

3.3.2. Preparation of lipid samples

Lipid samples for SPR experiments were prepared as follows. The phospholipid and cholesterol were first weighed to give the desired weight ratio and then dissolved in chloroform:methanol (3:1; v/v). The solvent was removed by a gentle stream of nitrogen gas. The lipid film thus formed was kept under high vacuum for 1 h and then hydrated with TBS-I (50mM Tris buffer, 0.15 M NaCl, 5 mM EDTA, pH 7.4). The lipid suspension was sonicated for 10 minutes using a probe sonicator, freeze-thawed thrice, using liquid nitrogen and sonicated again for 10 min to get unilamellar liposomes. The resulting sample was passed through a 0.22 mM syringe filter to remove any suspended particles. Phospholipid and cholesterol in the mixtures were estimated by determining the lipid-bound phosphate [Rouser et al., 1970] and cholesterol [Higgins, 1987].

3.3.3. Surface plasmon resonance experiments

Surface plasmon resonance experiments were performed using a BIAcore 2000 (Amersham Pharmacia Biotech) biosensor system. Experiments were performed at 6, 12, and 20°C. Binding of PDC-109 to lipid membranes was investigated as follows. A four-channel alkanethiol HPA chip was first cleaned by passing a 10 mM solution of n-octyl glucoside at a flow rate of 1 μl/min. The lipid sample, prepared as described above, was then loaded onto the chip and after the chip was saturated with the lipid, it was washed for 30 min with TBS-I, followed by a pulse of 10 mM NaOH to remove the multilamellar structures, yielding a single surface hybrid bilayer of lipid [Thomas et al., 1999]. The hybrid bilayer consists of alkanethiol monolayer attached to the chip on which the externally added lipid forms an additional monolayer. Different concentrations of PDC-109 were passed over this lipid surface and the resulting sensograms were recorded. From the sensograms binding parameters were calculated as described below.

3.3.4. SPR data analysis

Association (k_1) and dissociation (k_{-1}) rate constants were obtained by nonlinear fitting of the primary sensogram data using the BIA evaluation 3.0 software. The dissociation rate constant is derived using eq. (1):

$$R_t = R_{t0} e^{-k_{-1}(t-t0)}, \qquad (1)$$

where R_t is the response at time t, R_{t0} is the amplitude of the response at the time of addition of buffer (to dissociate bound PDC-109), and k_{-1} is the dissociation rate constant. The association rate constant k_1 can be derived from the measured k_{-1} values using eq. (2):

$$R_t = R_{Max}[1 - e^{-(k_1 C + k_{-1})(t - t0)}], \qquad (2)$$

where R_{Max} is the maximum response, C is the concentration of PDC-109 in the solution. The equilibrium constant (K_a) and the dissociation constant (K_d) were

obtained using the expressions $K_a = k_1/k_{-1}$ and $K_d = k_{-1}/k_1$. All sensograms were first corrected for bulk drift and analyzed for mass transport-influenced kinetics. All temperature dependent experiments were performed after both the flow cells and the samples were incubated at the desired temperature for 30 min. The ligand-binding parameters, namely concentration and response units (RU), obtained from the sensogram data, were analyzed according to the Scatchard method (Rao et al., 1999). Values of RU/[ligand] were plotted against RU, and K_a values were obtained from the slopes of the linear fits (slope = $-K_a$).

3.4. Results

To investigate the binding of PDC-109 to phosphatidylcholine membranes, the initial SPR experiments were carried out with monolayers of pure DMPC using the BIAcore biosensor system and the results obtained are shown in Fig. 3.1. The initial part of the data (up to ~ 15 or 20 s on the *x*-axis) corresponds to the passage of buffer over the sensor chip (baseline), after which the protein solution is passed over the chip. The rise in the signal with the progression of time reflects binding of protein to the hybrid lipid bilayer. When equilibrium is established, the response reaches a constant value and remains so until the protein solution that is being passed over the sensor chip is replaced with buffer. The decrease in response when buffer is passed over the sensor chip corresponds to the dissociation process. However, all the sensograms shown in Fig. 3.1 corresponding to different concentrations of the protein show an initial increase of the response, which reaches a high value (corresponding to maximum binding), but then decreases slowly (approximately between 75 and 175 s; the faster decrease after 175 s corresponds to a switch to the buffer). This indicates a loss of mass from the sensor chip surface and most likely suggests a loss of the lipid from the

surface of the chip. Gasset et al. [2000] have reported that binding of PDC- 109 to phosphatidylcholine vesicles leads to a disruption of the vesicle integrity, resulting in a leakage of the contents. However, they also observed that incorporation of cholesterol in DOPC vesicles stabilized the vesicle structure in a dose-dependent manner and reduced contents leakage. In view of these observations, we tested DMPC membranes containing varying amounts of cholesterol and noted that above 15–18% (wt/wt) cholesterol the hybrid bilayers remain stable, i.e., they do not suffer a loss in RU (mass) due to loss of phospholipid from the bilayers. Hence in all subsequent experiments membranes containing 20% (wt/wt) cholesterol were used. This would be equivalent to ~28–32% (mol/mol) of cholesterol for the different phospholipids investigated here.

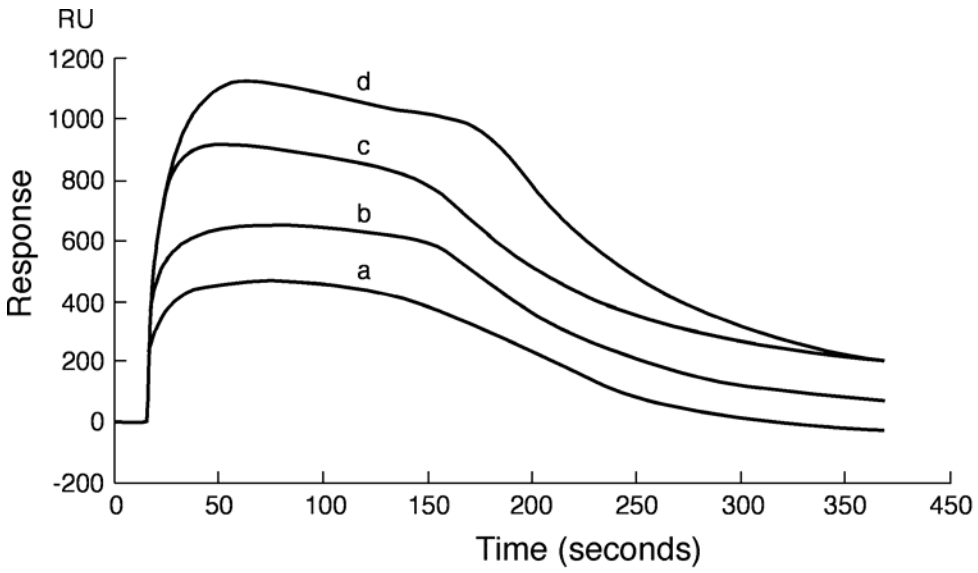

Fig. 3.1: Sensogram depicting the binding of PDC-109 to pure DMPC monolayer at 20°C. PDC-109 in varying concentrations was passed over a monolayer of DMPC: (a) 0.75 mM, (b) 1.0 mM, (c) 1.5 mM, and (d) 3.0 mM. The sensograms obtained show the distinct removal of the lipid from the monolayer, attesting to the fact that PDC-109 disrupts the membrane structure.

Representative sensograms recorded at 20°C, depicting the interaction of different concentrations of PDC-109 with hybrid bilayers made up of DMPC

containing 20% (wt/wt) cholesterol, immobilized on a sensor chip, are shown in Fig. 3.2A and a Scatchard analysis of the SPR data is shown in Fig. 3.2B. Unlike the profiles shown in Fig. 3.1, the SPR curves shown here do not indicate any slow decrease in response during the passage of the PDC-109 solution after equilibrium is attained. This clearly shows that mixing cholesterol with DMPC stabilizes the hybrid bilayer, and that there is no loss of lipid from the surface of the sensor chip.

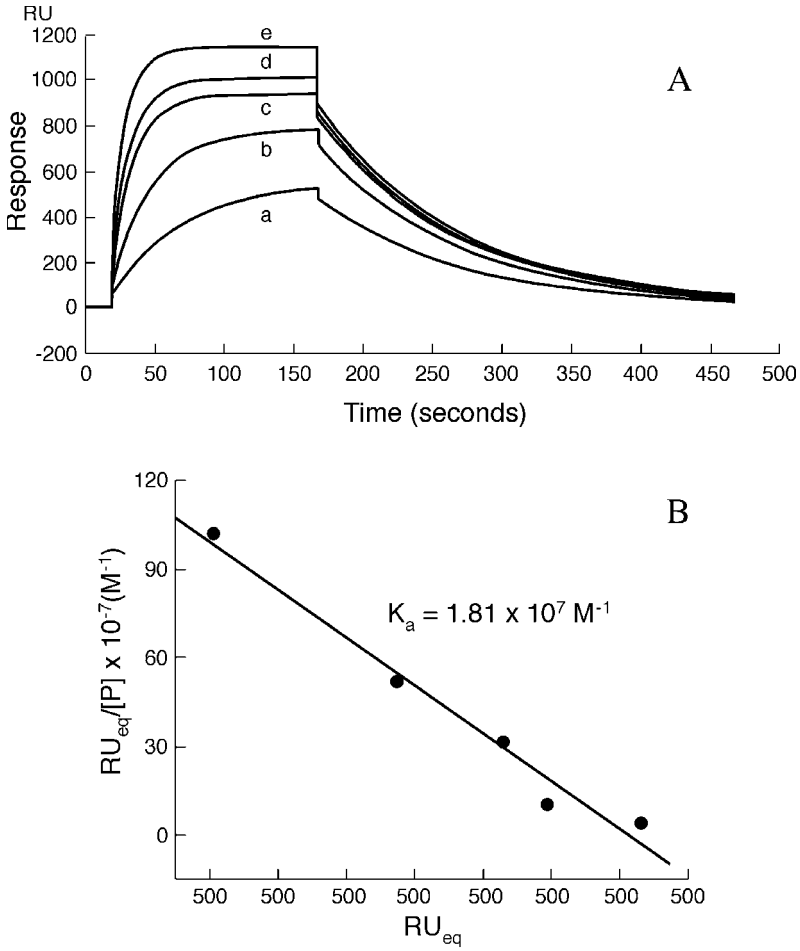

Fig. 3.2: (A) Sensograms depicting the concentration-dependent binding of PDC-109 to DMPC monolayers containing 20 (wt%) cholesterol at 20°C. PDC-109 in varying concentrations was passed over lipid monolayer of DMPC containing 20% wt/wt cholesterol at a flow rate of 10 ml/min: (a) 0.05 mM, (b) 0.15 mM, (c) 0.3 mM, (d) 1.0 mM, and (e) 3.0 mM. The sensogram was fitted using the linear least-squares method to obtain the association and dissociation rate constants. **(B) Scatchard plot depicting the analysis of the sensogram data.** From the slope the association constant was determined (slope = $-K_a$).

The SPR curves shown in Fig. 3.2A, fitted by mass transport limited analysis at 20°C, yielded the k_1 and k_{-1} values as 5.7×10^5 $M^{-1}s^{-1}$ and 2.7×10^{-2} s^{-1}, respectively. The residuals were found to be distributed equally for the association and dissociation parts, supporting the monoexponential nature of the interaction (data not shown). From the ratio k_1/k_{-1}, the equilibrium association constant, K_a, has been estimated to be 2.1×10^7 M^{-1}. Similar analysis was done at 6°C and 12°C also and the values of k_1, k_{-1}, and K_a obtained from this analysis are listed in Table 3.1. The values remain unchanged with increasing salt concentration up to 1 M (data not shown). Scatchard analysis of the data shown in Fig. 3.2A yielded a K_a value of 1.81×10^7 M^{-1} (Fig. 3.2B), which is in good agreement with the K_a value of 2.1×10^7 M^{-1} obtained from the k_1/k_{-1} ratio.

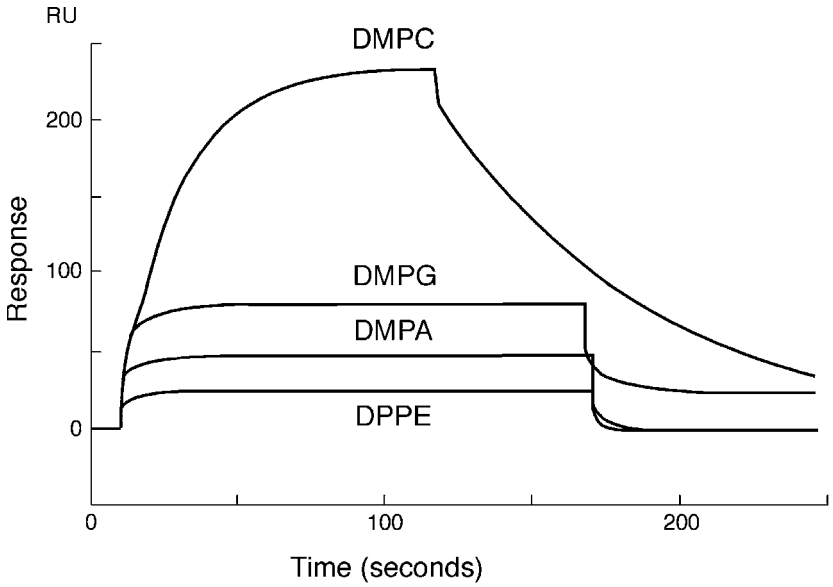

Fig. 3.3: Sensogram depicting the binding of PDC-109 to different lipid monolayers. PDC-109 was passed over different lipid monolayers (DMPC, DMPG, DMPA, and DPPE), containing 20% (wt/wt) cholesterol at 20°C. The concentrations of PDC-109 used were 0.05 μM, 20 μM, 100 μM, and 150 μM, respectively, for DMPC, DMPG, DMPA, and DPPE.

To determine the specificity and strength of binding of PDC-109 toward different phospholipids, SPR experiments were carried out with phospholipids bearing

different headgroup structures such as DMPC, DMPG, DMPA, and DPPE, containing 20% (wt/wt) cholesterol. Sensograms depicting the binding of PDC-109 to monolayers of these lipids, recorded at 20°C, are shown in Fig. 3.3. It is clear from this figure that while binding of PDC-109 to DMPC leads to a large response, thereby indicating good binding of the protein to DMPC membranes, its binding to DMPG and DMPA membranes, even at significantly higher concentrations, is associated with considerably smaller changes in the instrument response, suggesting much weaker binding of these two lipids. Binding to DMPE and DPPE yielded very low response and the data were not sufficiently reliable for determining the association and dissociation rate constants from the response curves.

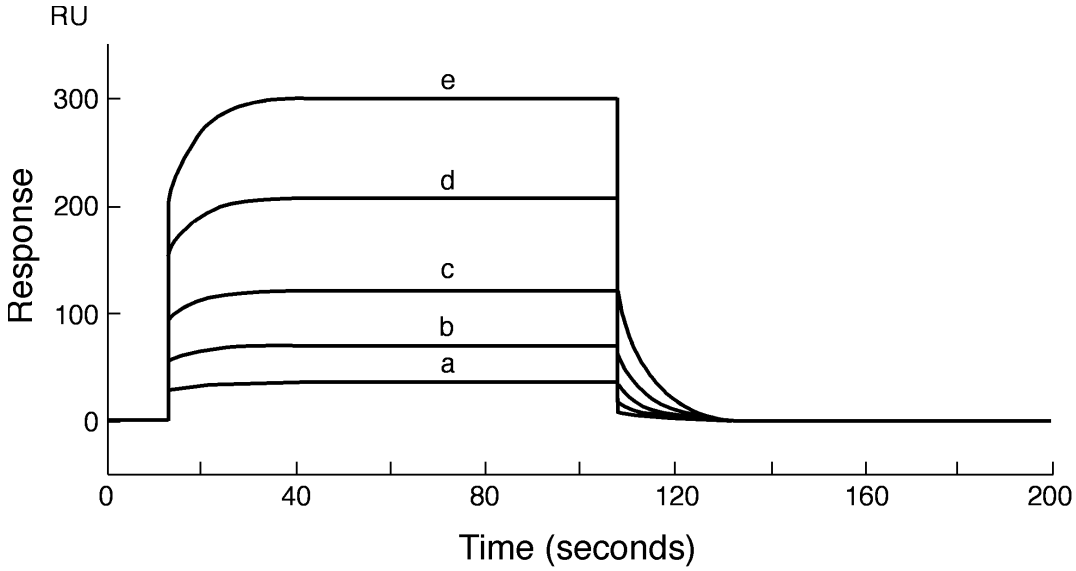

Fig. 3.4: Sensogram depicting the binding of PDC-109 to DMPG monolayer at 20°C. PDC-109 in varying concentrations was passed over a lipid monolayer of DMPG containing 20% wt/wt cholesterol at a flow rate of 10 ml/min: (a) 10 μM, (b) 20 μM, (c) 40 μM, (d) 80 μM, and (e) 150 μM. The sensogram was fitted using the linear least-squares method to obtain the association and dissociation constants.

Sensograms obtained at 20°C for the binding of different concentrations of PDC-109 with DMPG monolayers containing 20% (wt/wt) cholesterol are given in Fig. 3.4. The sensogram data were analyzed as described above for the interaction of

PDC-109 with DMPC/cholesterol monolayers. From the analysis, the association (k_1) and dissociation (k_{-1}) rate constants were obtained as 1.2×10^2 $M^{-1}s^{-1}$ and 0.11 s^{-1}, respectively. Association and dissociation rate constants were also obtained at 6°C and 12°C. The corresponding values of k_1, k_{-1}, and the equilibrium association constant, K_a, obtained from their ratio, are listed in Table 3.1. Similar measurements were also performed with DMPA and the kinetic rate constants and K_a value obtained are also listed in Table 3.1.

Table 3.1: Kinetic parameters and association constants obtained from the surface plasmon resonance experiments for the binding of PDC-109 to different phospholipid monolayers.

Lipid layer	T (°C)	k_1 ($M^{-1}s^{-1}$)	k_{-1} (s^{-1})	K_a (M^{-1})
DMPC	6	$1.9 (\pm 0.21) \times 10^5$	$1.1 (\pm 0.12) \times 10^2$	$1.73 (\pm 0.18) \times 10^7$
	12	$3.9 (\pm 0.42) \times 10^5$	$1.9 (\pm 0.19) \times 10^2$	$2.05 (\pm 0.21) \times 10^7$
	20	$5.7 (\pm 0.46) \times 10^5$	$2.7 (\pm 0.21) \times 10^2$	$2.11 (\pm 0.19) \times 10^7$
DMPA	6	$0.9 (\pm 0.11) \times 10^2$	$4.6 (\pm 0.63) \times 10^2$	$1.96 (\pm 0.16) \times 10^3$
	12	$1.1 (\pm 0.10) \times 10^2$	$8.1 (\pm 0.63) \times 10^2$	$1.36 (\pm 0.14) \times 10^3$
	20	$1.2 (\pm 0.15) \times 10^2$	$11.0 (\pm 0.93) \times 10^2$	$1.09 (\pm 0.12) \times 10^3$
DMPG	6	$3.6 (\pm 0.28) \times 10^2$	$4.2 (\pm 0.33) \times 10^2$	$8.57 (\pm 0.69) \times 10^3$
	12	$4.2 (\pm 0.39) \times 10^2$	$6.3 (\pm 0.51) \times 10^2$	$6.67 (\pm 0.63) \times 10^3$
	20	$5.3 (\pm 0.42) \times 10^2$	$9.0 (\pm 0.64) \times 10^2$	$5.89 (\pm 0.43) \times 10^3$

Number of experiments, $n = 4$.

Plots of $\ln(k/T)$ versus $(1/T)$ yielded straight lines for both the association and dissociation rate constants (Fig. 3.5). From the slopes of these plots, the activation enthalpies for the interaction of PDC-109 with different phospholipid/cholesterol membranes were obtained. Activation entropies and free energies were then calculated by the use of the following equations:

$$\Delta H^{\ddagger} = E_A - RT \qquad (3)$$

$$\ln(k/T) = -\Delta H^{\ddagger}/RT + \Delta S^{\ddagger}/R + \ln(k'/h) \quad (4)$$

$$\Delta G^{\ddagger} = \Delta H^{\ddagger} - T\Delta S^{\ddagger} \quad (5)$$

where k is the appropriate rate constant, k' is the Boltzmann constant, and h is Planck's constant. Activation parameters thus obtained, and the thermodynamic parameters, ΔH^{o}, ΔS^{o}, and ΔG^{o}, calculated from them, are listed in Table 3.2.

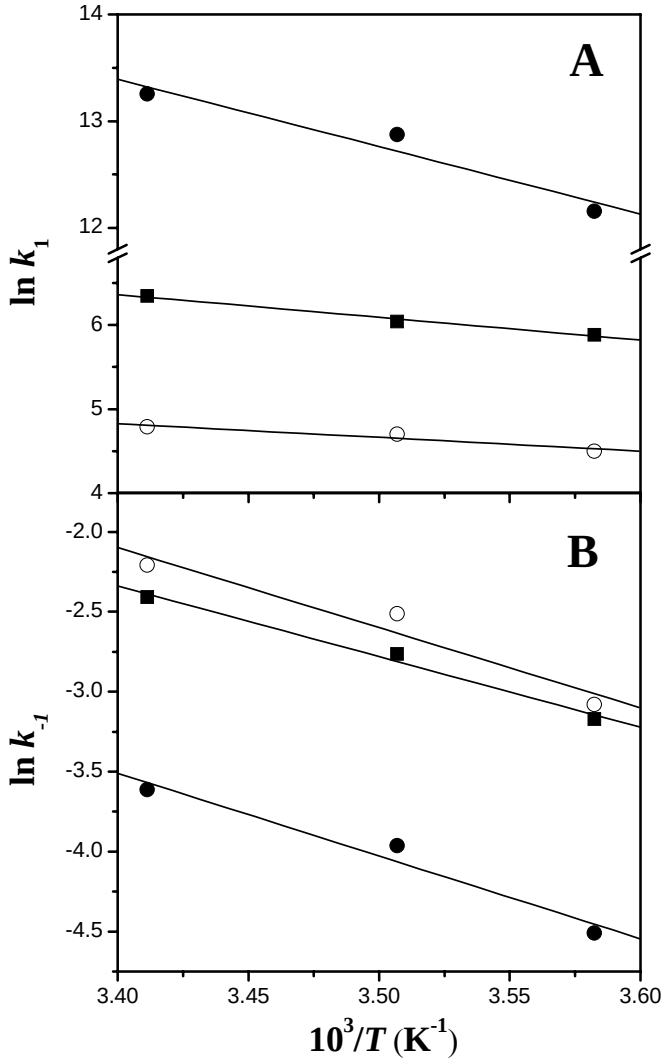

Fig. 3.5: Plots of ln (k/T) versus ($1/T$) for the association (A) and dissociation (B) rate constants. The data from SPR experiments carried out at different temperatures with (●) DMPC, (■) DMPG, and (○) DMPA containing 20% (wt/wt) cholesterol are shown.

Table 3.2: Activation parameters and thermodynamic parameters obtained for the interaction of PDC-109 with phospholipid/cholesterol membranes.

Lipid	Parameter								
	$\Delta H_a^{\ddagger}$	$\Delta H_d^{\ddagger}$	ΔH^o	$\Delta S_a^{\ddagger}$	$\Delta S_d^{\ddagger}$	ΔS^o	$\Delta G_a^{\ddagger}$	$\Delta G_d^{\ddagger}$	ΔG^o
DMPC	50.11	43.03	7.08	36.36	-128.00	164.36	39.45	80.6	-41.10
DMPA	11.32	41.64	-30.32	-166.28	-121.06	-45.22	60.07	77.1	-17.06
DMPG	16.48	36.74	-20.26	-136.39	-139.46	3.07	56.46	77.6	-21.26

Units are: $\Delta H_a^{\ddagger}$, $\Delta H_d^{\ddagger}$, ΔH^o, $\Delta G_a^{\ddagger}$, $\Delta G_d^{\ddagger}$ and ΔG^o: kJ.mol^{-1}; $\Delta S_a^{\ddagger}$, $\Delta S_d^{\ddagger}$, and ΔS^o: J.mol^{-1}.K^{-1}. The standard deviation of the parameters reported lie within 9% for ΔH and ΔG values (kJ.mol^{-1}) whereas for ΔS values (J.mol^{-1}K^{-1}) they are within 12% of the reported values (n=4).

3.5. Discussion

In view of the role of PDC-109 in the efflux of choline phospholipids and cholesterol, it is of particular interest to investigate its interaction with phospholipid membranes, especially those made up of PC and its mixtures with cholesterol. Though lipid selectivity of this protein has been characterized in considerable detail [Desnoyers & Manjunath, 1992; Ramakrishnan et al., 2001], the kinetics of its interaction with lipid membranes has not been investigated in detail so far. To investigate the kinetics and mechanism of interaction of PDC-109 with phospholipid membranes, SPR experiments were carried out in the present study. SPR is a very sensitive method for the analysis of macromolecule-ligand interactions and can provide information on association and dissociation rate constants as well as association constants from a single experimental run [Johnsson et al., 1991; Chaiken et al., 1992; O'Shannesy et al., 1993]. One of the main advantages of this method is that the mass change, taking place during the reaction is the only parameter monitored, obviating the need for

employing external labels such as chromophores, which can sometimes alter the reaction process [Schuck, 1997]. Also, the ability to form membrane assemblies allows the study, under physiological conditions, of cell membrane/surface-associated phenomena.

The loss of mass observed when PDC-109 was allowed to bind to DMPC monolayers (Fig. 3.1) is consistent with the fact that binding of this protein to PC vesicles results in a disruption of the vesicle integrity and contents leakage [Gasset et al., 2000]. However, addition of cholesterol (at 20% weight ratio) stabilizes the DMPC monolayers (Fig. 3.2), which is again consistent with the results of Gasset et al. [2000], who reported that cholesterol prevented disruption of DOPC membranes and contents leakage in a dose-dependent manner.

The association rate constant of 5.7×10^5 M^{-1} s^{-1} obtained for the binding of PDC-109 to DMPC/cholesterol monolayers at 20°C is approximately three to four orders of magnitude slower than the rate constants obtained for diffusion-controlled reactions. The dissociation of PDC-109 is also a single exponential process, and the dissociation rate constant of 2.7×10^{-2} s^{-1} clearly indicates that, upon binding, the protein is held quite strongly by the DMPC-cholesterol membranes.

The data presented in Fig. 3.3 clearly demonstrate that PDC-109 exhibits the highest binding affinity to PC membranes among the different phospholipids investigated in the present study. This is consistent with the results of the X-ray structure of PDC-109-phosphorylcholine complex, which clearly show that phosphorylcholine binds to each Fn2 domain of the protein via a cation-π interaction between the choline moiety and the indole side chain of a tryptophan residue and H-bond interactions of the phosphate group of the ligand with hydroxyls of exposed tyrosine residues [Wah et al., 2002]. However, because another zwitterionic lipid, PE,

is very poorly recognized, it is clear that, besides the charge state of the lipid molecules, steric complementarity is also an important factor governing the binding of PDC-109 to the membranes. This is supported by the observations that PDC-109 could be purified by affinity chromatography at high ionic strength on *p*-aminophenyl phosphorylcholine coupled to Sepharose, or quaternary methylamine coupled to silica or diethylaminoethyl group coupled to Sephadex and eluted by the specific ligand, phosphorylcholine [Desnoyers & Manjunath, 1993].

A comparison of the association and dissociation rate constants for the interaction of PDC-109 with membranes made up of different phospholipids shows that the strength of interaction is determined primarily by the association rate constant (see Table 3.1). Thus for the binding of PDC-109 to DMPC, DMPA, and DMPG, the k_1 values vary by ~3500 times whereas the variation in the values of k_{-1} is only ~3.5 fold. This results in a difference in the affinity by more than 10^4 times. The binding constants (K_a) are determined by the ratio of k_1 and k_{-1}. The value of K_a can, therefore, increase with either an enhancement in the values of k_1 or a diminution of k_{-1}. In general, for most biologic recognition processes including enzyme-substrate, lectin-sugar interactions, etc., it is usually the reduction in the dissociation rate constants which determines the affinities of cogners [Clegg et al., 1977]. In the case of PDC-109-phospholipid interaction, it is the enhanced k_1 that dictates the resultant affinities of binding. Hence, one of the striking findings of the present study is the observation that dramatic enhancements in the association rate constants with the change in the phospholipid headgroup underlie the specificities of these recognitions. These observations suggest that binding of PDC-109 to PC membranes require very few changes in the conformation of the protein, whereas binding to membranes made up of other phospholipids such as phosphatidylglycerol or phosphatidic acid probably need considerable changes in the conformation of the protein. This is also in agreement

with the crystal structure of PDC-109-phosphorylcholine complex, where the ligand binds quite snugly in the binding pocket on each Fn2 domain of PDC-109 [Wah et al., 2002].

In the studies reported in Chapter 2, ESR studies illustrate that besides spin labeled PC and sphingomyelin, the protein exhibits considerable selectivity for the spin-labeled analog of cholesterol, the cholestane spin-label, CSL, and that the presence of cholesterol in DMPC host matrix leads to an increase in the selectivity of PDC-109 for different spin-labeled phospholipids and sterol probes [Ramakrishnan et al., 2001; Swamy et al., 2002]. The data presented in Fig. 3.3 clearly show that despite the presence of 20 wt% cholesterol, the binding of PDC-109 to membranes bearing different phospholipids is considerably weaker than to those made up of PC. This is contrary to what one would expect if PDC-109 in its native conformation could recognize cholesterol at the membrane interface. One possible explanation for this is that in mixed lipid membranes containing phospholipids and cholesterol, the latter is sterically hindered by the phospholipid headgroups, and therefore is not accessible to PDC-109 present in the aqueous medium. Therefore, it may be expected that only upon binding to the membrane via the headgroup of choline-containing phospholipids would the PDC-109 protein be able to interact with cholesterol, as observed in the ESR experiments presented in Chapter 2 [see also Ramakrishnan et al., 2001; Swamy et al., 2002]. Independent ESR studies by Müller et al., [2002] also suggest that cholesterol does not interact directly with PDC-109, but is immobilized when PDC-109 binds to membranes containing both PC and cholesterol.

A comparison of the activation parameters given in Table 3.2 reveals the underlying thermodynamic factors that favor the strong binding of PDC-109 to DMPC as compared to DMPA and DMPG, which are recognized by this protein with considerably weaker affinity. From this Table it is seen that the binding of PDC-109

to DMPA and DMPG is accompanied by smaller activation enthalpies of association than for its binding to DMPC membranes. However, the positive activation entropy for the association with DMPC is contrasted by relatively large negative values of activation entropy for the binding to DMPA and DMPG membranes. These data thus indicate that the interactions of PDC-109 with different phospholipids are discriminated by disparate changes in activation entropies-being favorable for PC and sterically unfavorable for other phospholipids that do not possess the choline moiety in the headgroup structure. As a result, the free energy of activation for DMPC is considerably lower than the corresponding values for DMPA and DMPG. The enthalpies and entropies of activation for the dissociation process for all the three lipids are approximately in the same range, and therefore the relative affinities are primarily governed by the differences in the activation parameters, especially $\Delta S_a^{\ddagger}$. The positive entropic contribution associated with the binding of PDC-109 to PC membranes may arise from the disaggregation of the protein, which exists in an aggregated form in the native state, upon binding to the phosphocholine moiety, resulting in an increase in the entropy [see Gasset et al., 1997].

It is interesting to note that only a single exponential binding process could be detected by the SPR studies reported here, whereas in preliminary stopped-flow investigations monitoring changes in the protein fluorescence, Müller et al. [1998] observed that the binding of PDC-109 to DMPC unilamellar vesicles takes place by a biexponential process. FTIR experiments of Gasset et al. [2000] also suggest that PDC-109 undergoes a conformational change upon binding to PC membranes. However, since SPR detects only mass changes as a function of time, it may not be possible to detect subtle conformational changes that do not lead to any changes in the mass. Alternatively, it is also possible that a single step is observed in the present study because the acyl chain dynamics of the lipid molecules in the hybrid bilayer

used in the SPR experiments could be considerably different from those in the liposomes used by Müller et al. [1998]. As a result of such differences, the partial insertion of PDC- 109 into hydrophobic interior of the lipid membrane, which is observed in the earlier studies carried out with liposomes [Müller et al., 1998; Ramakrishnan et al., 2001], may not occur with the planar hybrid bilayers used in the SPR studies.

C-reactive protein, an acute phase protein found in most vertebrates, is another choline phospholipid binding protein that is well characterized. Binding of choline phospholipids to C-reactive protein occurs in a calcium-dependent manner [Volanakis & Wirtz, 1979; Sui et al., 1999] whereas their binding to PDC-109 is due to the specific interaction of the choline headgroup with the protein and does not require Ca^{2+} or other factors. Therefore, PDC-109 appears to be quite unique in its ability to recognize choline phospholipids without the need for any other factors.

In summary, in the studies reported in this chapter, the binding of PDC-109 to different phospholipid membranes has been investigated by the surface plasmon resonance technique. Binding of the protein to phosphatidylcholine membranes takes place with highest association rate constant and its dissociation is the slowest among the various phospholipids investigated. Binding of PDC-109 appears to be governed primarily by steric complementarity of the protein-binding site to the choline headgroup. Charge state of the lipid per se is not a significant factor in the recognition process as phosphatidylethanolamine is very poorly recognized by PDC-109.

Chapter 4

Thermodynamics of Phosphorylcholine and Lysophosphatidylcholine Binding to PDC-109

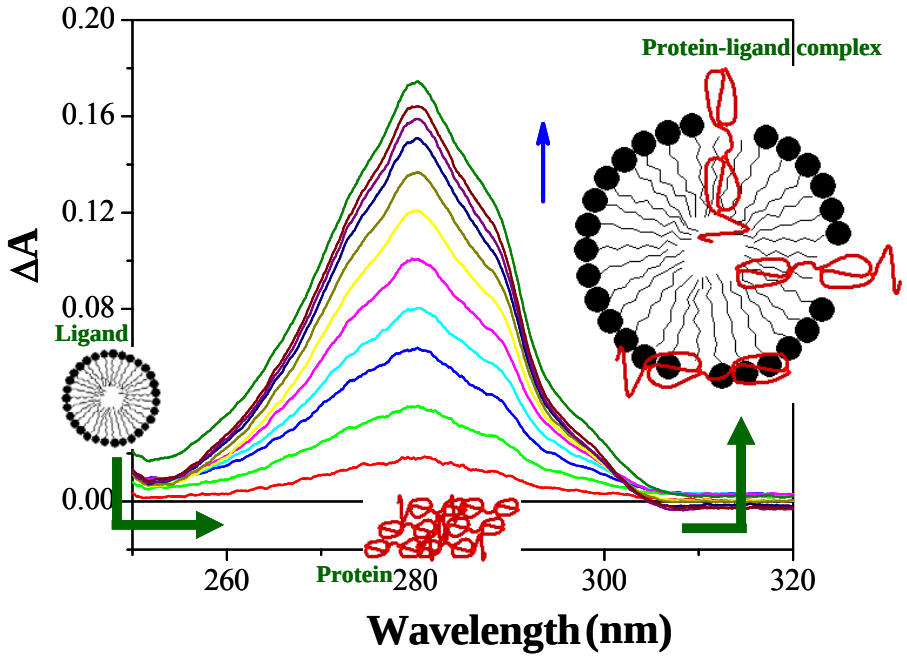

Anbazhagan, V. *and Swamy, M.J.* (2005) *Thermodynamics of phosphorylcholine and lysophosphatidylcholine binding to major protein of bovine seminal plasma, PDC-109.* ***FEBS Lett.*** *579: 2933-2938.*

4.1. Summary

PDC-109 binds to sperm plasma membranes by specific interaction with choline phospholipids and induces cholesterol efflux, a necessary event before capacitation – and subsequent fertilization – can occur. The binding of PrC and Lyso-PC with PDC-109 was investigated by monitoring the ligand-induced changes in the absorption spectrum of PDC-109. At 20°C, the association constants (K_a), for PrC and Lyso-PC were obtained as 81.4 M^{-1} and 2.02×10^4 M^{-1}, respectively, indicating that the binding of Lyso-PC to PDC-109 is 250 fold stronger than that of PrC. These studies show that while the choline moiety of phosphatidylcholine is specifically recognized by PDC-109, binding of PrC is quite weak and that the overall affinity of association of phosphatidylcholines strongly increases with the presence of the glycerol backbone and with each of the fatty acyl chains by two to three orders of magnitude. From the temperature dependence of the K_a values, enthalpy of binding (ΔH^o) and entropy of binding (ΔS^o), were obtained as -79.7 $kJ.mol^{-1}$ and -237.1 $J.mol^{-1}.K^{-1}$, for PrC and -73.0 $kJ.mol^{-1}$ and -167.3 $J.mol^{-1}.K^{-1}$, for Lyso-PC, respectively. These results demonstrate that although the binding of these two ligands is driven by enthalpic forces, smaller negative entropy of binding associated with Lyso-PC results in its significantly stronger binding.

4.2. Introduction

PDC-109 is the major protein of the bovine seminal plasma and is present at a concentration of ca. 15-25 mg/ml [Scheit et al., 1988]. Its 109-residue polypeptide chain is made up of two fibronectin type-II (Fn2) domains, preceded by a 23-residue *N*-terminal stretch, which is rich in acidic amino acids [Esch et al., 1983; Baker 1985; Seidah et al, 1987]. Recent biochemical and biophysical studies suggest that PDC-109 is a multifunctional protein, with at least two different types of physiologically significant binding interactions [Swamy, 2004]. Single-crystal X-ray diffraction studies have shown that each Fn2 domain can bind one choline phospholipid molecule by its specific interaction with the phosphorylcholine moiety and that the two binding sites are on the same face of the protein [Wah et al., 2002]. The interaction of PDC-109 with sperm plasma membranes results in an efflux of cholesterol and choline phospholipids, referred to as *cholesterol efflux*, which appears to be an important step in the capacitation process, which in turn is a necessary event before fertilization can occur [Thérien et al., 1998; Moreau & Manjunath, 1999]. PDC-109 also interacts with fucosylated oligosaccharides present on the oviductal epithelium in cow [Ignotz et al., 2001], and this has been postulated to be responsible for the maintenance of oviductal sperm reservoir [Gwathmey et al., 2003].

In view of the above, it is important to investigate the binding of different ligands to PDC-109 in order to understand its role in the fertilization process. In the spin-label ESR studies reported in Chapter 2 it was shown that upon binding to dimyristoylphosphatidylcholine (DMPC) membranes, PDC-109 penetrates into the hydrophobic interior of the membrane and that it also recognizes other phospholipids such as phosphatidylglycerol and phosphatidylserine, albeit weakly [Ramakrishnan et al., 2001]. Binding of PDC-109 decreases phospholipid mobility and abolishes the

lipid chain-melting phase transition [Ramakrishnan et al., 2001; Greube et al., 2001; Gasset et al., 2000]. Presence of cholesterol modulates the binding by increasing the association of different phospholipids and sterol probes with the protein, although the relative selectivity for individual lipid species was not significantly affected [Swamy et al., 2002]. SPR studies presented in Chapter 3 have shown that the binding of PDC-109 to phosphatidylcholine membranes is due to a combination of faster association rate constant and a slower dissociation rate constant, as compared to other phospholipids [Thomas et al., 2003]. In the present study the binding of PrC and Lyso-PC to PDC-109 has been investigated by absorption spectroscopy. The thermodynamic parameters associated in these interactions have been delineated by performing the binding studies at different temperatures. The results indicate that although the binding of both PrC and Lyso-PC to PDC-109 is driven by enthalpic forces, binding of PDC-109 to Lyso-PC is 250-fold stronger than its interaction with PrC due to a significantly smaller negative entropic contribution associated with the former.

4.3. Experimental Section

4.3.1. Materials

Phosphorylcholine chloride (Ca^{2+} salt) and Tris base were obtained from Sigma (St. Louis, MO, USA). Lyso-PC was a product of Avanti Polar Lipids (Alabaster, AL, USA). Sephadex G-50 (superfine) and DEAE Sephadex A-25 were purchased from Pharmacia (Uppsala, Sweden). PDC-109 was purified from bovine seminal plasma of healthy and reproductively active bulls by the combination of gel filtration and affinity chromatography as reported in Chapter 2. Concentration of PDC-109 was estimated

from its extinction coefficient of 2.5 for 1 mg/ml concentration at 280 nm [Calvete et al., 1996].

4.3.2. Binding of phosphorylcholine and Lyso-PC to PDC-109

Binding of PrC and Lyso-PC to PDC-109 was investigated by absorption spectroscopy. All experiments were carried out in 50 mM Tris-HCl buffer, pH 7.4, containing 0.5 M NaCl, 5 mM EDTA and 0.025% sodium azide (TBS). Absorption spectra were recorded on a Shimadzu UV-3101PC UV-Vis-NIR double-beam spectrophotometer using 1.0-cm path-length cells. Temperature was maintained constant (± 0.5 ^{o}C) by means of a Peltier device. Titrations were performed by adding small aliquots of the ligands from stock solutions (200 mM PrC, 2.0 mM Lyso-PC) to both the sample and reference cuvettes. The concentration of PDC-109 in different titrations ranged between 0.32 and 0.44 mg/ml. Spectra were recorded after an equilibration period of 2 min following each addition. All titrations were performed at least two times and the average values are reported.

4.3.3. Circular dichroism spectroscopy

Circular dichroism (CD) spectra were recorded at 25^{o}C on a Jasco-J-810 spectropolarimeter at a scan speed of 20 nm/min using 0.1-cm pathlength cylindrical quartz cells. Far-UV and near-UV spectra were recorded at PDC-109 concentration of about 0.16 mg/ml and 0.64 mg/ml, respectively. Data were collected with a response time of 2 s and a slit width of 1 nm. Each spectrum reported was the average of 20 consecutive scans from which buffer scans, recorded under the same conditions, were subtracted. The observed ellipticities were converted to mean residue ellipticities (Θ) using a mean molecular mass/residue of 117 [Esch et al., 1983].

4.4. Result and Discussion

Previous binding studies have demonstrated that PDC-109 specifically recognizes choline phospholipids such as phosphatidylcholine and sphingomyelin, among the different types of lipids tested [Desnoyers & Manjunath, 1992]. Affinity chromatographic experiments in which PrC was successfully used as the eluting ligand showed that the protein specifically recognizes the choline moiety in choline phospholipids [Desnoyers & Manjunath, 1993]. PDC-109, which exists as a polydisperse aggregate in solution, is converted into dimers upon binding of PrC [Gasset et al., 1997]. The X-ray structure of the PDC-109/PrC complex showed that each Fn2 domain binds one molecule of PrC [Wah et al., 2002]. Although it is known from earlier reports that both PrC and Lyso-PC bind to PDC-109 and that the binding affinity for the interaction of PDC-109 with Lyso-PC is higher than the affinity of its interaction with PrC [Desnoyers & Manjunath, 1992, 1993; Gasset et al., 1997; Müller et al., 1998, 2002], the association constants and thermodynamic forces that govern the interaction of choline-containing ligands to this protein were not known. In this study we have investigated the binding of PrC and Lyso-PC to PDC-109, in order to obtain the association constants that characterize the respective binding reactions and to delineate the thermodynamic forces that control their interaction.

When PDC-109 was titrated with PrC, small but reproducible changes were observed in the protein absorption spectrum. Difference spectra displayed an increase in the absorption intensity in the wavelength range of ca. 250-300 nm, with maximum change in absorption around 289 nm and a second peak centered around 280 nm, signifying the perturbation of aromatic side chains of Tyr and Trp (not shown). Titration of PDC-109 with choline chloride led to very small changes in the absorption spectrum of the protein, precluding the analysis of the titration data to

obtain the association constant. On the other hand, titration of the protein with Lyso-PC resulted in a considerably larger increase in the absorption intensity of the protein in the same spectral region (Fig. 4.1A). Further, as seen in the difference spectra (Fig. 4.1B), the change in the absorption intensity at 280 nm was considerably larger than that at 289 nm, indicating that Tyr residues are perturbed more in the case of Lyso-PC binding.

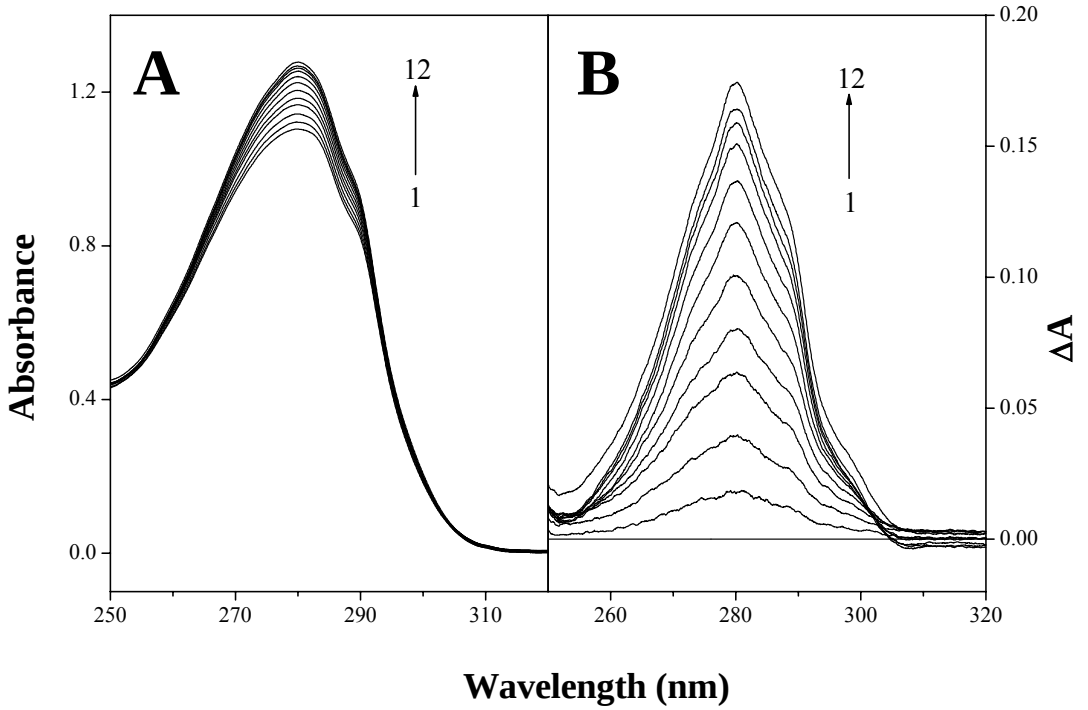

Fig. 4.1: Absorption titration of PDC-109 with Lyso-PC. A) Absorption spectra of PDC-109 alone (spectrum 1) and PDC-109 in the presence of different concentrations of Lyso-PC (spectra 2-12). B) Difference absorption spectra obtained by subtracting the spectrum of PDC-109 alone from the spectra of PDC-109 obtained in the presence of different concentrations of Lyso-PC. The difference spectra with increasing intensities were obtained in the presence of increasing concentrations of Lyso-PC.

These observations are consistent with the three-dimensional structure of PDC-109/PrC complex, obtained from single-crystal X-ray diffraction studies [Wah et al, 2002], where it was observed that binding of PrC is guided by a cation-π interaction between the quaternary ammonium group and the indole side chain of a core tryptophan residue in the ligand binding site, with additional hydrogen bonding

interactions between the phosphate group of PrC and side chains of one or two tyrosine residues (Fig. 4.2). Although the crystal structure suggested that the quaternary ammonium group interacts with the indole side chain of Trp47, in solution a similar interaction with the indole moiety of Trp58 is also quite probable; such an interaction requires only a rotation around the C-C bond between the two methylene units of phosphorylcholine.

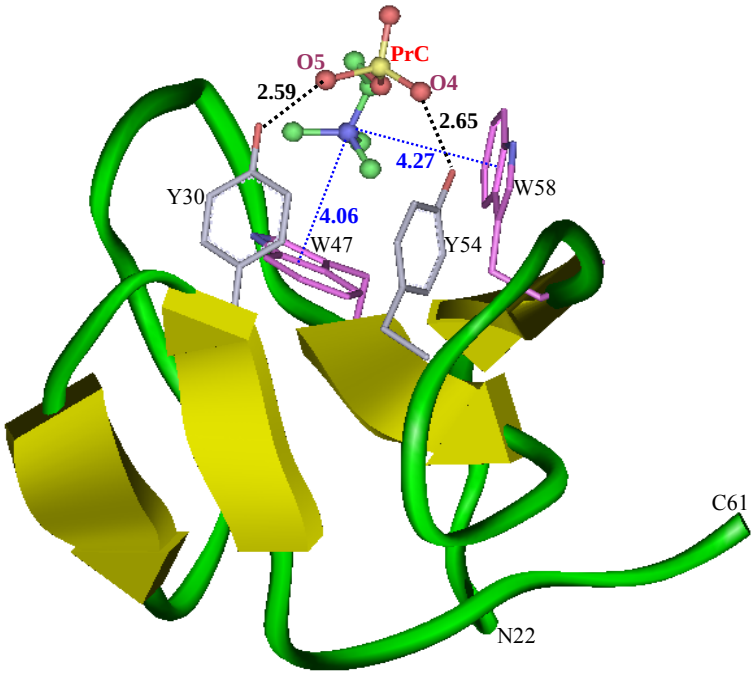

Fig. 4.2: Structure of a Fn2 domain of PDC-109 with bound PrC molecule. The structure was generated using the Insight II software (Accelrys Inc.) from the coordinates in pdb (id = 1h8p). The backbone is shown as a ribbon and the side chains of Y30, Y54, W47 and W58, which interact with the ligand are shown as sticks. Hydrogen bonds between the hydroxyls of Y30 and Y54 and the phosphate oxygens are indicated by black dotted lines. The cation-π interaction of the quaternary ammonium group with W47 and W58 are indicated by blue dotted lines with the distances between the quaternary nitrogen and the centroid of the indole moiety. Distances are shown in Å.

Binding of PrC and Lyso-PC to PDC-109 was monitored by following changes in the absorbance at 289 nm and 280 nm, respectively. Typical binding curves for the association of PrC and Lyso-PC with PDC-109 are shown in the insets of Figs. 4.3A and 4.3B, respectively. These binding curves show that the change in the absorption

intensity decreases with increasing ligand concentration, displaying saturation behavior. At the highest concentrations of the ligands used in the binding titrations performed at 20°C (binding curves shown in the insets of Figs. 4.3A and 4.3B), the ratios PrC/PDC-109 and Lyso-PC/PDC-109 (monomer) are 656 and 4.5 and clearly indicate that Lyso-PC exhibits a significantly higher binding strength as compared to PrC. These results are in agreement with the observations of Müller et al. [1998], who investigated the interaction of Lyso-PC and PrC with PDC-109 at 30°C by fluorescence spectroscopy.

In order to obtain the association constants, K_a, the binding data were analyzed according to the expression [Chipman et al., 1967]:

$$\text{Log } \{\Delta A/(A_c - A_\infty)\} = \log K_a + \log [L]_f \qquad (1)$$

where ΔA is the change in absorbance at any point of the titration, A_c is the corresponding absorption intensity of the protein, A_∞ is the absorption intensity of the protein that is fully saturated with the ligand and $[L]_f$, the free ligand concentration, is given by:

$$[L]_f = [L]_t - \{(\Delta A/\Delta A_\infty).[P]_t\} \qquad (2)$$

where $[P]_t$ is the total protein concentration, $[L]_t$ is the total ligand concentration and ΔA_∞ is the change in absorbance at saturation binding. Because the 3-dimensional structure of PrC/PDC-109 complex [Wah et al., 2002] has clearly shown that each molecule of PDC-109 binds two molecules of PrC, in the analysis of the titration data the protein concentration was taken as twice the concentration of PDC-109 monomer, i.e., the concentration of the Fn2 domains.

Equation 1 shows that the X-intercept of a plot of $\log\{\Delta A/(A_c - A_\infty)\}$ versus $\log[L]_f$ will yield $-pK_a$ for the association of PrC (or Lyso-PC) with PDC-109. Representative plots of this type corresponding to the interaction of PrC and Lyso-PC

with PDC-109 at 20°C are given in Figs. 4.3A and 4.3B, respectively. From the X-intercepts of these plots the K_a values characterizing the binding of PrC and Lyso-PC to PDC-109 were obtained as 81.4 M^{-1} and 2.02×10^4 M^{-1}, respectively.

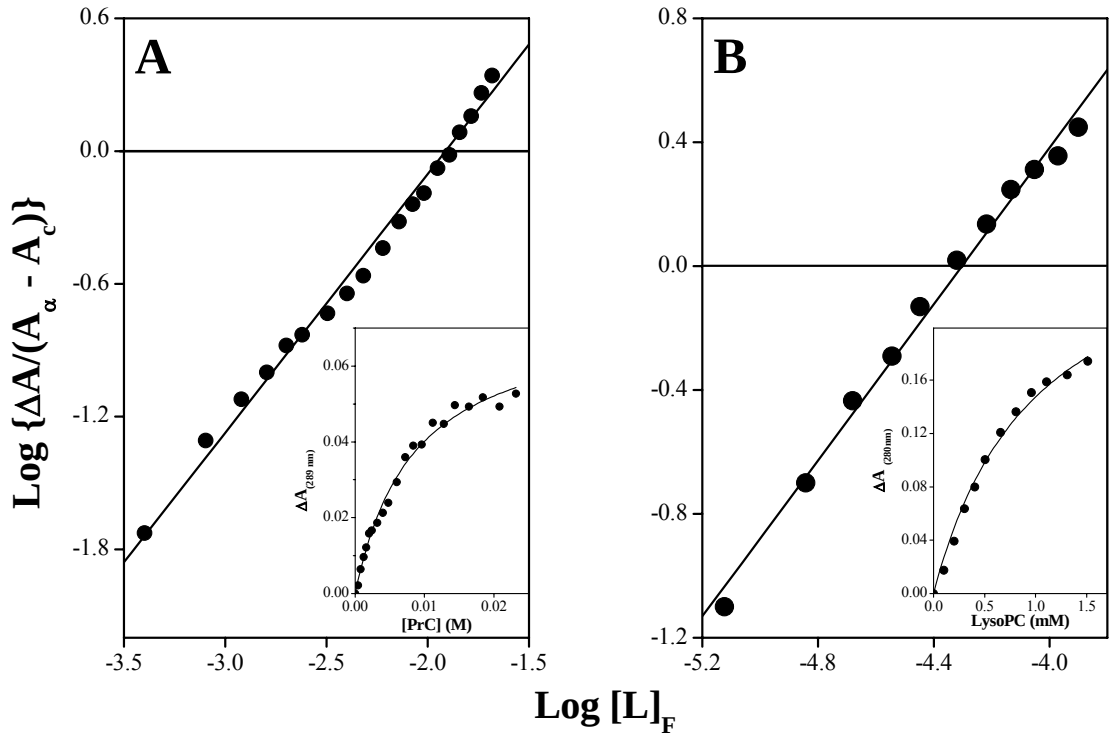

Fig. 4.3: Analysis of the absorption titration of PDC-109 with (A) PrC and (B) Lyso-PC. The titration data were analysed according to Chipman et al. [1967]. The insets show binding curves of ΔA versus $[L]_f$.

It is seen that the data shown in Figs. 4.3A and 4.3B exhibit linear dependence within the range of experimental error, suggesting that despite the minor differences in the mode of binding of PrC to the different Fn2 domains of the protein as observed in the PrC/PDC-109 complex crystal structure [Wah et al., 2002], the binding strength for the interaction of PrC with the different Fn2 domains of PDC-109 is most likely comparable. In other words, the affinities with which different Fn2 domains of the PDC-109 dimer bind PrC appear to be nearly the same.

In order to obtain the thermodynamic parameters associated with the interaction of PrC and Lyso-PC, binding titrations were performed at different temperatures. The association constants were then obtained by analyzing the titration data as described above and the values obtained at different temperatures are listed in Table 4.1. It is clear from the values presented in this Table, the association constants (K_a) decrease with increase in temperature for both PrC and Lyso-PC.

Table 4.1: Association constants, K_a, determined from the absorption titrations at different temperatures for the binding of phosphorylcholine and Lyso-PC to PDC-109.

T (^oC)	Phosphorylcholine	Lyso-PC
	K_a (M^{-1})	$10^{-3} \times K_a$ (M^{-1})
15	99.0 ± 1.1	----
20	81.4 ± 0.1	20.2 ± 0.4
25	33.2 ± 0.7	11.2 ± 0.9
30	28.3 ± 0.5	5.6 ± 0.7
35	11.8 ± 1.3	5.3 ± 0.2

From the K_a values, changes in the Gibbs free energies have been calculated using eq. (3) as ΔG^o = -10.7 kJ.mol^{-1} and -24.3 kJ.mol^{-1} for the interaction of PDC-109 with PrC and Lyso-PC, respectively.

$$\Delta G^o = -RT \ln K_a \qquad (3)$$

The thermodynamic parameters, enthalpy of binding (ΔH^o) and entropy of binding (ΔS^o) associated with the interaction of PrC and Lyso-PC were obtained by means of van't Hoff plots (Fig. 4.4) according to the expression:

$$\ln K_a = (- \Delta H^o/RT) + (\Delta S^o/R) \qquad (4)$$

The enthalpy and entropy of binding for PrC were obtained as ΔH^o = -79.7 kJ.mol^{-1} and ΔS^o = -237.1 J.mol^{-1}.K^{-1}, whereas the corresponding values for the binding of Lyso-PC were determined to be ΔH^o = -73.0 kJ.mol^{-1} and ΔS^o = -167.3 J.mol^{-1}.K^{-1}.

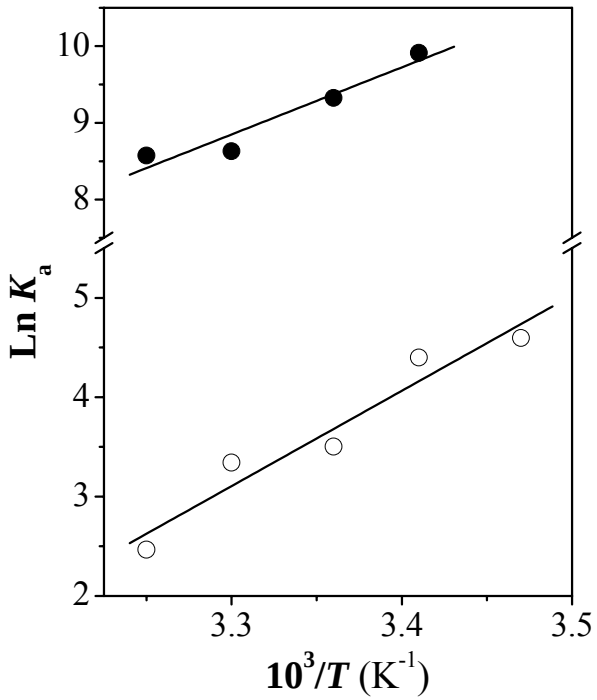

Fig. 4.4: Van't Hoff plots for the interaction of phosphorylcholine (○) and Lyso-PC (●) with PDC-109.

It is instructive to compare the K_a values and thermodynamic parameters obtained for the association of PrC and Lyso-PC with PDC-109 (Table 4.1). The K_a value for the lyso-PC/PDC-109 interaction obtained at 20^{o}C is 2.02 × 10^4 M^{-1}, which is about 250-fold higher than the value of 81.4 M^{-1} obtained for the association of PrC with PDC-109 at the same temperature. A comparison of the thermodynamic parameters obtained with PrC and Lyso-PC clearly shows that although the binding of PrC is associated with a slightly larger (negative) change in enthalpy as compared to

Lyso-PC, the smaller negative contribution from entropy of binding overrides this difference, resulting in a much stronger association of Lyso-PC with PDC-109.

Previous CD spectroscopic studies have shown that PrC binding leads to notable changes in the secondary and tertiary structure of PDC-109 [Gasset et al., 1997]. However, the effect of Lyso-PC binding on the structure of this protein was not known. In order to investigate this and to compare the effect of these two ligands on the structure of PDC-109 under similar conditions, we have recorded the CD spectra of PDC-109 in TBS (pH 7.4). The far-UV and near-UV CD spectra of PDC-109 alone and in the presence of PrC and Lyso-PC are shown in Figs. 4.5A and 4.5B, respectively.

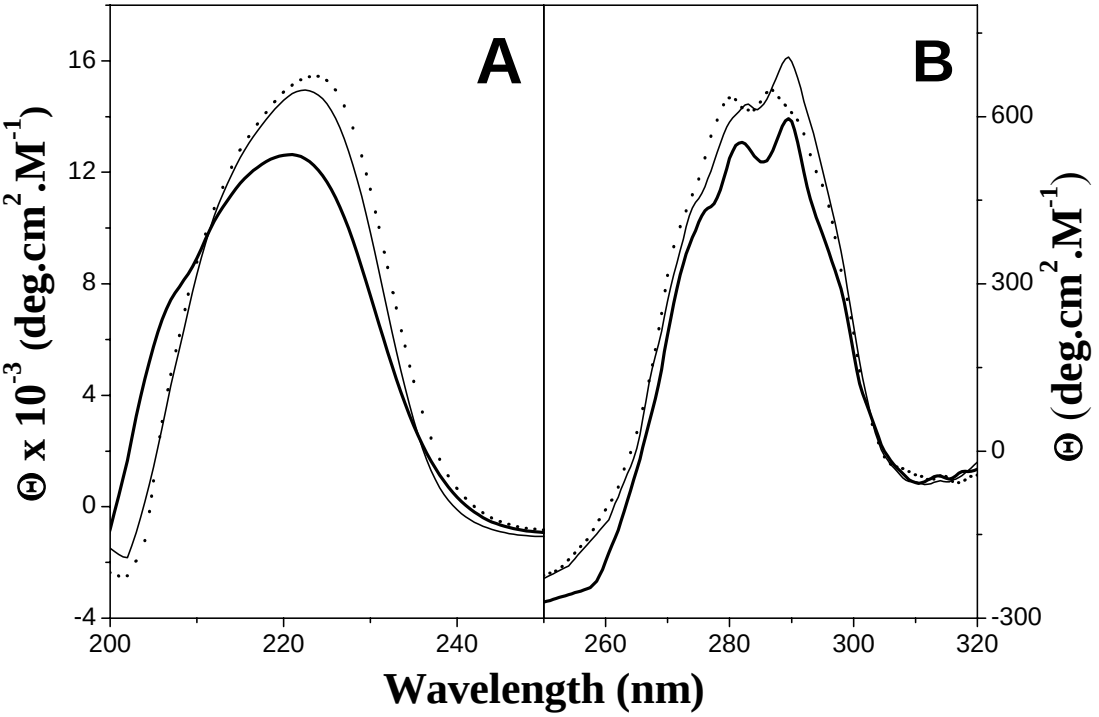

Fig. 4.5: CD spectra of PDC-109 in the absence and in the presence of PrC and Lyso-PC. (A) Far-UV region and (B) near-UV region. (– –) PDC-109 alone, (——) PDC-109 + 20 mM PrC, (------) PDC-109 + 0.2 mM Lyso-PC.

Consistent with the previous reports, the far-UV CD spectrum of PDC-109 is characterized by a broad positive band centered at ca. 225 nm, which appears to be due to the unusually high content of aromatic amino acids and disulfide bonds in this protein [Gasset et al., 1997]. Analysis of the far UV CD spectra to obtain secondary structure composition was not possible due to the lack of appropriate protein reference data set [Esch et al., 1983; Gasset et al., 1997]. Binding of either PrC or Lyso-PC results in a considerable increase in the intensity of this band with the magnitude of change associated with the binding of Lyso-PC being larger. These results, together with the results of absorption titrations presented above, which showed larger changes in the difference spectra in the presence of Lyso-PC, clearly indicate that the binding of Lyso-PC induces larger perturbations in the secondary structure of PDC-109. The near-UV CD spectra of PDC-109 exhibit similar trends, with two overlapping positive bands at 282 and 289.5 nm, which become more intense in the presence of PrC with practically no shift in the band position. In the presence of Lyso-PC also two closely spaced and overlapping bands are seen; however, these bands are slightly blue shifted and occur at 280 and 286.5 nm. Although X-ray studies have shown that binding of PrC leads to conformational changes in the polypeptide backbone of PDC-109 [Wah et al., 2002], changes observed in the far and near UV CD spectra upon binding of PrC or Lyso-PC could arise in part due to the changes in the quaternary structure of the protein, as it has been demonstrated earlier that this protein, which exists as a polydisperse aggregate in solution, is converted to the dimeric form upon ligand binding [Gasset et al., 1997].

In Chapter 3, surface plasmon resonance studies have been reported, which showed that association of PDC-109 with DMPC/cholesterol mixtures is entropically favored, with binding enthalpy (ΔH^o) and entropy (ΔS^o) values of 7.08 kJ.mol^{-1} and 164.36 J.mol^{-1}.K^{-1}, respectively [Thomas et al., 2003]. Comparing the thermodynamic

parameters obtained for the interaction of PrC and Lyso-PC with these values indicates that going from PrC to Lyso-PC to DMPC, the binding enthalpy becomes progressively less favorable, whereas the entropy of binding becomes increasingly favorable. However, the net result is that the free energy of binding becomes more favorable, resulting in a stronger binding of DMPC as compared to Lyso-PC, which in turn binds more strongly than PrC. Although several possibilities can be suggested for the above changes in the binding enthalpy and binding entropy for the interaction of the above three ligands with PDC-109, it is important to obtain structural information on the complexes of PDC-109 with Lyso-PC and diacyl PC in order to gain molecular level understanding on the factors leading to the energetic changes with respect to the binding of these ligands to PDC-109.

Results from a number of studies indicate that PDC-109 exhibits an obligatory requirement for choline-containing lipids in order to bind to lipid membranes [Desnoyers and Manjunath 1992,1993; Müller et al., 1998; Ramakrishnan et al., 2001; Thomas et al., 2003]. Indeed, the X-ray structure of PrC/PDC-109 complex [Wah et al., 2002] clearly shows that specific recognition of the phosphorylcholine moiety by each Fn2 domain of the protein is mediated by a cation-π interaction between the quaternary ammonium group and a core tryptophan and several hydrogen bonds between the phosphate group of the ligand and the hydroxyl groups of tyrosine residues (Fig. 4.2). The present results clearly show that despite the obligatory requirement of the choline moiety for PDC-109 to bind to lipid membranes, binding of phosphorylcholine to this protein is quite weak, with an association constant of 81.4 M^{-1} at 20^{o}C. The association becomes 250 fold stronger by the attachment of the glycerol backbone and the acyl chain in Lyso-PC, with a K_a of 2.02×10^4 M^{-1} at the same temperature. Comparison with the SPR results shows that the strength of binding of the diacyl lipid, DMPC ($K_a = 2.1 \times 10^7$ M^{-1}) is further increased by three

orders of magnitude [Thomas et al., 2003]. These results show that the additional interactions with the acyl chain(s) further stabilize the binding of Lyso-PC and DMPC with PDC-109. However, phospholipids with other head groups are very poorly recognized [Desnoyers and Manjunath 1992; Müller et al., 1998; Ramakrishnan et al., 2001; Thomas et al., 2003], clearly indicating the requirement of both phosphorylcholine moiety and the hydrophobic acyl chain region of the choline phospholipids for the optimal interaction of PDC-109 with sperm cell membranes. Phosphatidylcholine, which is the major lipid of the sperm plasma membrane, thus appears to have been chosen for this regulatory step in the sperm cell maturation prior to fertilization.

In summary, the studies presented in this chapter demonstrate that the higher affinity of Lyso-PC towards PDC-109 as compared to PrC is due to a smaller (negative) entropy associated with its binding. Comparison of these results with the results obtained by the SPR method for the interaction of PDC-109 with DMPC membranes indicates that the acyl chain(s) of Lyso-PC and DMPC also contribute positively towards their binding with the protein, thus strengthening the overall binding strength.

Chapter 5

Fluorescence Spectroscopic Investigations on the Interaction of PDC-109 with Phosphorylcholine and Choline Phospholipid Membranes

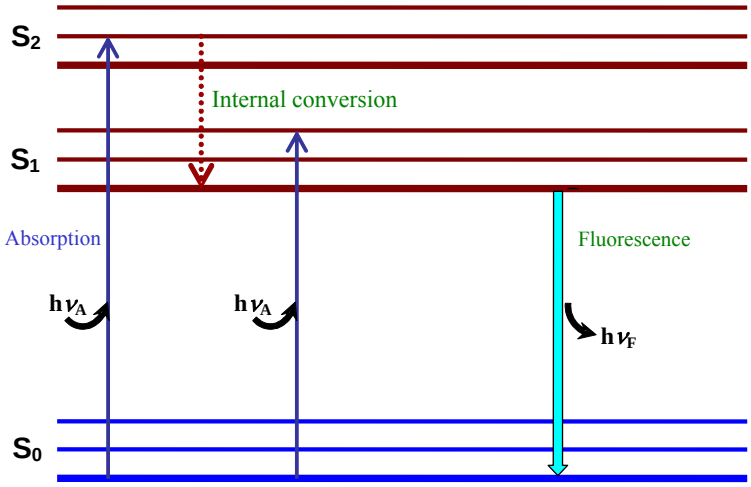

Jablonski Diagram

***Anbazhagan, V.**, Paul, A. and Swamy, M.J.* (2005) *Fluorescence spectroscopic investigations on the interaction of PDC-109, a multifunctional protein from bovine seminal plasma with phosphorylcholine and lipid membranes.* (to be communicated).

5.1. Summary

PDC-109, the multifunctional protein from bovine seminal plasma binds with high selectivity to choline containing phospholipids on the sperm plasma membrane and stimulates cholesterol and phospholipid efflux, which is a crucial event in sperm capacitation which primes the spermatozoa before fertilization. In the studies reported in this chapter, the environment and accessibility of tryptophan residues of PDC-109 in the native state, upon binding to phosphorylcholine, Lyso-PC micelles and DMPC membranes as well as upon denaturation, have been investigated by fluorescence quenching, time-resolved fluorescence measurements and red-edge excitation shift studies. The extent of quenching of the protein intrinsic fluorescence by acrylamide, succinimide, cesium ion (Cs^+) and iodide ion (I^-), at a quencher concentration of 0.5 M was 91.9%, 77.4%, 44.8% and 35.2%, respectively. Binding of PrC, Lyso-PC and DMPC to PDC-109 resulted in a progressive decrease in the degree of quenching, indicating that while the head group phosphorylcholine moiety is critical for the recognition of the choline phospholipids by the protein, the acyl chain(s) stabilize the binding and result in further tightening of the protein structure, leading to decreased accessibility of the Trp residues to different quenchers. A red-edge excitation shift (REES) of 4 nm was observed with native PDC-109, suggesting that the microenvironment of Trp residues in this protein has a reduced mobility and that the reorientation of the solvent water molecules around them is considerably restricted. Interestingly, even upon denaturation with 6 M Gdn.HCl, PDC-109 exhibits a REES of 4 nm, clearly indicating that the structural and dynamic features of the microenvironment around the tryptophan residues are retained even after denaturation. Upon binding of PDC-109 to DMPC membranes and Lyso-PC vesicles the REES values were reduced to 2.5 nm and 1.0 nm, respectively, which has been interpreted as due to the penetration of the segments of the protein containing majority of the

tryptophan residues into the hydrophobic interior of the membrane, where the red-edge effects have been shown to be considerably reduced. Time-resolved fluorescence experiments yielded biexponential decay curves with different lifetimes for native PDC-109 and the DMPC-membrane-bound form.

5.2. Introduction

As discussed in Chapter 1, PDC-109 binds to sperm plasma membranes by specific interaction with choline phospholipids and induces cholesterol efflux, which is a critical step in the process of capacitation. In view of this, it is essential to understand the interaction of this protein with membranes containing-choline phospholipids. The spin-label ESR studies presented in Chapter 2 demonstrated that upon binding to PC membranes PDC-109 penetrates into the hydrophobic interior of the membrane, resulting in the direct interaction of segments of the protein with lipid acyl chains. SPR studies described in Chapter 3 showed that the higher affinity of PDC-109 towards choline phospholipids is due to a faster association rate and a slower dissociation rate as compared to other phospholipids such as phosphatidylglycerol and phosphatidic acid. Thermodynamic studies on the binding of PrC and Lyso-PC to PDC-109 presented in Chapter 4 indicated that although the phosphorylcholine head group of choline phospholipids is the obligatory structural determinant that is recognized by the protein, the glycerol moiety and the acyl chain(s) of Lyso-PC and diacyl PC contribute positively to the binding and stabilize the interaction.

Although these studies have yielded much valuable information on the interaction of PDC-109 with membranes, molecular features of the interaction are still not very clear. For example, Gasset et al. [2000] have shown that PDC-109 undergoes a conformational change upon binding to PC membranes. The ESR studies presented

in Chapter 2 show that some segments of PDC-109 penetrate into the hydrophobic interior of the membrane. However, it is not clear as to which regions of the protein are embedded into the membrane interior. Additional studies are therefore necessary in order to understand this aspect better. The application of fluorescence spectroscopy to the study of the structure and conformation of proteins has proved to be very fruitful over the past few decades [Grinvald & Steinberg, 1976; Eftink & Ghiron, 1981; Lakowicz, 1999]. Particularly, the emission characteristics of tryptophan residues in proteins provide a convenient handle to investigate changes in the conformation/structure of proteins resulting from a variety of factors such as substrate/ligand binding, association/dissociation of subunits in oligomeric proteins, and unfolding. From the primary structure of PDC-109, it can been seen that there are five tryptophan residues at positions 47, 58, 90, 93 and 106 [Esch et al., 1983], whose fluorescence properties can be monitored to investigate changes in its conformation and to study the effect of ligand binding. In previous studies, it has been shown that the intrinsic fluorescence spectrum of PDC-109 in aqueous buffer exhibits a maximum emission at 342 nm, which is blue shifted to 337 nm upon binding of phosphorylcholine with a concomitant increase in the emission intensity, whereas binding of both Lyso-PC and PC SUVs resulted in a shift of the emission maximum to 333 nm accompanied by an increase in the emission intensity [Müller et al., 1998]. The changes in the protein fluorescence intensity have also been monitored by the stopped-flow technique to obtain information on the kinetics of its interaction with DMPC SUVs.

In the studies presented in this chapter, systematic studies have been carried out on the intrinsic fluorescence of PDC-109 in the native state, in the presence of different ligands (PrC, Lyso-PC micelles and DMPC SUV), and upon denaturation. The accessibility of the fluorescent Trp residues has been investigated by quenching

studies employing two neutral quenchers, acrylamide and succinimide, a cationic quencher, cesium ion (Cs^+) and an anionic quencher, iodide ion (I^-). In addition, time-resolved fluorescence studies have been carried out in order to investigate the heterogeneity in the Trp environment. Finally, the effect of changing excitation wavelength on the wavelength of maximum emission, commonly referred to as red-edge excitation shift (REES), has been investigated in order to obtain information on the environment and organization of the Trp residues in this protein in the native state, upon denaturation and when bound to PrC, Lyso-PC and DMPC. REES is mostly observed with polar fluorophores in motionally restricted media such as viscous solutions or condensed phases where the dipolar relaxation time for the solvent shell around a fluorophore is comparable to or longer than its fluorescence lifetime [Demchenko, 2002; Chattopadhyay, 2003]. It provides information about the relative rates of solvent (water in biological systems) relaxation dynamics which is not possible to obtain by other techniques, thus making REES extremely useful since hydration plays a crucial modulatory role in a large number of important cellular events including protein folding, lipid-protein interactions and ion transport [Mentre, 2001; Kouyama et al., 2004].

5.3. Materials and Methods

5.3.1. Chemicals

Acrylamide, urea, guanidine hydrochloride, phosphorylcholine, choline chloride, and β-mercaptoethanol were purchased from Sigma (St. Louis, MO, USA). KI was purchased from Qualigens (Mumbai, India). Dimyristol phosphatidylcholine (DMPC) and lysophosphatidylcholine (Lyso-PC) were from Avanti polar lipids (Alabaster, AL). All other chemicals used were of analytical grade and were obtained from local

suppliers. PDC-109 was purified from the seminal plasma of healthy and reproductively active bulls as reported in Chapter 2. Buffers were prepared in glass double distilled and deionized water.

5.3.2. Preparation of liposomes

Lipids dissolved in dichloromethane in a glass test tube were dried under a gentle stream of nitrogen gas and the final traces of the solvent were removed by vacuum desiccation for ca. 3 hours. The dried lipid film was hydrated by vortexing for 5 min with TBS-I to give the desired lipid concentration. Small unilamellar vesicles (SUV) were prepared by sonication of the lipid suspension in a bath sonicator for 30 min at room temperature.

5.3.3. Steady State fluorescence measurements

Steady state fluorescence measurements were performed using a Spex model Fluoromax-3 spectrofluorimeter at 25^{o}C, with both the excitation and emission band pass filters set at 3 nm. All fluorescence studies were carried out on PDC-109 samples in TBS-I with $OD_{280nm} < 0.1$. Protein samples were excited at 280 nm and emission spectra recorded between 310 and 390 nm, except for the REES experiments where the excitation wavelength ranged between 280 and 307 nm and emission spectra was recorded between 320 and 390 nm. Titrations were performed by adding small aliquots of the quenchers from 5 M stock solutions in TBS-I to the protein. Stock solution of KI contained 0.2 mM sodium thiosulfate to prevent the formation of triiodide. Experiments were performed in triplicate and the average results are given.

5.3.4. Fluoresence lifetime measurements

Time-resolved fluorescence measurements were performed on an IBH time correlated single-photon counting spectrofluorimeter equipped with a nanoLED excitation source

(IBH) and a cooled microchannel plate photomultiplier tube from Hamamatsu (Model 5000U-09B). Samples of $OD_{280nm} < 0.1$ in $1 \times 1 \times 4.5$ cm quartz cells were exited at 281 nm and emission was monitored at the wavelength indicated in parentheses: native PDC-109 (340 nm), denatured protein (347 nm), PDC-109 + phosphorylcholine (336 nm), PDC-109 in the presence of Lyso-PC micelles or DMPC SUV (333 nm). All experiments were performed using excitation and emission slits with a nominal bandpass of 12 nm or less. Lamp profiles were measured at the excitation wavelength using Ludox (colloidal silica) as the scatterer. To optimize the signal/noise ratio, 5000 photon counts were collected in the peak channel. The sample and the scatter were alternated after every acquisition to ensure compensation for shape and timing drifts occurring during the period of data collection. This arrangement also prevents any prolonged exposure of the sample to the excitation beam, thereby avoiding any possible photodamage to the fluorophore. The resultant fluorescence decay curves were deconvoluted with the instrument response function and analyzed by a multiexponential iterative fitting program supplied by IBH.

5.4. Result

The effect of ligand binding on the intrinsic fluorescence properties of PDC-109 was investigated earlier by Müller et al. [1998]. They observed that binding of PrC, phosphatidylcholine and Lyso-PC, all resulted in a significant increase in the fluorescence intensity of the protein with a concomitant blue shift in the emission λ_{max}. In order to compare the results obtained under similar instrumental conditions and with the same protein sample, these measurements have repeated. The results are qualitatively very similar to those obtained by Müller et al. [1998]. The fluorescence spectra of PDC-109 in the native state and in the presence of PrC, Lyso-PC and

DMPC are shown in Fig. 5.1. The excitation wavelength used in these experiments was 280 nm.

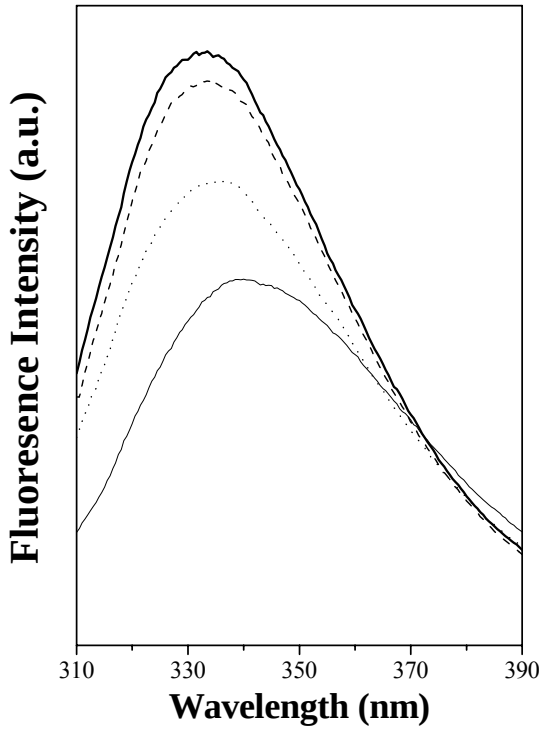

Fig. 5.1: Fluorescence spectra of PDC-109 obtained under different conditions. Native protein (thin line); in the presence of 20 mM PrC (dotted line); in the presence of 0.15 mM Lyso-PC (dashed line) and in the presence of 0.15 mM DMPC (thick line). Excitation wavelength = 280 nm.

From Fig. 5.1 it is seen that the fluorescence emission spectrum of PDC-109 exhibits a maximum at 340 nm, which is blue shifted to 335.5 nm with about 27% increase in the intensity in the presence of 20 mM PrC. In the presence of 0.15 mM Lyso-PC the emission λ_{max} shifted to 333.5 nm with ca. 54% increase in the fluorescence intensity, whereas upon binding to 0.15 mM DMPC the emission maximum shifted to 333 nm, accompanied by nearly 62% increase in the emission intensity.

5.4.1. Quenching of the intrinsic fluorescence of PDC-109

Fluorescence spectra of PDC-109 in the native state and in the presence of increasing concentrations of acrylamide and iodide ion are shown in Figs. 5.2A and 5.2C, respectively. Figures 5.2B and 5.2D show fluorescence spectra of PDC-109 bound to DMPC SUVs in the absence and in the presence of increasing concentrations of acrylamide and iodide ion, respectively. In each case, spectrum 1, which exhibits the highest intensity, corresponds to PDC-109 (or PDC-109 bound to DMPC SUVs) in the absence of any quencher, and the spectrum with the lowest intensity corresponds to that recorded in the presence of 0.5 M quencher. The remaining spectra correspond to those recorded in the presence of different concentrations of the quencher and in each case as the quencher concentration is increased, the fluorescence intensity was found to decrease. The spectra presented in Figs. 5.2A and 5.2C show that while acrylamide quenches the protein fluorescence significantly, quenching with iodide is considerably reduced. At 0.5 M concentration of the quencher, acrylamide and iodide quenched about 91.9% and 35.2% of the fluorescence intensity, respectively, of the native protein. For native PDC-109 the emission maximum is slightly blue shifted upon quenching with 0.5 M acrylamide (spectrum 17, Fig. 5.2A), whereas in the presence of 0.5 M iodide no blue shift was observed. From Figs. 5.2B and 5.2D, it is seen that upon binding to DMPC vesicles the accessibility of the Trp residues of the protein is considerably decreased, resulting in a decrease in the extent of quenching to 81% and 22.3%, with acrylamide and iodide, respectively, at 0.5 M concentration of the quencher. Quenching studies with succinimide and Cs^+ also gave qualitatively similar spectra, and the extent of quenching observed with them at 0.5 M concentration was 77.4% and 44.8%, which decreases significantly to 34.3 and 15.6%, respectively, upon binding to DMPC SUV (spectra not shown). In addition to the studies carried out on the native protein and in the presence of DMPC SUV, fluorescence studies were also carried out in the presence of phosphorylcholine and

Lyso-PC. The extent of quenching observed in each case is given in Table 5.1. With each quencher, the quenching observed in the presence of DMPC was less than that in the presence of Lyso-PC which in turn was less than that in the presence of PrC.

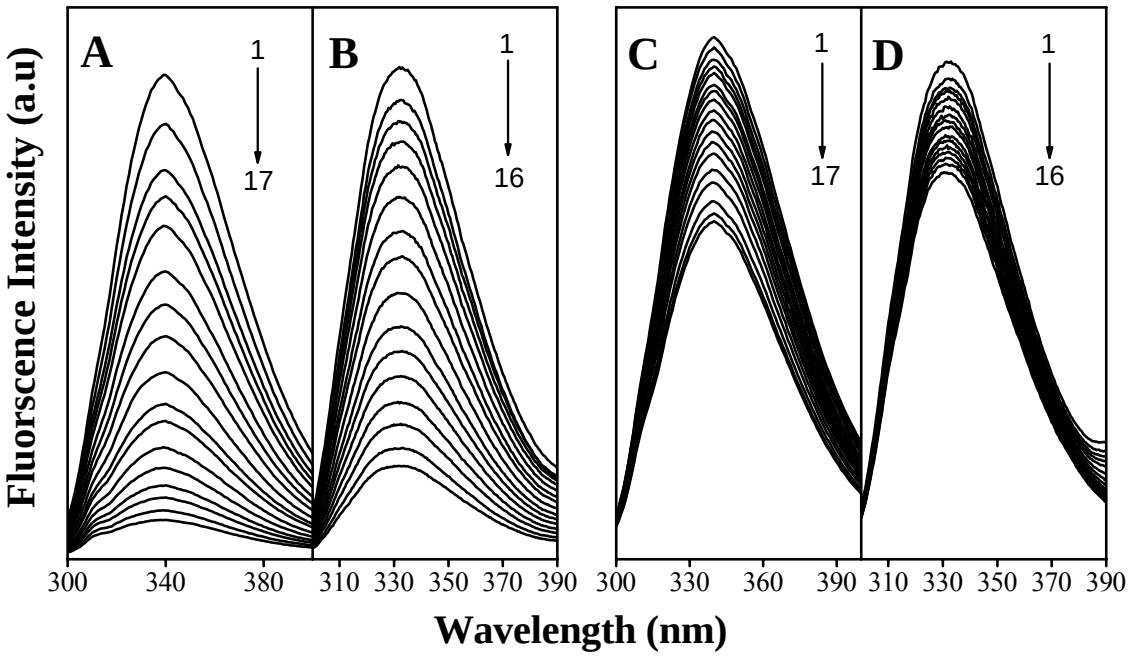

Fig. 5.2: Quenching of PDC-109 fluorescence by acrylamide (A and B) and iodide (C and D) in the native state and upon binding to DMPC membranes. A and C, native PDC-109; B and D, PDC-109 bound to DMPC membranes.

In order to investigate the effect of denaturation on the quenching with neutral and ionic quenchers, quenching studies were carried out with acrylamide and iodide ion upon denaturing the protein with 6 M guanidine hydrochloride (Gdn.HCl) in the absence and in the presence of 10 mM β-mercaptoethanol (β-ME). Denaturation results in a red shift of the emission maximum from 340 nm (for the native protein) to 348 nm in presence of 6 M Gdn.HCl, and to 349.5 nm in the presence of 6 M Gdn.HCl and 10 mM β-ME. The extent of quenching observed with 0.5 M acrylamide and I^- also increased to 96% and 47.4%, respectively, in the presence of 6 M Gdn.HCl. In the presence of 6 M Gdn.HCl and 10 mM β-ME, these values

increased further to 96.7% and 48.4%, respectively, for studies with acrylamide and iodide ion.

5.4.2. Stern-Volmer analysis of quenching data

The quenching data for the various quenchers was initially analyzed by the Stern-Volmer equation [Lehrer, 1971], which is given below:

$$F_o/F_c = 1 + K_{SV}[Q] \qquad (1)$$

where F_o and F_c are the respective fluorescence intensities, corrected for dilution, in the absence and presence of quencher, [Q] is the resultant quencher concentration and K_{SV} is the Stern-Volmer quenching constant of the protein for a given quencher. A plot of F_o/F_c as a function of [Q] is then referred to as a Stern-Volmer plot.

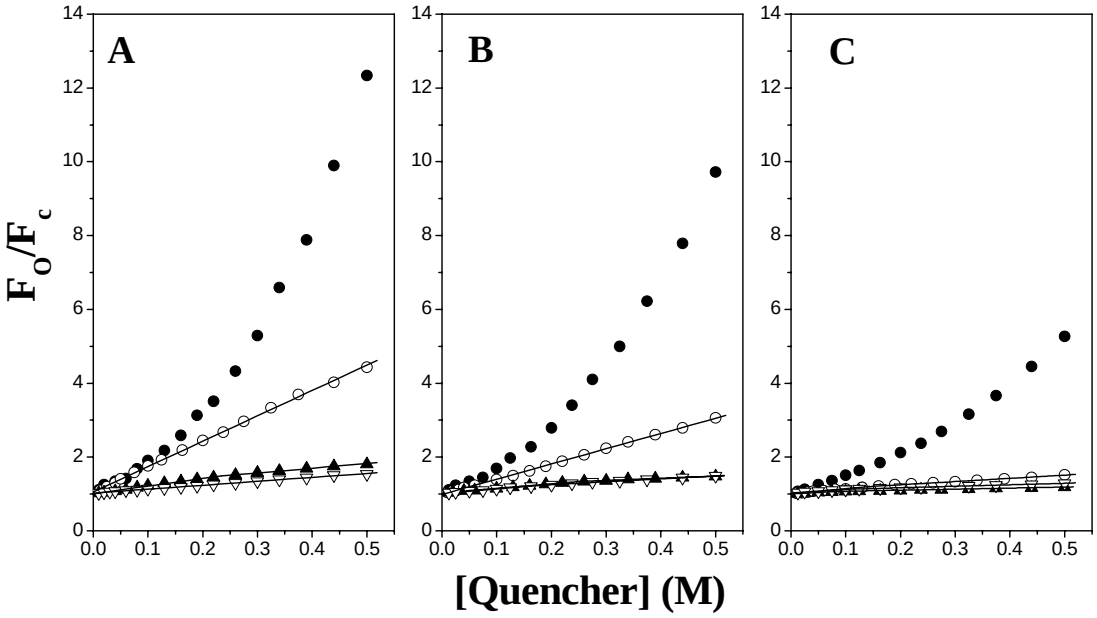

Fig. 5.3: Stern-Volmer plots of fluorescence quenching data for PDC-109 under different conditions. A) Native PDC-109, B) PDC-109 with bound *O*-phosphorylcholine, C) PDC-109 in the presence of DMPC small unilamellar vesicles. Quenchers used are: (●) acrylamide, (O) succinimide, (▲) cesium ion, (△) iodide ion.

Stern-Volmer plots of the quenching data for native PDC-109, PDC-109 in the PrC bound form and upon binding to DMPC SUVs, are shown in Figs. 5.3A, 5.3B and

5.3C, respectively. Each panel presents the Stern-Volmer plots for all the four quenchers. It is seen from this figure that under all conditions, Stern-Volmer plots for acrylamide quenching exhibit upward curvature, indicating that a combination of dynamic and static quenching mechanisms operate for this quencher. For succinimide, the Stern-Volmer plots are linear for the native PDC-109 and its PrC complex, but become biphasic (i.e., contain two linear parts that differ in the slope) upon binding to DMPC membranes. This is more clearly seen in Fig. 5.4, which gives the Stern-Volmer plots for succinimide, I^- and Cs^+ in the presence of Lyso-PC and DMPC. Further, it is seen that both I^- and Cs^+ also give biphasic plots with PDC-109

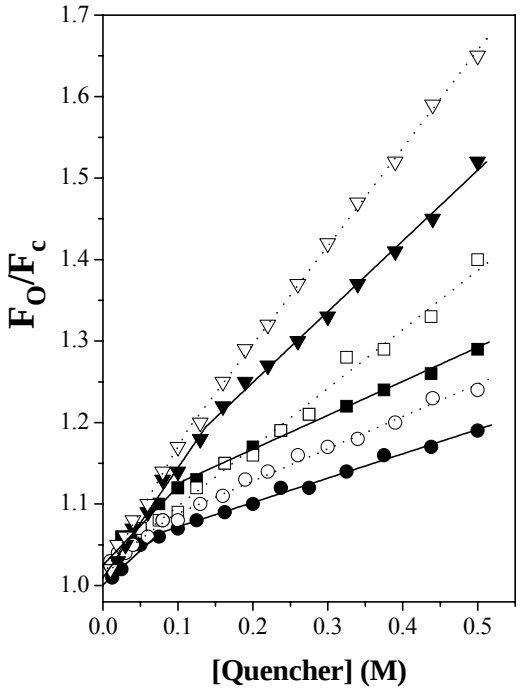

Fig. 5.4: Stern-Volmer plots of fluorescence quenching data for PDC-109 bound to Lyso-PC (open symbols) and DMPC (solid symbols). (▼,▽) succinimide, (■,□) iodide ion, (●,○) cesium ion.

when bound to Lyso-PC and DMPC. In addition, biphasic plots are also seen with I^- and Cs^+ for the native protein and its complex with PrC (not shown). From the slopes of the linear and biphasic plots obtained with different quenchers, Stern-Volmer

quenching constants, K_{SV1} and K_{SV2}, were determined and listed in Table 5.1. In addition, the corresponding bimolecular quenching constants, k_q ($k_q = K_{SV}/\tau_o$ where τ_o is the average lifetime of fluorescence decay) for succinimide, I^- and Cs^+ ion are also calculated from the K_{SV} values and the average lifetimes obtained from time-resolved fluorescence decay measurements (see Section 5.4.3). The values obtained are also listed in Table 5.1.

Table 5.1: Summary of parameters obtained from intrinsic fluorescence quenching and time-resolved fluorescence measurements on PDC-109.

Quencher/ Condition	K_{sv1} (M^{-1})	$k_{q1} \times 10^{-9}$ ($M^{-1}s^{-1}$)	K_{sv2} (M^{-1})	$K_{q2} \times 10^{-9}$ ($M^{-1}s^{-1}$)	Percent Quenching
Acrylamide					
Native	1.93	1.24	-	-	91.9
With 20 mM PrC	2.58	1.71	-	-	89.6
With 0.15 mM LysoPC	-	-	-	-	89.6
With 0.15 mM DMPC	0.51	0.32	-	-	81.0
In 6 M Gdn.HCl	1.69	0.66	-	-	96.0
In 6 M Gdn HCl &10 mM β-ME	2.29	1.02	-	-	96.7
Iodide					
Native	1.67	1.07	1.06	0.68	35.2
With 20 mM PrC	1.21	0.80	0.78	0.52	32.7
With 0.15 mM LysoPC	1.30	0.78	0.72	0.43	28.5
With 0.15 mM DMPC	0.95	0.61	0.41	0.26	22.3
In 6 M Gdn.HCl	1.74	0.68	-	-	47.4
In 6 M Gdn HCl 10 mM β-ME	1.91	0.85	-	-	48.9
Succinimide					
Native	6.87	4.40	-	-	77.4
With 20 mM PrC	4.12	2.91	-	-	67.3
With 0.15 mM LysoPC	1.61	0.96	1.22	0.73	39.8
With 0.15 mM DMPC	1.39	0.89	0.86	0.55	34.3
Cesium					
Native	2.07	1.35	1.24	0.79	44.8
With 20 mM PrC	1.24	0.82	0.59	0.39	32.7
With 0.15 mM LysoPC	0.68	0.41	0.40	0.24	19.4
With DMPC	0.81	0.52	0.29	0.19	15.6

When the Stern-Volmer plots show upward curvature, it is possible to analyze the quenching data by eq. (2), which allows the resolution of the static and dynamic components [Lakowicz, 1999]:

$$F_o/F_c = (1 + K_{SV}[Q])\,(1 + K_S[Q]) \qquad (2)$$

where K_{SV} is the dynamic Stern-Volmer quenching constant, K_S is the static quenching constant and [Q] is the quencher concentration. In this equation, the dynamic component of the quenching can be determined by lifetime measurements, according to the following expression [Lakowicz, 1999]:

$$\tau_o/\tau = 1 + K_{SV}[Q] \qquad (3)$$

where τ_o is the average lifetime of the fluorophores in the absence and τ is the average lifetime in the presence of the quencher at a concentration of [Q].

However, the upward curving Stern-Volmer plots obtained with acrylamide for PDC-109 under different conditions could not be resolved by eq. (2), as attempts to fit the data using this equation did not succeed. It is possible that the quenching data requires more than one dynamic and/or static quenching constants.

5.4.3. Lifetime measurements of fluorescence emission

The fluorescence decay curves of native PDC-109, in the presence of 0.15 mM DMPC and 6 M Gdn.HCl, obtained from the time resolved measurements, are given in Fig. 5.5. In addition, fluorescence lifetime measurements were also carried out in the presence of 20 mM PrC and 0.15 mM Lyso-PC. In each case, the decay curves could be best fitted to a biexponential function ($\chi^2 \leq 1.1$). Monoexponential fits gave considerably larger errors ($\chi^2 > 1.8$), whereas triexponential fits did not significantly reduce the errors. From the biexponential fits two decay times, τ_1 and τ_2 with corresponding weight factors, α_1 and α_2 were obtained for the Trp fluorescence of PDC-109 in all the above mentioned conditions. For native PDC-109, the lifetime

values were obtained as 1.07 and 2.72 ns ($\chi^2 \leq 1.05$), whereas in the presence of 0.15 mM DMPC the lifetimes obtained were 0.64 and 2.27 ns ($\chi^2 \leq 1.09$). For the protein denatured with 6 M Gdn.HCl, the biexponential fits yielded lifetime value of 0.95 and 3.15 ns ($\chi^2 \leq 1.13$), whereas for the protein in the presence of 6 M Gdn.HCl and 10 mM β-mercaptoethanol lifetime values of 0.88 and 2.76 ns ($\chi^2 \leq 1.04$) were obtained. These values, together with the values obtained in the presence of PrC and Lyso-PC are listed in Table 5.2.

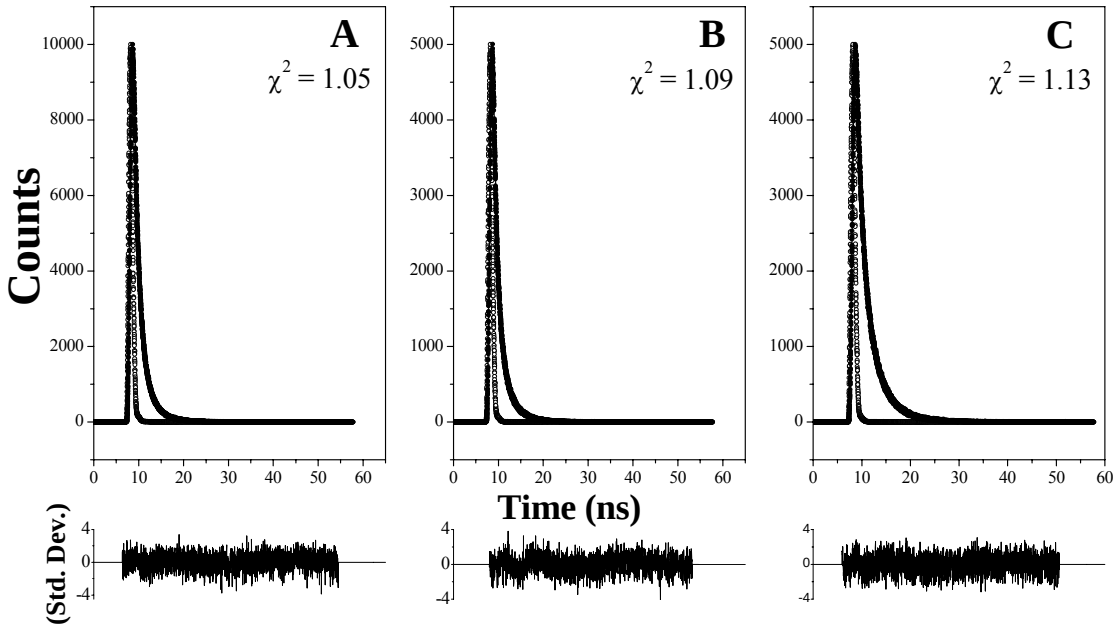

Fig. 5.5: Time-resolved fluorescene decay profiles. (A) native PDC-109, (B) in the presence of 0.15 mM DMPC, and (C) upon denaturation with 6 M Gdn.HCl. The solid lines correspond to the nonlinear least square fit of the experimental data to biexponential functions. The lower panels represent the residuals.

The average lifetimes of fluorescence decay for PDC-109 under different conditions were calculated from the values of lifetime, τ_i and the corresponding preexponential weighting factors, α_i, listed in Table 5.2, with the use of the following equations [Grinwald & Steinberg, 1974]:

$$\tau = \Sigma_i \alpha_i \tau_1 / \Sigma_i \alpha_i \qquad (5)$$

$$\langle\tau\rangle = \Sigma_i\alpha_i\tau^2_i/\Sigma_i\alpha_i\tau_i \qquad (6)$$

where τ and $\langle\tau\rangle$ are the average fluorescence lifetimes estimated by the two different approaches. For native PDC-109, values of τ and $\langle\tau\rangle$ are obtained as 1.42 and 1.56 ns, respectively. In the presence of 0.15 mM DMPC, these values change marginally to 1.06 and 1.57 ns respectively, whereas the corresponding values obtained in the presence of 20 mM PrC are 1.19 and 1.51 ns, respectively. Denaturation with 6 M Gdn.HCl and reduction with 10 mM β-ME increases the average lifetime to 2.56 and 2.25 ns, respectively. These values as well as the average lifetimes obtained in the presence of Lyso-PC and with denatured and reduced and denatured PDC-109 are presented in Table 5.2.

Analysis of the lifetime decay profiles also yielded the relative contributions of each component to the total fluorescence intensity. For native PDC-109, the component with the shorter lifetime of 1.07 ns contributed 80% of the total fluorescence intensity, with the remaining 20% intensity arising from the component with the longer lifetime of 2.72 ns. In the presence of 20 mM PrC, 0.15 mM Lyso-PC and 0.15 mM DMPC the contribution of the shorter lifetime decreased to about 65, 68 and 74%, respectively. Denaturation with 6 M Gdn.HCl and denaturation in the presence of β-ME resulted in the increases in the contribution of longer lifetime component to 45 and 46%, respectively.

In the presence of 0.5 M acrylamide and 0.5 M iodide lifetimes of both the shorter lifetime component and longer lifetime component decreased. For the native protein in the presence of PDC-109 the two lifetimes observed are 0.66 ns and 1.48 ns whereas the corresponding values obtained in the presence of 0.5 M iodide are 0.53 ns and 1.49 ns (Table 5.2). Under all conditions, both the lifetimes decreased significantly in the presence of acrylamide, clearly indicating the dominant

contribution of dynamic quenching process with this quencher, although the upward curving profiles have indicated the presence of some static component as well. For the native protein, in the presence of 0.5 M acrylamide contribution of the shorter lifetime component increased to 91%, whereas in the presence of 0.5 M concentration of the charged quencher I^-, it decreased to 63% of the total intensity. With acrylamide a moderate increase in contribution of the shorter lifetime component was observed under different conditions, except in the presence of PrC, where the longer lifetime component increased from 35 to 43% (Table 5.2).

Table 5.2: Lifetimes of fluorescence decay of PDC-109 under different conditions, the corresponding pre-exponential factors and the calculated average lifetimes.

Sample description	α_1	τ_1 (ns)	α_2	τ_2 (ns)	τ	$\langle\tau\rangle$
Native PDC-109	0.80	1.07	0.20	2.72	1.42	1.56
PDC-109 + 20 mM PrC	0.65	0.74	0.35	2.03	1.19	1.51
PDC-109 + 0.15 mM Lyso-PC	0.68	0.73	0.32	2.30	1.23	1.67
PDC-109 + 0.15 mM DMPC	0.74	0.64	0.26	2.27	1.06	1.57
PDC-109 in 6 M Gdn.HCl	0.55	0.95	0.45	3.15	1.94	2.56
PDC-109 in 6 M Gdn HCl + 10 mM β-ME	0.54	0.88	0.46	2.76	1.74	2.25
PDC-109 + 0.5 M iodide ion	0.63	0.53	0.37	1.49	0.89	1.12
PDC-109 + 0.5 M acrylamide under different conditions						
Native PDC-109	0.91	0.66	0.09	1.48	0.73	0.81
PDC-109 + 20 mM PrC	0.57	0.35	0.43	0.82	0.55	0.65
PDC-109 + 0.15 mM Lyso-PC	0.74	0.61	0.26	1.89	0.94	1.28
PDC-109 + 0.15 mM DMPC	0.79	0.54	0.21	1.98	0.84	1.25
PDC-109 in 6 M Gdn.HCl	0.72	0.66	0.28	2.01	1.04	1.39
PDC-109 in 6 M Gdn HCl + 10 mM β-ME	0.65	0.52	0.35	1.43	0.84	1.06

In order to estimate the dynamic quenching constants for acrylamide, which yielded upward curving Stern-Volmer plots, time-resolved fluorescence measurements were performed in the presence of different concentrations of acrylamide with PDC-109 in the native state, in the presence of 20 mM PrC or 0.15 mM DMPC, upon

denaturation with 6 M Gdn.HCl, and upon denaturation and reduction of the disulfide bonds with 10 mM β-mercaptoethanol. In each case the data could be best fit to biexponential functions and from the two lifetimes obtained the average fluorescence lifetime, τ was calculated using eq. (6). It has been observed in all cases that τ decreases linearly with increasing acrylamide concentration. From linear plots of τ_o/τ versus acrylamide concentration (Fig. 5.6), the dynamic quenching constant, K_{SV1}, were obtained. These values are also listed in Table 5.2.

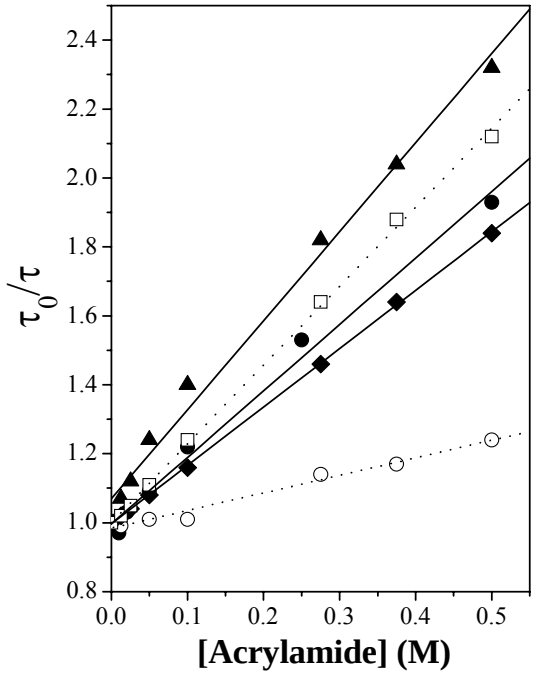

Fig. 5.6: Plots of τ_0/τ versus acrylamide concentration for the quenching of PDC-109 intrinsic fluorescence. (●) native protein, (O) in the presence of DMPC SUV, (▲) in the presence of 20 mM PrC, (◆) in the presence of 6 M Gdn.HCl, (□) in the presence of 10 mM β-ME and 6 M Gdn.HCl.

5.4.4. Red-edge excitation shift of tryptophan fluorescence

Red-edge excitation shift (REES) represents a unique and powerful approach that can be used to directly monitor the dynamics of the environment around a fluorophore in a complex biological system [Chattopadhyay, 2003]. The shift in the maximum of

fluorescence emission of the Trp residues of PDC-109 as a function of excitation wavelength under different conditions is shown in Fig. 5.7.

As the excitation wavelength is changed from 280 nm to 307 nm, the emission maximum of native PDC-109 is shifted from 340 nm to 344 nm for native protein, which corresponds to a REES of 4 nm. Further red shift may be observed if the sample can be excited at wavelengths beyond 307 nm; however, it was not possible to obtain reliable spectral data for excitation beyond 307 nm due to a combination of low signal/noise ratio and artifacts arising due to the presence of residual intensity from the solvent Raman peak that sometimes remained despite background subtraction. Interestingly, PDC-109 upon denaturation also shows a REES of 4 nm, with the wavelength of maximum emission shifting from 348 nm to 352 nm, when the excitation wavelength was shifted from 280 nm to 307 nm.

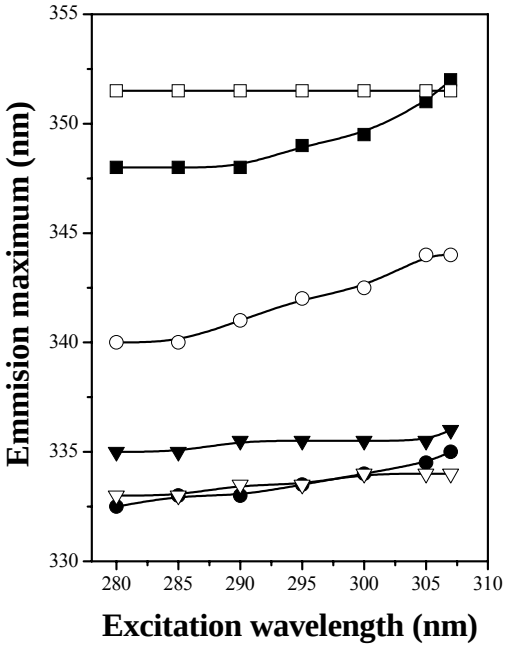

Fig. 5.7: Effect of changing excitation wavelength on the emission maximum of PDC-109. (○) native protein, (▼) in the presence of 20 mM PrC, (●) in the presence of 0.15 mM DMPC, (▽) in the presence of 0.15 mM Lyso-PC, (■) upon denaturation with 6 M Gdn.HCl. (□) corresponds to L-tryptophan in 6 M Gdn.HCl.

As already noted above, binding of PrC to PDC-109 results in a blue shift of the emission maximum from 340 nm to 335 nm, when excited at 280 nm. Increasing the excitation wavelength did not affect the wavelength of the emission maximum significantly; excitation at 307 nm resulted in a shift of the emission maximum to about 336 nm, that is, a REES of only 1 nm is observed. Binding of PDC-109 to DMPC SUV leads to a decrease in the REES to 2.5 nm, whereas upon binding to Lyso-PC micelles, the REES is further reduced to 1 nm.

5.5. Discussion

Among the three aromatic amino acids in proteins, namely tryptophan, tyrosine and phenylalanine, tryptophan is the dominant intrinsic fluorophore. The most valuable feature of the Trp fluorescence is its high sensitivity to the local environment. Changes are often observed in Trp emission spectra in response to conformational transitions in proteins, ligand binding or denaturation [Lakowicz, 1999]. Previous studies of Müller et al. [1998] have shown that fluorescence spectral properties of PDC-109 are significantly altered by its interaction with PrC, Lyso-PC micelles and DMPC SUV. This is consistent with the presence of Trp residues in the PrC binding site of the two Fn2 domains of PDC-109 [Wah et al., 2002]. In the light of these observations a detailed characterization of the fluorescence properties of PDC-109 has been taken up in this study. Experiments were performed with PDC-109 in the native state and upon ligand (PrC, Lyso PC and DMPC unilamellar vesicles) binding by several fluorescence approaches, viz., investigation of the steady-state fluorescence properties, quenching of the protein fluorescence by neutral as well as charged quenchers, time-resolved fluorescence studies and by red-edge excitation shift studies. The results obtained are discussed here.

Consistent with the results obtained by Müller et al. [1998], it was observed that the emission λ_{max} of PDC-109 is blue shifted upon interaction with PrC, Lyso-PC micelles and DMPC SUV (Fig. 5.1). These observations fully support the interpretation that upon binding of these ligands the microenvironment of Trp residues of PDC-109 becomes more hydrophobic [Müller et al., 1998]. It is likely that binding of PrC, the soluble head group moiety of phosphatidylcholine, results in the displacement of bound water molecules in the ligand binding site of the protein, thus making the environment of the tryptophan side chains in the binding site less polar. On the other hand, FTIR studies have shown that binding of PDC-109 to PC membranes results in conformational changes in the protein [Gasset et al., 2000] and the ESR studies presented in Chapter 2 have shown that upon binding to DMPC membranes part of the protein penetrates into the hydrophobic core of the membrane, at least up to the 14^{th} C-atom of the acyl chains. Therefore, it is possible that some of the Trp residues are buried in the membrane interior and thus experience a nonpolar environment.

Further investigations on the exposure and microenvironment of the Trp residues in PDC-109 were carried out by the solute perturbation technique employing small molecular weight quenchers. The polar but neutral molecules acrylamide and succinimide can diffuse into the protein interior and quench the fluorescence of even partially buried Trp residues, whereas the charged species, Cs^+ and I^- can quench only surface-exposed Trp residues and their quenching efficiency will be affected by the presence of charged residues in the neighborhood of the fluorophores. Thus by the use of all the above four quenchers one can obtain complementary information regarding the exposure of the Trp residues of proteins [Lakowicz, 1999; Kenoth & Swamy, 2003; Sultan & Swamy, 2005].

The emission λ_{max} observed at 340 nm (spectrum 1, Fig. 5.2A) indicates that Trp residues are the major contributors to the fluorescence of PDC-109 and that the indole side chains are partially exposed to the aqueous medium. The slight blue shift in the emission λ_{max} upon quenching with 0.5 M acrylamide (spectrum 17, Fig. 5.2A), suggests that there is some heterogeneity in the microenvironment of the Trp residues and shows that the more solvent exposed Trp residues are more readily quenched by acrylamide.

The red shift in the emission maximum of PDC-109 to 348 nm upon denaturation with 6 M Gdn.HCl indicates greater exposure of the Trp residues to the polar aqueous environment. This is also evident from the increase in the extent of quenching observed for the quenchers in the presence of 6 M Gdn.HCl. The further red shift in the emission λ_{max} to 349.5 nm when PDC-109 was denatured in the presence of β-ME indicates the complete exposure of the Trp residues to the solvent because Trp alone in water emits around 350 nm [Lakowicz, 1999]. These results suggest that some residual structure that is present in the unreduced, but denatured protein, becomes completely unordered, or nearly so, when the disulfide bonds are broken.

The quenching data presented in Table 5.1 demonstrate that interaction of phosphorylcholine and choline phospholipids, Lyso-PC and DMPC, alters the accessibility of Trp residues to the quenchers, indicating that ligand-induced conformation changes modify the penetration of the quencher into the protein matrix. Quenching profiles obtained with acrylamide for native PDC-109 and for PDC-109 in the presence of different ligands, which show a positive curvature, clearly indicate that the quenching has both dynamic and static components. While the dynamic quenching constant could be estimated by time-resolved fluorescence measurements (Tables 5.1 and 5.2), it was not possible to estimate the static quenching constants by

analyzing the quenching data according to eq. (2). This suggested that the mechanism of quenching by acrylamide may be more complex, involving more than one static quenching constant. Because each PDC-109 molecule has 5 Trp residues, in principle they can give rise to 5 sets of static and dynamic quenching constants.

While the Stern-Volmer plots obtained with succinimide are linear for the quenching of native PDC-109 as well as in the presence of the soluble ligand, PrC, the Stern-Volmer plots obtained with both I^- and Cs^+ are biphasic (Fig. 5.3). This clearly indicates that while the neutral succinimide is able to access all the Trp residues with equal facility, the charged quenchers see a heterogeneity in the Trp environment. This is consistent with the inability of I^- and Cs^+ to penetrate into the protein interior. However, the quenching profiles with succinimide also become biphasic when the protein is bound to Lyso-PC micelles and DMPC SUV. This indicates that in the presence of Lyso-PC and DMPC, some of the fluorophores are less accessible even to this neutral quencher and strongly supports the interpretation that part of the protein penetrates into the membrane interior [Müller et al., 1998; Ramakrishnan et al., 2001], with some of the Trp residues deeply embedded in the hydrophobic core.

As PDC-109 contains 5 Trp residues, the REES of 4 nm observed with the native protein (corresponding to a shift in the excitation wavelength from 280 nm to 307 nm) is likely to be an average effect; however, such an effect implies that the water molecules in the vicinity of at least some of the Trp residues experience a rather restricted motion resulting in their significant slowing down of their reorientation. Interestingly, PDC-109 upon denaturation also shows a REES of 4 nm, with the wavelength of maximum emission shifting from 348 nm to 352 nm, when the excitation wavelength was shifted from 280 nm to 307 nm. With erythroid spectrin also the Trp fluorescence exhibited a REES of 3 nm upon denaturation, which was interpreted as due to the retention of some of the structural and dynamical features of

the microenvironment of the Trp residues even after denaturation [Chattopadhyay et al., 2003]. Thus the observation REES with denatured PDC-109 indicates that the microenvironment of the Trp residues in this protein is retained to a significant extent, such that even after denaturation reorientation of the solvent water molecules surrounding them is rather restricted. It is possible that some ordered water molecules are retained in the vicinity of the Trp residues. Alternately, some residual order may remain in the protein structure because of the presence of the disulfide bonds in the protein, which restricts the motion of some of the Trp residues and the water molecules in their vicinity.

In the PrC-bound form, PDC-109 exhibits a REES of only 1 nm, that is a shift of the emission maximum from 335 nm to 336 nm. This is significantly smaller than the REES of 4 nm observed with the native protein and implies that the restricted motion of the water molecules in the neighborhood of the Trp residues, which leads to the observed REES with the native protein, is not seen upon binding of PrC. As mentioned earlier, the blue shift in the emission maximum of PDC-109 resulting from PrC binding indicates that the environment of the Trp residues becomes less polar, and suggests that water molecules may be removed from the binding site when the ligand binds. Therefore, it is likely that when PrC binds to PDC-109 the water molecules that are in the microenvironment of the Trp residues in the ligand binding site are removed and hence the REES is reduced. Alternately, the reduction in the REES, resulting from the binding of PrC may be related to the change in the oligomeric state of the protein, which exists as a polydisperse aggregate in the native form but dissociates to yield dimers upon binding of PrC [Gasset et al., 1997]. It is possible that in the aggregated protein, the solvent water molecules in the proximity of Trp residues relax more slowly than in the dimer.

The reduction in the REES when PDC-109 is bound to Lyso-PC micelles (1 nm) and DMPC vesicles (2.5 nm) shows that upon binding to DMPC or Lyso-PC, the Trp environment is more dynamic than in the native form. That is, a majority of the Trp residues of PDC-109 are in a more dynamic environment in the membrane bound form. It has been shown by Chattopadhyay and Mukherjee that the rates of solvent relaxation in membranes are depth-dependent, and the deeper regions of membrane display less-pronounced red-edge effects [Chattopadhyay & Mukherjee, 1999a,b]. Thus it would appear that upon binding to the DMPC membranes and Lyso-PC micelles, a majority of the Trp residues in PDC-109 would be deeply embedded into the membrane interior. This is consistent with the spin label ESR studies and hydropathy analysis presented in Chapter 2. Spin label ESR studies indicated that upon binding to PC membranes, segments of PDC-109 penetrate into the membrane interior and directly interact with the lipid acyl chains up to the 14^{th} C-atom of the *sn*-2 acyl chain. Hydropathy analysis suggested that regions of PDC-109 corresponding to residues 43-76 and 82-100 may preferentially partition into the interfacial region of the membrane, which could result in the penetration of shorter regions into the hydrophobic core of the membrane; in particular, regions corresponding to residues 43-50 and 90-96 were predicted to penetrate into the membrane interior. Pertinently, three of the five Trp residues of PDC-109, namely W47, W90 and W93 are present in these two regions, strongly suggesting that they may reside in the membrane interior when bound to DMPC liposomes.

In summary, the fluorescence properties of PDC-109 have been investigated in this chapter by a variety of approaches. Quenching studies indicate that ligand binding shields the Trp residues from different quenchers, with shielding ability following the order: PrC < Lyso-PC < DMPC, indicating that while the protein binds to PC containing membranes by specific recognition of the phosphorylcholine moiety,

the acyl chains of the lipid also interact with the protein, resulting in a further tightening of the protein structure. Results obtained from REES experiments suggested that when PDC-109 binds to choline phospholipid membranes some of the Trp residues of the protein most likely get embedded in the hydrophobic interior of the membrane.

Chapter 6

Isothermal Titration Calorimetric studies on the Interaction of PDC-109 with Phospholipid Membranes and Micelles

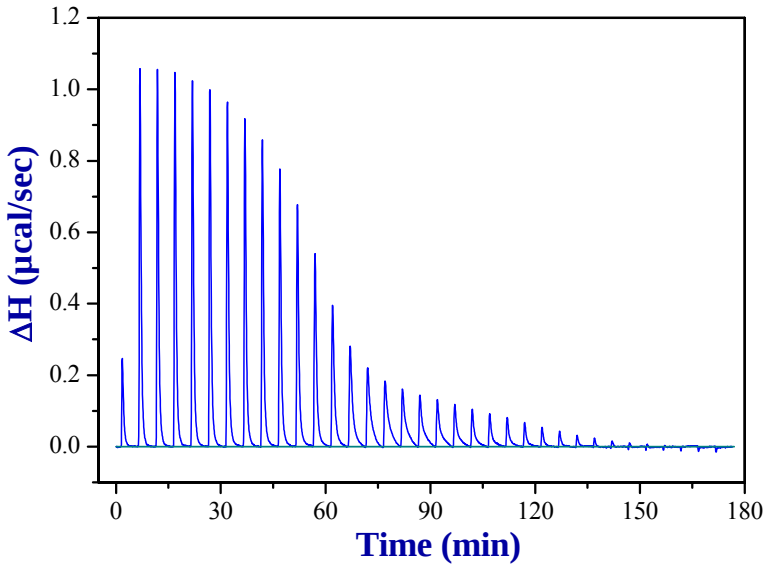

Raw ITC data for the titration of protein with lipid

Anbazhagan, V. *and Swamy, M.J. Isothermal titration calorimetric study on the interaction of PDC-109, the major protein from bovine seminal plasma with Phospholipid membranes and micelles.* (to be communicated)

6.1. Summary

The interaction of PDC-109 with phospholipid membranes and Lysol-PC micelles was investigated by isothermal titration calorimetry (ITC). Binding of PDC-109 to dimyristoylphosphatidylcholine and dipalmitoylphosphatidylcholine (DPPC) small unilamellar vesicles were analyzed in terms of a single type of binding sites on the protein for the choline phospholipids. The stoichiometry of binding for the PDC-109/DMPC interaction was determined as 7.4 lipids per protein monomer at 20°C, but increased at lower temperatures. At 20°C, the binding constant, K_a, and thermodynamic parameters, ΔG^o, ΔH^o and ΔS^o for this interaction were found to be $(4.39 \pm 0.04) \times 10^5$ M^{-1}, -7.58 kcal.mol^{-1}, 4.05 ± 0.05 kcal.mol^{-1} and 39.6 cal.mol^{-1}.K^{-1}, respectively. Qualitatively similar results were obtained for the interaction of PDC-109 with DPPC membranes. These observations indicate that binding of PDC-109 to choline phospholipids is entropically favored with negative contribution from enthalpy of binding. Enthalpies and entropies of binding to both DMPC and DPPC increased with increase in temperature, with large positive changes in the heat capacities (ΔC_p), which could be due to an increase in the exposure of the hydrophobic region of the membrane to water, or due to the membrane incorporation of some polar residues of the protein. Enthalpy-entropy compensation was observed for the interaction of PDC-109 with PC membranes, suggesting that water structure plays an important role in the binding process. Also, the slope of the enthalpy-entropy plot was estimated as 0.67, which is consistent with entropic contributions driving the binding reaction. Binding data for the interaction of PDC-109 with Lyso-PC micelles could not be satisfactorily analyzed with one type of binding sites; it was necessary to invoke two sets of binding sites on the protein – one set of low-affinity sites (with a K_a of 6.9×10^3 M^{-1} at 20°C) and another set of high-affinity sites (with a K_a of 9.79×10^5 M^{-1} at 20°C). Binding to both these sites is exothermic with ΔH^o values of -17.56 ±

0.33 kcal.mol^{-1} and -2.58 ± 0.44 kcal.mol^{-1}, for the low and high affinity sites, respectively, at 20^{o}C. K_a values for Lyso-PC binding to the low affinity sites increase with temperature whereas those for the high affinity sites decrease with increase in temperature. The thermodynamic parameters indicate that Lyso-PC binding to the high affinity sites is favored by both entropic and enthalpic contributions, with the entropic contribution being larger, whereas binding of Lyso-PC to the low-affinity sites is enthalpically driven, with a negative entropic contribution.

6.2. Introduction

In view of the ability of PDC-109 to induce cholesterol efflux from sperm cell plasma membranes [Thérien et al., 1998], it is important to understand the molecular basis of interaction of the various components to the protein. Studies reported in Chapters 2-5 have shown that PDC-109 penetrates into the hydrophobic interior of the membrane up to the 14th C-atom of lipid acyl chains [Ramakrishnan et al., 2001; Swamy et al., 2002] and that the higher affinity of PDC-109 for choline phospholipids is due to faster association and slower dissociation rate constants for PC as compared to other phospholipids [Thomas et al., 2003]. Further, it has been shown that although the binding of choline phospholipids is due to the specific recognition of the phosphorylcholine moiety, the glycerol back bone and acyl chains of the lipid also interact positively with the protein, thus stabilizing the binding significantly [Anbazhagan and Swamy, 2005]. Finally, the fluorescence spectroscopic studies reported in Chapter 5 indicated that upon binding of PDC-109 some of the Trp residues get deeply embedded in the interior of the membrane.

Although the above studies have yielded considerable valuable information on the specificity of PDC-109 to various lipid membranes and mechanism of its

interaction with phospholipid membranes, a complete thermodynamic description of the binding of this protein to phospholipids was not reported. In the studies reported in this chapter, the interaction of PDC-109 with several phospholipids was investigated by employing isothermal titration calorimetry (ITC). The effect on cholesterol on the binding of PDC-109 to phosphatidylcholine membranes was also investigated by ITC. The energetics of binding of Lyso-PC micelles and phospholipid bilayers were compared and analyzed to understand the nature of the interactions involved in the binding process.

6.3. Materials and Methods

6.3.1. Materials

Phosphorylcholine chloride (Ca^{2+}), choline chloride and tris(hydroxymethyl)-aminomethane (Tris base) were obtained form Sigma (St. Louis. MO). Sephadex G-50 (superfine) and DEAE Sephadex A-25 were purchased from Pharmacia Biotech (Uppsala, Sweden). DMPC, DMPG, DMPE, Lyso-PC, cholesterol, dipalmitoylphosphatidylcholine (DPPC), dioleylphophatidylcholine (DOPC) and dioleylphosphatidylethanolamine (DOPE) were obtained from Avanti Polar Lipids (Alabster, AL). PDC-109 was purified from bovine seminal plasma from healthy and reproductively active bulls as reported in Chapter 2. All other chemicals used were of analytical grade and obtained from local suppliers.

6.3.2. Preparation of liposomes

Either phospholipid alone or a mixture of lipid and cholesterol, dissolved in dichloromethane was taken in a glass tube to give the desired final composition. The solvent was evaporated under a gentle stream of nitrogen and then subjected to

vacuum-desiccation for at least 4 hours. The dried lipid mixture was then hydrated above the gel-fluid phase transition temperature by vortexing for 5 minutes with Tris buffered saline (50 mM Tris-HCl, pH 7.4, 150 mM NaCl, 5mM EDTA and 0.025 % NaN_3). Multilamellar vesicles (MLVs) were prepared by 8 freeze thaw cycles to get a homogenous suspension. Small unilamellar vesicles (SUV) were prepared by sonication of the lipid suspension in a bath sonicator for 30 min at room temperature.

6.3.3. Turbidimetry

Binding of PDC-109 to phospholipid multilamellar vesicles was investigated by turbidimetry. Sample turbidity was measured at 333 nm with increasing protein concentration using an Analytikjena Spekol 1200 UV-Vis single beam spectrophotometer using a 1-cm pathlength cell.

6.3.4. Isothermal titration calorimetry

Isothermal titration calorimetry experiments were performed using a Microcal high-sensitivity VP-ITC instrument (Northampton, MA, USA). Solutions were degassed under vacuum prior to use. Binding of PDC-109 to phosopholipid membranes and Lyso-PC micelles was studied at various temperatures as follows. Typically, 25-50 consecutive injections of 5 μL aliquots of the protein (250-500 μM in protomer) were injected from the syringe into the cell of 1.445 mL filled with 24 – 90 μM of lipid (unless otherwise indicated), present as SUV. To minimize the contribution to binding heat from dilution, the final dialyzate obtained after the protein was dialyzed was used to hydrate the lipid film which was then sonicated as described above to obtain the SUV. Injections were made at intervals of 180sec, and to ensure proper mixing during and after each injection, a constant stirring speed of 300 rpm was maintained during the experiment. Control experiments were performed by titrating PDC-109 solution into a buffer solution and the resulting heats were subtracted from

measured heats of binding. The binding curves were analyzed using the Origin software provided by Microcal. The equilibrium association constant (K_a), the enthalpy of binding (ΔH^o), and the stoichiometry parameter (n, the number of lipid molecules bound per each protein molecule (monomer of PDC-109)) were obtained from curve fitting of the experimental data to '*one set of sites*' model for DMPC. The areas under the peaks correspond to the heat released during the reaction, resulting from the addition of the protein/lipids into the solution containing SUVs/PDC-109. The values of K_a and ΔH^o obtained from curve fitting were used to calculate the standard free energy change (ΔG^o) and the standard entropy change (ΔS^o) for the binding using the equation:

$$\Delta G^o = -RT\ln K_a = \Delta H^o - T\Delta S^o$$

6.4. Results

6.4.1. Binding and soulbilization of phospholipid membranes by PDC-109

The binding of PDC-109 to multilamellar vesicles of phospholipids indicated that binding results in a partial solubilization of the vesicles as could be observed by a decrease of the sample turbidity. In the studies reported in Chapter 2 this property was utilized to investigate the binding of PDC-109 to multilamellar vesicles (MLVs) of DMPC and DMPC/cholesterol by turbidimetry. Here the turbidimetric analysis has been extended to investigate the binding of PDC-109 to other phospholipids, namely DMPG and DMPE. To make an appropriate comparison of the data collected under similar conditions, the experiment with DMPC was performed again. Fig. 6.1 gives the results of binding experiments where the turbidity of MLVs of phospholipid was monitored at 333 nm as a function of protein concentration. From this figure, it is seen that turbidity of the DMPC sample decreases initially rather steeply upon

addition of PDC-109 and then decreases more gradually as the protein concentration is increased further. Qualitatively similar results were obtained with DMPG, although considerably higher concentrations of the protein were required to decrease the turbidity of the DMPG membranes to a comparable level, indicating the lower affinity that characterizes the interaction of phosphatidylglycerol with PDC-109. On the other hand, turbidity of DMPE MLVs was practically unaffected by the addition of increasing concentrations of PDC-109, clearly showing that PDC-109 exhibits little or no interaction with phosphatidylethanolamine, which is consistent with earlier reports [Ramakrishnan et al., 2001; Thomas et al., 2003].

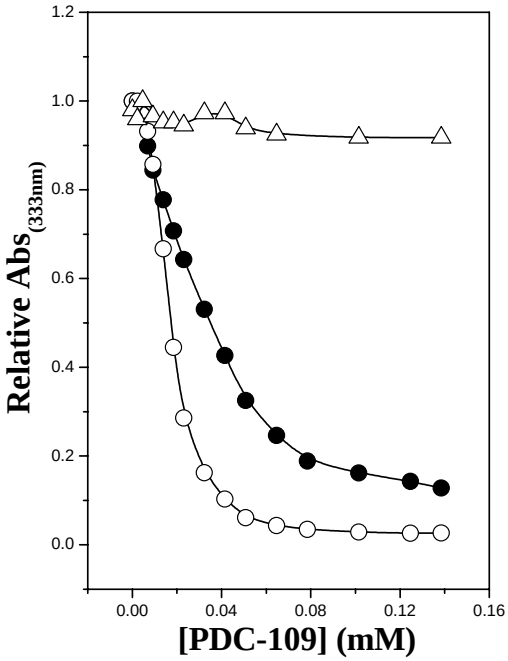

Fig. 6.1: Binding of PDC-109 to phospholipids multilamellar vesicles, monitored by turbidimetry. (●) DMPC; (○) DMPG and (Δ) DMPE. The samples were subjected to 7 free-thaw cycles, and the turbidity was measured spectrophotometrically at 333 nm.

6.4.2. *Thermodynamics of PDC-109 binding to phospholipid SUVs*

Thermodynamic parameters characterizing the interaction of PDC-109 with different phospholipids were obtained from ITC studies. Initial studies were carried out with

phosphatidylcholines because earlier studies, including those reported in chapters 2-5 clearly show that PDC-109 specifically recognizes choline phospholipids. Figures 6.2A and 6.2B show representative ITC profiles for the binding of PDC-109 to DMPC

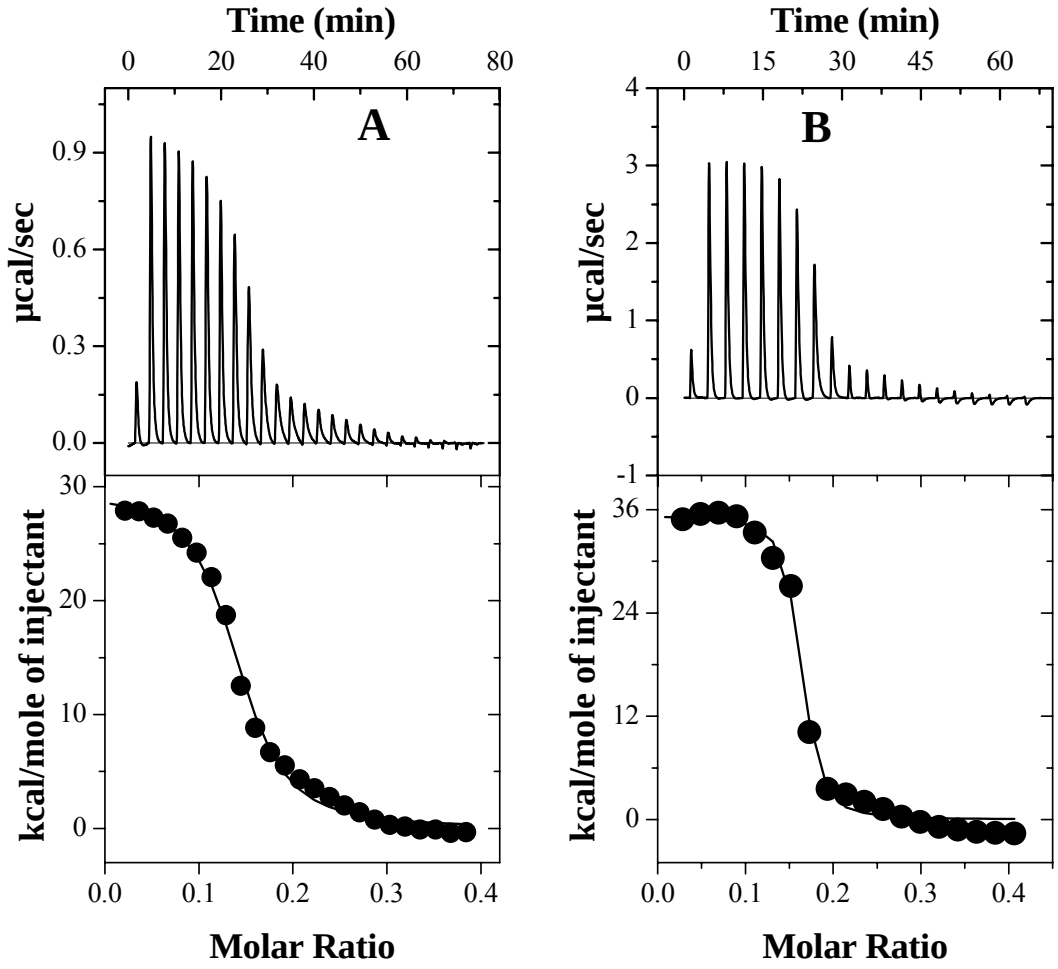

Fig. 6.2: Calorimetric titrations of PDC-109 with (A) DMPC at 20°C and (B) DPPC at 39°C. Injection volumes were 5 µL in both cases. The upper panels show the raw data for the titration of 88 and 87 µM lipid vesicles with 250 and 500 µM of protein for DMPC and DPPC, respectively. The lower panels show the integrated data obtained from the raw data shown in the upper panel, after subtracting the dilution experiments. The solid line in the bottom panels represents the best curve fit to the experimental data, using the '*one set of sites*' model from Microcal Origin.

and DPPC small unilamellar vesicles at 20°C and 39°C, respectively. Injection of 5 µL aliquiots of PDC-109 into the suspension of DMPC and DPPC resulted in large

endothermic peaks, indicating that the binding process is associated with positive enthalpy change. The magnitude of the endothermic peaks decreased with increase in injection number, showing saturation of the binding sites at high protein concentrations. The data could be fit satisfactorily by nonlinear least squares method to '*one set of sites*' binding model from Microcal Origin. Stoichiometry (*n*) and thermodynamic parameters ΔG^o, ΔH^o and ΔS^o for the binding of DMPC and DPPC to PDC-109 at different temperatures, obtained from this analysis, are listed in Table 6.1. The association constant, K_a, and the thermodynamic parameters ΔG^o, ΔH^o and ΔS^o for the binding for DMPC at 20°C were determined to be 4.39 (± 0.04) × 10^5 M^{-1}, -7.58 k.cal.mol^{-1}, 4.05 (± 0.05) kcal.mol^{-1}, and 39.6 cal.$mol^{-1}.K^{-1}$, respectively. Corresponding parameters obtained for the PDC-109/DPPC interaction at 39°C were found to be 2.45 (± 0.65) × 10^6 M^{-1}, -9.13 kcal.mol^{-1}, 5.45 (± 0.09) kcal.mol^{-1}, and 46.7 cal.$mol^{-1}.K^{-1}$, respectively. These values indicate that the binding of PDC-109 to both DMPC and DPPC is governed by a positive entropic contribution, which more than compensates the positive enthalpy value that contributes negatively towards the binding process.

The turbidimetric studies presented in Fig. 6.1 indicate that PDC-109 exhibits some interaction with DMPG whereas it does not interact with DMPE. In order to investigate whether these observations could be verified by calorimetric titrations, ITC experiments were carried out with both DMPG and DMPE. Titration of DMPE SUV with PDC-109 yielded isotherms that were comparable to those obtained when protein was injected into buffer, suggesting that the interaction is too weak to be observed by this method. On the other hand, titration of DMPG SUV with PDC-109 gave detectable and reproducible changes in the enthalpy and the data could be analyzed by the '*one set of sites*' model (Fig. 6.3), and the parameters obtained form the analysis are presented in Table 6.1. It is seen from this Table that binding of PDC-109 to

DMPG is also driven by entropic forces, with enthalpy of binding contributing negatively towards the binding process. However, the K_a value of 4.0×10^3 M^{-1} and the stoichiometry of 80 (± 34) lipids per protomer of the protein indicate that the binding of PDC-109 to this lipid is considerably weaker than its interaction with DMPC and DPPC.

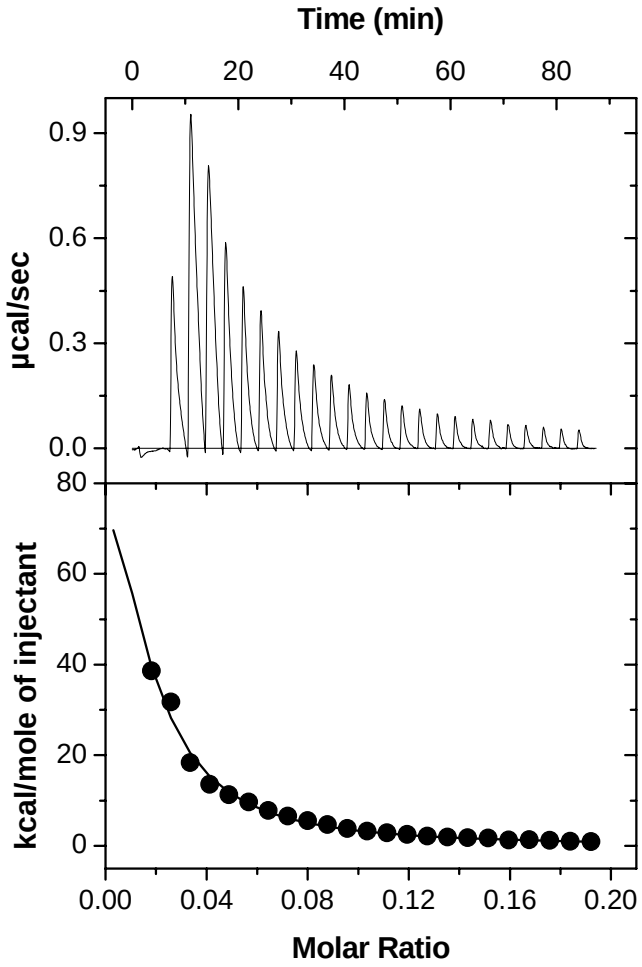

Fig. 6.3: Titration calorimetry of PDC-109 binding to DMPG SUVs at 20°C. Aliquots of PDC-109 (5 µL) from a 460 µM stock solution in the syringe were added to the lipid suspension (210 µM) in the sample cell. The upper panel shows the raw data for the titration and the lower panel shows the integrated data obtained from the raw data, after subtracting the control data from a dilution experiment. The solid line in the lower panel corresponds to the non-linear least squares fit to '*one set of sites*' model. Temperature = 20°C.

Table 6.1: Temperature dependence of the thermodynamic parameters for the binding of PDC-109 to phospholipids. The binding data were analyzed in terms of a '*one set of sites*' model.

Temp. (^oC)	n	K $\times 10^{-5}$ (M^{-1})	$-\Delta G^o$ ($kcal.mol^{-1}$)	ΔH^o ($kcal.mol^{-1}$)	ΔS^o ($cal.mol^{-1}.K^{-1}$)
DPPC					
20	21.4 ± 2.00	0.41 ± 0.19	6.20 ± 0.12	0.54 ± 0.04	22.9
25	13.4 ± 0.58	0.98 ± 0.33	6.82 ± 0.09	1.36 ± 0.06	27.4
30	8.72 ± 0.17	2.58 ± 0.66	7.51 ± 0.64	4.2 ± 0.10	38.6
36	7.10 ± 0.04	29.6 ± 6.3	9.16 ± 0.94	5.54 ± 0.06	47.5
39	6.48 ± 0.06	24.5 ± 6.5	9.13 ± 0.97	5.50 ± 0.09	46.7
DMPC					
10	21.7 ± 0.56	3.10 ± 0.83	7.12 ± 0.04	1.18 ± 0.04	29.3
15	13.9 ± 0.75	3.89 ± 0.05	7.38 ± 0.01	2.12 ± 0.11	33.0
20	7.35 ± 0.13	4.39 ± 0.04	7.58 ± 0.02	4.05 ± 0.05	39.6
DMPG					
20	80.2 ± 34	0.04 ± 0.02	4.77 ± 0.54	2.16 ± 0.01	23.6

6.4.3. Effect of temperature

The effect of temperature on the thermodynamic parameters associated with the binding was investigated by ITC at different temperatures between 10 and 39^{o}C for PDC-109 interacting with SUV of DMPC and DPPC. The data presented in the Table 6.1 show that the number of lipid molecules corresponding to each bound protein decreases with increasing temperature, whereas the binding enthalpies, entropy and binding constant (K_a) increase with temperature (Fig. 6.4). Fig. 6.4A and 6.4B show that ΔH^o and ΔS^o show a linear temperature dependence. The K_a values for DMPC are linear in the range studied (Fig. 6.4C), but for DPPC the values increase in a linear fashion initially, but steep, non-linear increase is seen at higher temperatures. From the slopes of the linear least squares fits of the enthalpy data, shown in Fig. 6.4A, the heat capacity changes (ΔC_p) were obtained as 287 and 289 $cal.mol^{-1}.K^{-1}$ for the binding of DMPC and DPPC, respectively.

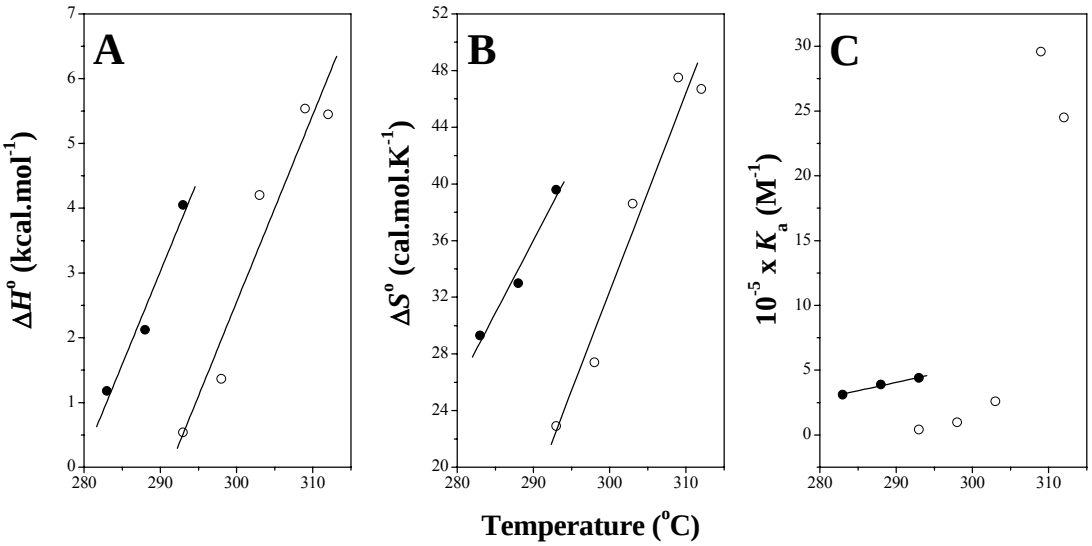

Fig. 6.4: Temperature dependence of (A) reaction enthalpies, (B) entropies and (C) association constants for PDC-109 binding to DMPC (●) and DPPC (○) SUV. From the slope of the linear least squares fits in A, the ΔC_p values were obtained.

6.4.4. Effect of PDC-109 on lipid phase transition

The ITC experiments described above, in which the interaction of PDC-109 with DMPC and DPPC SUV was investigated, were all done below the gel-liquid crystalline phase transition. In order to investigate the effect of the phase structure of the lipid on the thermodynamics of the binding, calorimetric titrations were also carried out with DMPC, DPPC and DOPC in their liquid crystalline phase. Isotherms obtained at 30^{o}C with DMPC and at 20^{o}C with DOPC are shown in Fig. 6.5. In sharp contrast to the isotherms obtained with DMPC and DPPC in the gel phase, the isotherms obtained in the liquid crystalline phase indicate that the binding of PDC-109 to these choline phospholipids is associated with an exothermic heat of binding for the initial injections, which become endothermic as the titration progresses. A qualitatively similar binding isotherm was obtained when DPPC in the liquid crystalline phase (45^{o}C) was titrated with PDC-109. However, these data could not be fit satisfactorily by the '*one set of sites*' model or the '*two sets of sites*' model or the

'*sequential binding*' model. Hence no further experiments were carried out in the liquid crystalline phase with these lipids.

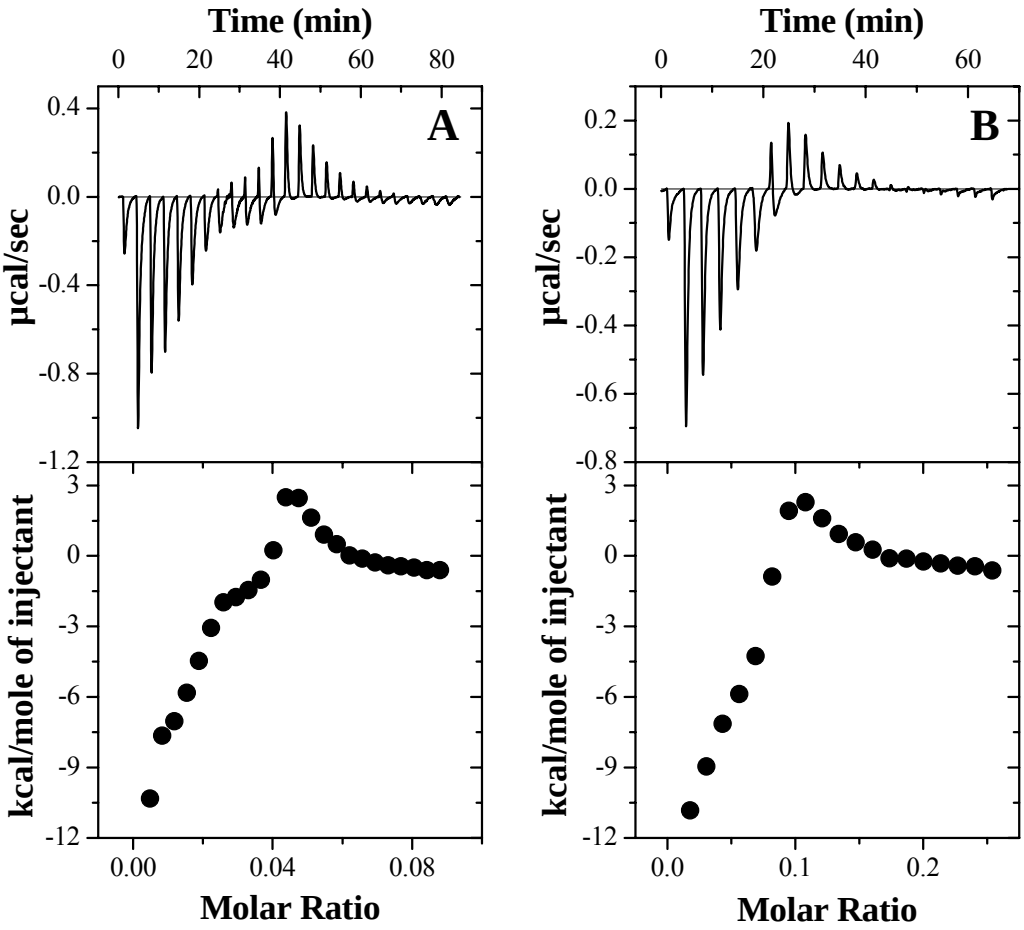

Fig. 6.5: Titration calorimetry of (A) DMPC at 30°C and (B) DOPC SUVs at 20°C with PDC-109. Aliquots of PDC-109 (5 µL each) were added to the lipid suspension in the sample cell. The upper panels show the raw data from the calorimetric titrations. The corresponding heats of reaction obtained by integration of the raw data are given in the lower panels.

6.4.5. Effect of cholesterol on the binding of PDC-109 to phosphatidylcholine membranes

In order to investigate the influence of cholesterol on the binding of PDC-109 to DMPC model membranes, ITC studies were carried out with DMPC SUV containing

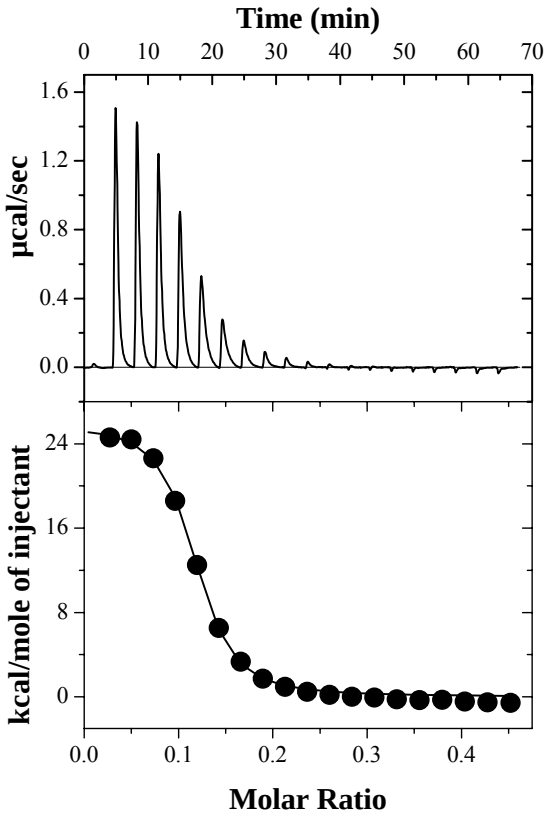

Fig. 6.6: ITC data for binding of PDC-109 to DMPC SUVs containing 25 mol% cholesterol at 20°C. The upper panel shows a calorimetric traces, each peak corresponds to the injection of 5 µL of lipid suspension into the reaction cell (V = 1.43 mL). Heat of reaction as a function of injection number obtained by integration of the calorimeter traces are given in the bottom panel. The heat of dilution was measured in a separate control experiment and was subtracted for calculation of the binding isotherm.

25 mol% cholesterol. A representative calorimetric titration performed at 20°C, depicting the injection of 5 µL aliquots of 500 µM PDC-109 into the reaction vessel containing 76 µM DMPC/cholesterol (25 mol% cholesterol) is shown in Fig. 6.6. From this figure it is seen that the binding reaction is endothermic, and that the heat change associated with each injection decreases monotonically with increase in the injection number until saturation is achieved (Fig. 6.6). The data could be satisfactorily analyzed by a nonlinear least squares fit to '*one set of sites*' model. The

Table 6.2: Temperature dependence of the thermodynamic parameters for the binding of PDC-109 to DMPC/cholesterol mixture. The data were analyzed in terms of a '*one-set of sites*' model.

Temp. (^{o}C)	n	K_a $\times 10^{-5}$ (M^{-1})	$-\Delta G^o$ kcal.mol^{-1}	ΔH^o kcal.mol^{-1}	ΔS^o cal.mol^{-1}.K^{-1}
10	21.5 ± 0.87	2.13 ± 0.35	6.91 ± 0.24	1.17 ± 0.04	27.6
15	11.0 ± 0.12	2.60 ± 0.25	7.15 ± 0.05	2.24 ± 0.02	32.5
20	9.08 ± 0.09	3.90 ± 0.43	7.51 ± 0.42	2.86 ± 0.03	35.3
25	7.37 ± 0.11	3.97 ± 0.64	7.65 ± 0.58	2.64 ± 0.05	34.5
30	6.22 ± 0.25	3.91 ± 1.60	7.76 ± 0.97	1.67 ± 0.08	31.1

parameters n, K_a, ΔG^o, ΔH^o and ΔS^o obtained from the fits for the data obtained at different temperatures are summarized in Table 6.2. At 20^{o}C the binding parameters K_a, ΔG^o, ΔH^o and ΔS^o obtained for the interaction of PDC-109 to DMPC membranes containing 25 mol% cholesterol are: 3.9 (± 0.43) × 10^5 M^{-1}, -7.51 kcal.mol^{-1}, 2.86 (± 0.03) kcal.mol^{-1}, and 35.3 cal.mol^{-1}.K^{-1}, respectively. From the data presented in Table 6.2, it is observed that the values of n decrease with increase in temperature, whereas the values of K_a, ΔH^o and ΔS^o exhibit a biphasic dependence on temperature. This is clearly seen in Fig. 6.7, where the values of K_a, ΔH^o and ΔS^o are plotted as a function of temperature.

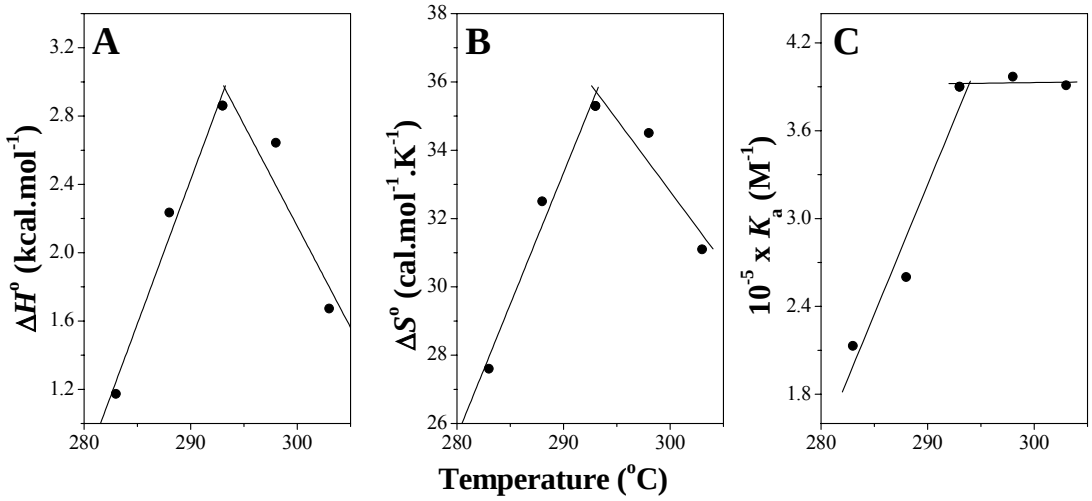

Fig. 6.7: Temperature dependence of (A) reaction enthalpies, (B) entropies and (C) association constants for PDC-109 binding to DMPC/cholesterol (3:1; mol) membranes.

6.4.6. Binding of PDC-109 to Lyso-PC micelles

A typical ITC isotherm for the binding of PDC-109 to Lyso-PC micelles at 20^{o}C is shown in Fig. 6.8. In this experiment 5 μL aliquots of a 10.88 mM solution of Lyso-PC were added to a 1.445 ml sample of 0.400 - 0.450 mM in the calorimeter cell at intervals of 200 seconds (Fig. 6.8). From this figure it is seen that the exothermic heat of binding exhibits an initial increase, reaches a maximum at a molar ratio of ca. 1.0 and then decreases monotonically with successive injections until saturation is

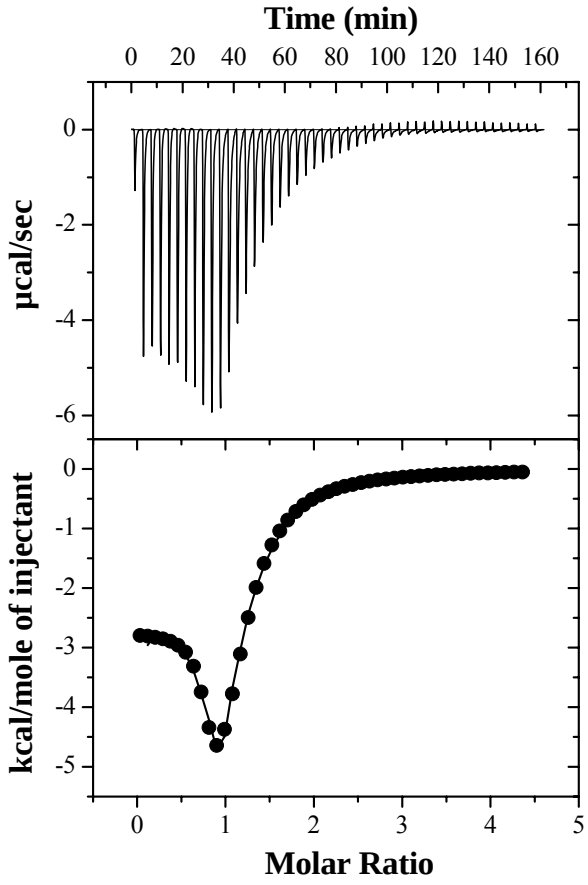

Fig. 6.8: Calorimetric titrations of PDC-109 with Lyso-PC in Tris I buffer, pH 7.4. The upper panels show the raw data for the titration of 450 μM protein with 10.88 mM Lyso-PC. The lower panel shows the integrated values obtained from the raw data, after subtracting the data from a dilution experiment. The solid line in the lower panel represents the best curve fit to the experimental data, using the '*two sets of sites*' model from Microcal Origin.

achieved. A plot of the incremental heat released as a function of the Lyso-PC/PDC-109 ratio is shown in the lower panel of Fig. 6.8, together with a non-linear least squares fit to the '*two sets of sites*' binding model. The parameters obtained from the fits are presented in Table 6.3.

The binding constants presented in Table 6.3 indicate the presence of two sets of binding sites; one set of low-affinity sites and a second set of high-affinity sites. At 20°C the analysis yielded n_1 = 4.76 (± 0.23), K_a = 6.9 (± 0.01) × 10^3 M^{-1}, ΔG_1^o = -5.15 (± 0.01) kcal. mol^{-1}, ΔH_1^o = -17.56 (± 0.33) kcal.mol^{-1}, and ΔS_1^o = -42.4 cal.mol^{-1}.K^{-1} for the low-affinity sites, and n_2 = 1.04 (± 0.01), K_a = 9.79 (± 0.05) × 10^5 M^{-1}, ΔG_2^o = -8.04 (± 0.02) kcal. mol^{-1}, ΔH_2^o = -2.58 (± 0.44) kcal.mol^{-1}, and ΔS_2^o = 18.7 cal. mol^{-1}.K^{-1}. While binding to both types of sites is exothermic in nature, binding to the low-affinity sites is associated with a considerably larger change in the enthalpy, but is significantly offset by a negative entropy change. On the other hand, binding of Lyso-PC to the high-affinity sites is associated with a smaller change in enthalpy, but a significantly positive entropy value increases the binding affinity. The association constant corresponding to the binding of Lyso-PC to the low affinity sites increases with temperature whereas the corresponding binding constant for the high affinity sites decreases with increasing temperature (Table 6.3).

Plots depicting the temperature dependence of ΔH^o, ΔS^o and K_a for the binding of PDC-109 to Lyso-PC are shown in Fig. 6.9. For the low-affinity sites, enthalpy of binding decreases with increase in temperature (Fig. 6.9A). However, the entropy of binding increases (that is, the values become smaller, although their contribution to the free energy of binding is still negative), and the change in ΔS^o is steeper (Fig. 6.9B) and hence results in a net increase in the ΔG^o, which is reflected in an increase in the K_a values (Table 6.3; Fig. 6.9C). On the other hand, for the high-affinity sites

the binding enthalpy increases with temperature, whereas the entropy values decrease with temperature. The decrease in ΔS^o is larger than that required to compensate the increase in ΔH^o, thus resulting in a decrease in the K_a values.

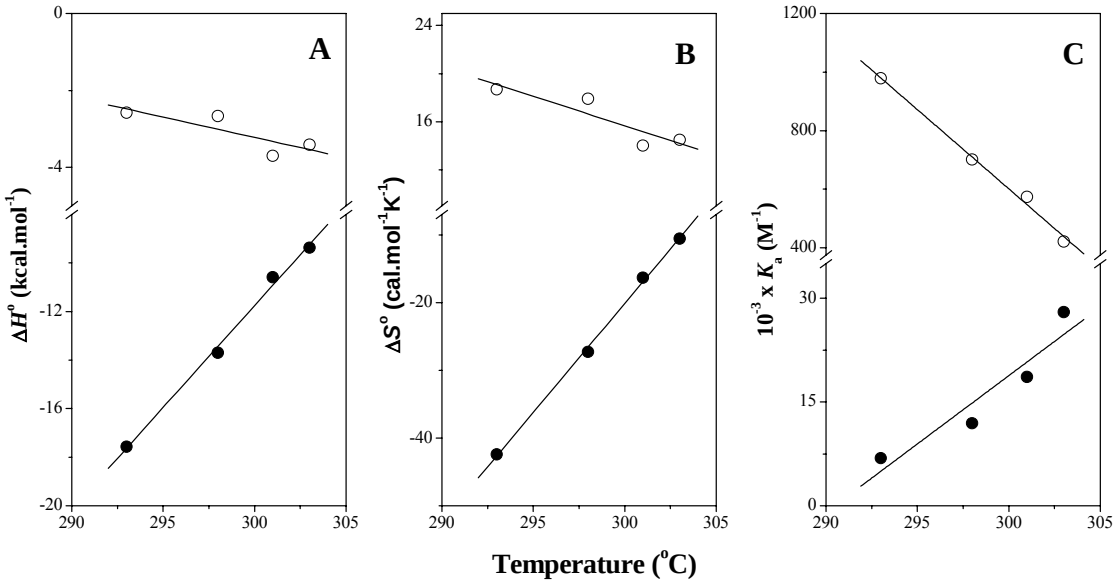

Fig. 6.9: Temperature dependence of (A) reaction enthalpies, (B) entropies and (C) association constants for PDC-109 binding to Lyso-PC micelles. From the slope of the linear least squares fits in A, the ΔC_p values were obtained. (O) high-affinity sites, (●) low-affinity sites.

Table 6.3: Calorimetric data of Lyso-PC binding to PDC-109. The data were analyzed in terms of '*two sets of sites*' model.

Parameters	Temperature (^{o}C)			
	20	25	28	30
n_1	4.76 ± 0.23	3.45 ± 0.12	4.76 ± 3.17	2.13 ± 0.68
$K_1 \times 10^{-4}$ (M^{-1})	0.69 ± 0.01	1.19 ± 0.09	1.83 ± 0.25	2.80 ± 0.08
ΔG_1^o (kcal. mol^{-1})	-5.15 ± 0.01	-5.57 ± 0.04	-5.89 ± 0.07	-6.17 ± 0.05
ΔH_1^o (kcal.mol^{-1})	-17.56 ± 0.33	-13.70 ± 0.53	-10.85 ± 2.2	-9.37 ± 0.27
ΔS_1^o (cal.mol^{-1}. K^{-1})	-42.4	-27.3	-16.9	-10.6
n_2	1.04 ± 0.01	0.88 ± 0.06	1.64 ± 0.22	1.64 ± 0.24
$K_2 \times 10^{-5}$ (M^{-1})	9.79 ± 0.05	7.01 ± 0.15	6.37 ± 2.74	4.21 ± 0.38
ΔG_2^o (kcal. mol^{-1})	-8.04 ± 0.02	-7.98 ± 0.09	-7.94 ± 0.82	-7.81 ± 0.24
ΔH_2^o (kcal.mol^{-1})	-2.58 ± 0.44	-2.66± 0.12	-3.79 ± 0.12	-3.41 ± 0.30
ΔS_2^o (cal.mol^{-1}. K^{-1})	18.7	17.9	14.0	14.5

6.4. Discussion

In order to investigate the energetics that characterize the interaction of PDC-109 with phospholipid membranes, ITC experiments have been carried out in this study. ITC is the most appropriate method for such a study because one gets directly the heat absorbed/released corresponding to each injection of the titration. A number of studies have been published recently exploiting this method for investigating the interaction of peptides and proteins with membranes [cf. Wieprecht et al., 1999; Arnulphi et al., 2004; Torrecillas et al., 2004; Abraham et al., 2005].

In the SPR studies reported in Chapter 3 a K_a value of 2.11×10^7 M^{-1} was obtained for the interaction of PDC-109 with DMPC membranes containing 20 wt% cholesterol. This value is considerably higher than the values obtained here for the interaction of PDC-109 with DMPC or DMPC/cholesterol membranes at the same temperature. It is possible that the binding strength is different because of the differences in the membranes structure between the two studies. In the SPR studies, hybrid bilayers of the lipid obtained by coating a lipid monolayer on alkanethiol coated sensor chip. In the ITC studies small unilamellar vesicles, which are intrinsically highly curved, are used.

The positive values of enthalpy and entropy obtained for the binding of PDC-109 to DMPC and DPPC membranes clearly indicate that the binding is entropy-driven. This observation may be interpreted in terms of the binding taking place due to the classical hydrophobic effect. The data presented in Table 6.1 and Fig. 6.4 show that the enthalpy of binding for both DMPC and DPPC increases with increase in temperature, yielding large positive heat capacity changes (ΔC_p) of 287 and 289 $cal.mol^{-1}.K^{-1}$ for the binding of PDC-109 to DMPC and DPPC, respectively. This

large positive ΔC_p is quite unusual as both classical and nonclassical hydrophobic effects are characterized by a negative heat capacity change [Wieprecht et al., 1999]. However, such large positive ΔC_p values can be explained if one assumes that binding of PDC-109 results in the exposure of a larger hydrophobic surface area to water. There are at least two lines of evidence that support this explanation. One is the ability of PDC-109 to induce leakage of contents from large unilamellar vesicles of phosphatidylcholine [Gasset et al., 2000]. Such a leakage would necessarily imply the presence of openings or defects in the membrane, which would lead to an exposure of hydrophobic portions of the membrane to the solvent water. The other evidence is the partial solubilization of vesicles by PDC-109 when it binds to multilamellar vesicles or large unilamellar vesicles, resulting in the formation of smaller particles as observed by turbidimetric studies presented above [see also Ramakrishnan et al., 2001; M.J. Swamy, unpublished observations]. Because such small particles have to be highly curved, water penetration into the hydrophobic region of the membrane will be higher upon binding of PDC-109 to the lipid membranes. Formation of highly curved lipid structures is also supported by ^{31}P-NMR studies, which demonstrated that binding of PDC-109 to DMPC multilamellar vesicles results in isotropic ^{31}P-NMR signal, indicating that the lipid exists in highly curved structures in the presence of PDC-109 [R.S. Damai & M.J. Swamy, unpublished observations]. Finally, it is also possible that a part of the positive ΔC_p could arise from the insertion of some polar residues of the protein into the hydrophobic portion of the membrane. Such an explanation has also been considered for rationalizing the positive ΔC_p values observed for the binding of magainin peptides to membranes [Wieprecht et al., 1999] The fluorescence spectroscopic studies reported in Chapter 5 indicate that some of the Trp residues of PDC-109 may be embedded in the hydrophobic interior of the membrane. As the Trp residues are generally known to preferentially partition into the interfacial region of the membrane, it is likely that their insertion into the nonpolar

membrane interior may lead to a positive ΔC_p. This is in accord with the ESR studies reported in Chapter 2, where it was shown that PDC-109 perturbs DMPC membranes up to the 14th C-atom of the acyl chains [Ramakrishnan et al., 2001].

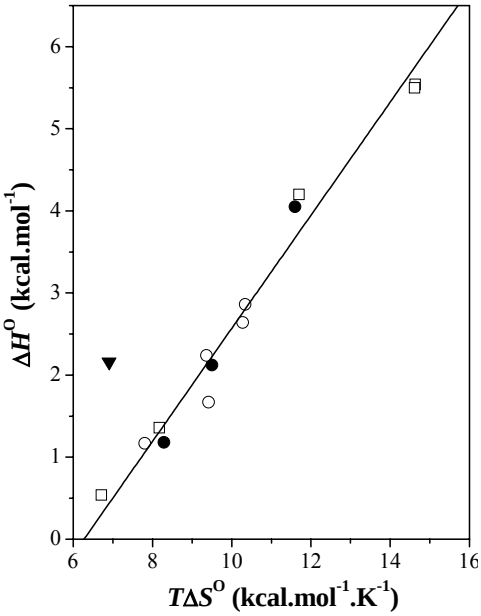

Fig. 6.9. Enthalpy-entropy compensation plot for the interaction of PDC-109 with phospholipid membranes. The straight line corresponds to a linear least squares fit. The point corresponding to DMPG was not included in the fit. (□) DPPC, (●) DMPC, (○) DMPC with 25 mol% cholesterol, (▼) DMPG.

The enthalpy and entropy values associated with the binding of PDC-109 to DMPC, DPPC and DMPC/cholesterol membranes increase with increasing temperature (Tables 6.1 and 6.2). An enthalpy-entropy compensation plot (ΔH^o versus $T\Delta S^o$) for the binding data obtained with the above membranes as well as DMPG membranes is shown in Fig. 6.9. It is seen from this figure while a close enthalpy-entropy compensation is observed for the binding of PDC-109 to choline phospholipid containing membranes, binding of this protein to DMPG membranes does not fall in line with the above data. It is possible that PDC-109 binds to DMPG membranes by a mechanism that is different from its interaction with PC-containing membranes. The significantly different stoichiometry (n = 80.2 ± 34 lipids/protein

monomer at 20^{o}C) as compared to the stoichiometry observed with DMPC and DPPC (n ≈ 21 lipids/protein monomer) also is consistent with this interpretation. The slope of the fit in Fig. 6.9 is 0.67. An exact compensation of enthalpy by entropy would be expected to yield a slope close to 1.0 [Eads et al., 1998]. On the other hand, deviation of this would indicate the predominance of one of these factors over the other. If the slope is larger than one then it would indicate that the binding is primarily enthalpy driven, whereas a slope that is significantly smaller than 1.0 is suggestive of a process that is predominantly entropy-driven [Munske et al., 1984; Sigurskjold & Bundle, 1992]. Therefore, the observation of enthalpy-entropy compensation strongly suggests that binding of PDC-109 to membranes containing PC is driven predominantly by entropic forces.

In the presence of cholesterol PDC-109 binds to DMPC membranes by an endothermic process at temperatures corresponding to the gel phase as well as the fluid phase of DMPC alone. These results are consistent with the abolition of the gel-fluid phase transition and the rigidification of liquid crystalline phase of diacyl phosphatidylcholine membranes by cholesterol. This is also consistent with the potentiation of PDC-109-DMPC interaction by cholesterol [Swamy et al., 2002]. Additionally, it is observed that the thermodynamic parameters K_a, ΔH^o and ΔS^o exhibit a biphasic temperature dependence, with the values of enthalpy and entropy of binding increasing in the gel phase region of DMPC (10 - 20^{o}C), whereas they decrease at higher temperatures corresponding to the liquid crystalline phase of the lipid. These results suggest that the binding at low temperatures is associated with a positive change of ΔC_p which becomes negative at higher temperatures. These changes could be related to differences in the hydration of the membrane surface at different temperatures. Alternately, they may reflect differences in the organisation of water molecules around the protein/ligand.

For the binding of PDC-109 to Lyso-PC, the reaction enthalpies become less exothermic with increasing temperature in the low-affinity binding sites and more exothermic in the high-affinity binding sites, yielding a large positive heat capacity change of 839.07 cal.mol^{-1}K^{-1} for the low-affinity sites, and -105.51 cal.mol^{-1}K^{-1} for the high affinity sites (Fig. 6.9A). The positive ΔC_p value for the low-affinity sites can be explained in the same way as explained for the binding of PDC-109 to DMPC and DPPC above, that is binding of the protein results in an exposure of large hydrophobic areas (most likely from the lipid acyl chains) to the solvent water. In addition, some polar residues of the protein may become embedded in the hydrophobic part of the Lyso-PC micelles. The negative value of ΔC_p observed for the binding of PDC-109 to the high-affinity sites can be explained in terms of the burial of some nonpolar parts of the protein in the hydrophobic regions of the Lyso-PC micelles. This is then due to the classical hydrophobic effect. This explanation is consistent with the conformational changes in the protein, resulting from the binding reaction [Gasset et al., 2000]. The conformational change in PDC-109 upon binding to Lyso-PC was supported by the blue shift in fluorescence emission maximum of PDC-109 from 340 nm to 333 nm [Gasset et al., 2000]. Although these studies suggest that there are two types of binding sites for the interaction between PDC-109 and Lyso-PC, the molecular features that are responsible for this are not clear. Further, the studies presented in Chapter 4 indicated only a single type of binding sites on PDC-109. Thus there seems to be some discrepancy between the two studies. However, it is likely that the absorption changes followed for investigating the binding in the studies presented in Chapter 4 do not detect one of the two types of binding reactions, because such binding may not yield significant changes in the protein absorption spectra, when compared with the changes observed with binding to the other type of sites.

For phosphatidylcholines in the absence and in the presence of cholesterol, the number of binding sites is found to decrease with temperature, that is, the number of lipid molecules associated with each protein molecule decreases as the temperature is increased (Tables 6.1 and 6.2). It is well known that the cross-sectional area of lipids increases with increase in temperature [Marsh, 1990]. Assuming that the area of the protein which interacts with the lipid membrane does not change significantly in the temperature range studied, it is expected that the number of lipid molecules that would be associated with the protein would decrease as the temperature is increased. However, it is possible that other factors, which are yet to be identified, may also contribute to the change in the stoichiometry.

In summary, the energetics of interaction of PDC-109 with phospholipids has been investigated by isothermal titration calorimetry. It has been found that the binding of PDC-109 to gel phase lipids is primarily driven by a classical hydrophobic effect, with a positive entropic contribution. A positive change in the ΔC_p observed for the binding of PDC-109 to membranes containing phosphatidylcholine is likely due to the exposure of hydrophobic surfaces to water, which are consistent with the high surface curvature of the protein-lipid recombinants, observed by ^{31}P-NMR spectroscopy. For the binding of PDC-109 to DMPC/cholesterol (3:1; mol) membranes a biphasic temperature dependence was observed for the enthalpy, entropy and K_a, which could be due to differences in the water structure around the protein, membrane or the protein-lipid recombinant. This is further supported by enthalpy-entropy compensation for the binding of PDC-109 to membranes containing choline phospholipids, underscoring the role of water in the overall binding process.

Chapter 7

General Discussion and Conclusions

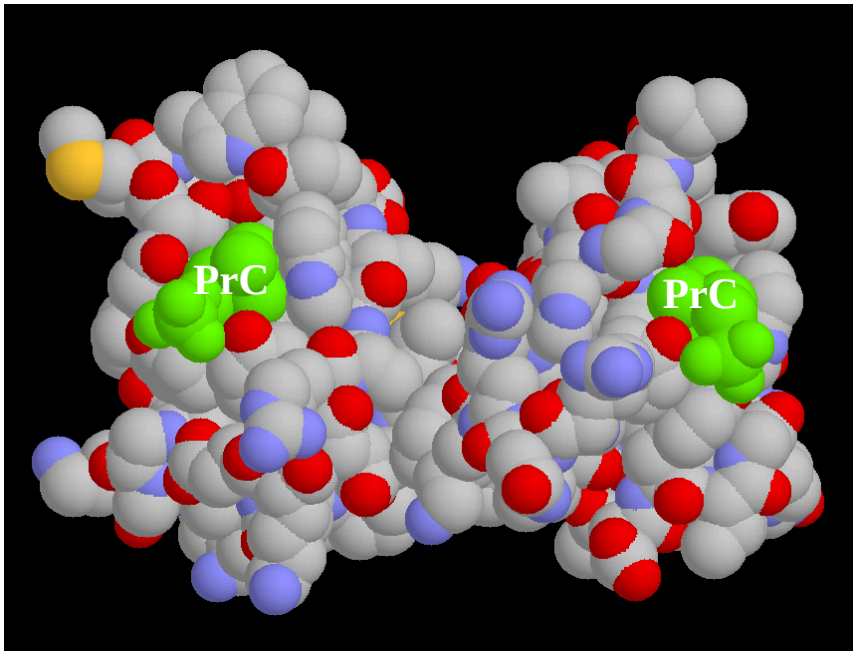

7.1. General discussion and conclusion

As mentioned in Chapter 1, the major objective of the present study is to investigate the interaction of the major protein from bovine seminal plasma, PDC-109 with phospholipid membranes, in order to understand the lipid specificity of this protein, the mechanism of its binding to lipid membranes, to characterize the effect of its binding to lipid membranes and to characterize the thermodynamic forces that govern its interaction with different lipids and ligands. The studies reported in Chapters 2-6 clearly show that these objectives are mostly fulfilled. In the following paragraphs, the results obtained in these studies are discussed and their implications are discussed in terms of the physiological role of PDC-109 in cholesterol efflux and sperm capacitation, which is a necessary event before fertilization can occur.

In the studies presented in Chapter 2, lipid selectivity and specificity of PDC-109 were investigated by ESR spectroscopy. The interaction of PDC-109 with membranes made up of phosphatidylcholine and phosphatidylcholine/cholesterol mixtures bearing probe amounts of different spin-labeled phospholipids and steroid probes was investigated by electron spin resonance (ESR) spectroscopy. PDC-109 shows the selectivity for different lipids in the following order: phosphatidylcholine ≈ sphingomyelin ≥ phosphatidic acid (pH 6.0) > phosphatidylglycerol ≈ phosphatidylserine ≈ androstanol > phosphatidylethanolamine ≥ *N*-acyl phosphatidylethanolamine >> cholestane. Thus, lipids bearing the phosphocholine moiety in the head group are clearly the lipids most strongly recognized by PDC-109. However, these studies demonstrate that this protein also recognizes other lipids such as phosphatidylglycerol and the sterol androstanol, albeit with somewhat reduced affinity. Further membrane perturbation of the protein showed that upon binding to PC membranes PDC-109 penetrates into the hydrophobic interior of the membrane

(up to 14th C atom of the lipid acyl chain). Additionally, the presence of cholesterol has been shown to modulate the binding by increasing the association of different phospholipids and sterol probes with the protein, although the relative selectivity for individual lipid species was not significantly affected.

The kinetics and mechanism of the interaction of PDC-109 with phospholipid membranes were investigated by the surface plasmon resonance technique. Interaction of PDC-109 to different phospholipid membranes containing 20% cholesterol (wt/wt) indicated that the binding occurs by a single step mechanism. From the kinetic data, the association constant for the binding of PDC-109 to different phospholipids investigated decrease in the order: DMPC > DMPG > DMPA > DMPE. Binding of PDC-109 to PC membranes is due to a combination of faster association rate constant and a slower dissociation rate constant, as compared to other phospholipids. Analysis of the activation parameters indicates that the binding of PDC-109 with DMPC membranes is favored by a positive entropic contribution, whereas negative entropic contribution is primarily responsible for the rather weak interaction of this protein with DMPA and DMPG.

The binding of PrC and (Lyso-PC) to PDC-109 investigated by difference absorption spectroscopy show that Lyso-PC binds 250 fold stronger than that of PrC. Monitoring the temperature dependence of the binding process the thermodynamic forces that govern the interaction have been delineated. The binding of both these ligands were driven by enthalpic forces, however smaller negative entropy of binding associated with Lyso-PC results in the significantly stronger binding. Further, by comparing with the SPR results it was shown that binding of the diacyl lipid, DMPC to PDC-109 results in an increase in the association constant by nearly three orders of magnitude as compared to Lyso-PC. These results show that the acyl chain(s) stabilize the binding of Lyso-PC and DMPC with PDC-109. CD studies showed that

the binding of these ligands induce conformational changes in the protein. Binding of PrC or Lyso-PC results in considerable increases in the intensity in the far-UV CD. The magnitude of change associated with the binding of Lyso-PC is larger, clearly indicating that the binding of Lyso-PC induces larger perturbation in the secondary structure of PDC-109.

Considering the conformational changes in PDC-109 induced by the binding to choline phospholipids, Trp fluorescence was used as tool to investigate the protein conformation in the presence of PrC, Lyso-PC and DMPC membranes. Two neutral quenchers (acrylamide and succinimide), one anionic (I^-) and one cationic (Cs^+) quencher were employed in these experiments. The degree of quenching for the protein decreases upon binding to PrC, Lyso-PC and DMPC, with the maximum decrease to DMPC membrane bound state and minimum with PrC. These results indicate that while the head group choline moiety of phosphatidylcholine is critical for the recognition of the lipid by the protein, the acyl chains of the lipid stabilize the binding, leading to a further tightening of the protein structure, which results in a decrease in the accessibility to different quenchers. Interestingly both the native and denatured protein exhibits a REES of 4 nm, clearly indicating that some of the structural and dynamic features of the microenvironment around the Trp residues are retained even after denaturation. The REES values decrease to 2.5 nm and 1.0 upon binding of the protein to DMPC membranes and Lyso-PC micelles, respectively. This has been interpreted as resulting from the penetration of the segments of the protein containing majority of the Trp residues into the hydrophobic interior of the membrane, where the red-edge effects are considerably reduced.

Isothermal titration calorimetry, a highly sensitive tool for determining the binding of proteins to lipid membranes was used to derive key information on the energetics of PDC-109 binding to lipid bilayers and micelles. Thermodynamic

parameters obtained for the binding of DMPC and DPPC to PDC-109 indicate that the binding is driven by entropic forces with negative enthalpic contribution. Large values of ΔC_p were observed for both, suggesting that binding of the protein to these two choline phospholipids results is the exposure of hydrophobic areas (presumably from the lipid acyl chains) to water. Further, the presence of cholesterol in the DMPC membrane modulates the binding of PDC-109 to the membranes at temperatures above the phase transition temperature of DMPC alone. Interestingly, Lyso-PC binds to PDC-109 with two set of binding sites. The thermodynamic parameters associated with Lyso-PC binding to the high-affinity sites is aided by both entropic and enthalpic contributions, mostly favored by positive entropy, whereas the binding to the second and low-affinity set of sites is enthalpically driven.

The studies presented in this thesis will improve our understanding about the interaction of PDC-109 with the lipid membranes. Interaction of PDC-109 with sperm plasma membranes, mediated by the binding of this protein to lipids, plays a crucial in inducing an efflux of cholesterol and choline phospholipids from the spermatozoa, referred to as *cholesterol efflux*, which appears to be an important step in the capacitation process, which in turn is a necessary event before fertilization can occur. Therefore, understanding the molecular features of the interaction of PDC-109 with lipid membranes is a crucial step, before the role of this protein in regulating capacitation can be understood. Such an understanding will be of considerable practical importance in veterinary and human medicine, e.g., for birth control and *in vitro* fertilization.

References

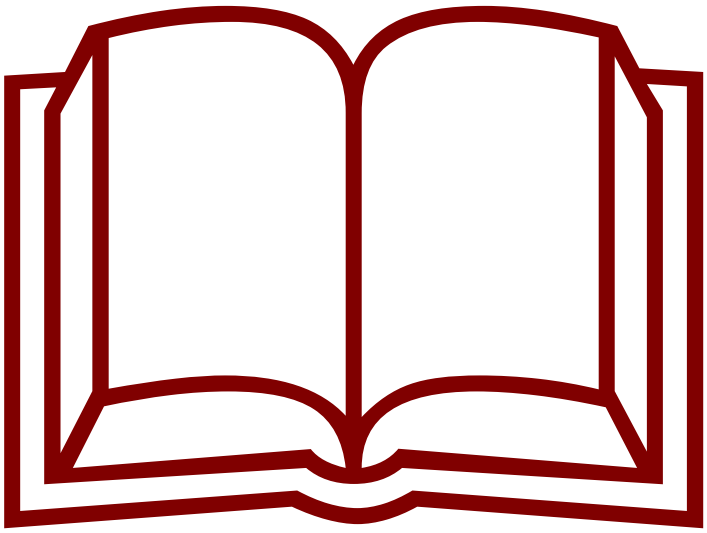

Abraham, T., Lewis, R.N.A.H., Hodges, R.S. & McElhaney, R.N. (2005) Isothermal titration calorimetry studies of the binding of a ration designed analogue of the antimicrobial peptide gramicidin S to phospholipids bilayer membranes. *Biochemistry* **44:** 2103-2112.

Anbazhagan, V. & Swamy M.J. (2005) Thermodynamics of phosphorylcholine and lysophosphatidylcholine binding to major protein of bovine seminal plasma, PDC-109. *FEBS Lett.* **579:** 2933-2938.

Aracava, Y., Smith, I. C. P. & Schreier, S. (1981) Effect of amphotericin-B on membranes - a spin probe study. *Biochemistry* **20:** 5702–5707.

Arunlphi, C., Jin, L., Tricerri, M.A. & Jonas, A. (2004) Enthalpy-drive apolipo-protein A-I and lipid bilayer interaction indicating protein penetration upon binding. *Biochemisry* **43:** 12258-12264.

Aumüller, G., Vesper, M., Seitz, J., Kemme, M. & Scheit, K-H. (1988) Binding of a major secretory protein from bull seminal vesicles to bovine spermatozoa. *Cell Tissue Res.* **252:** 377-384.

Austin, C.R. (1952) The "capacitation" of the mammalian sperm. *Nature* **170:** 326

Awano, M., Kawaguchi, A. & Mohri, H. (1993) Lipid composition of hamster epididymal spermatozoa. *J Reprod Fertil.* **99:** 375-383.

Baker, M.E. (1985) The PDC-109 protein from bovine seminal plasma is similar to the gelatin-binding domain of bovine fibronectin and a kringle domain of human tissue-type plasminogen activator. *Biochem. Biophys. Res. Commun.* **130:** 1010-1014.

Banyai, L., Trexler, M., Koncz, S., Gyenes, M., Sipos, G. & Patthy, L. (1990). The collagen-binding site of type-II units of bovine seminal fluid protein PDC-109 and fibronectin. *Eur J Biochem.* **193:** 801-806.

Bergeron, A., Villemure, M., Lazure, C. & Manjunath, P. (2005) Isolation and characterization of the major proteins of ram seminal plasma. *Mol Reprod Dev.* **71:** 461-470.

Biltonen, R.L., Lathrop, B., Heimburg, T. & Bell, J.D. (1990) Aspects of the activation of phospholipase A_2 on lipid bilayer surfaces. In: Biochemistry, Molecular Biology, and Physiology of Phospholipase A_2 and its Regulatory Factors (Mukherjee, A.B., Ed.), Plenum Press, New York. pp. 85-103.

Blondelle, S.E., Lohner, K. & Aguilar, M. (1999) Lipid-induced conformation and lipid-binding properties of cytolytic and antimicrobial peptides: determination and biological specificity. *Biochim Biophys Acta.* **1462:** 89-108.

Boisvert, M., Bergeron, A., Lazure C. & Manjunath, P. (2004) Isolation and characterization of gelatin-binding bison seminal vesicle secretory proteins. *Biol Reprod.* **70:** 656-61.

Brantmeier, S.A., Grimmer, R.R., Ax, R.L. (1987) Concentration of high density of lipoproteins vary among follicular sizes in the bovine. *J. Dairy Sci.* **70:** 2145-2149.

Bräuer, C. & Scheit, K.H. (1991) Characterization of the gene for the bovine seminal-vesicle secretory protein SVSP109. *Biochim. Biophys. Acta.* **1090:** 259-260.

Calvete, J. J., Paloma, F. V., Sanz, L. & Romero, A. (1996) A procedure for the large-scale isolation of major bovine seminal plasma proteins. *Protein Exp. Purif.* **8:** 48-56.

Calvete, J.J., Mann, K., Schafer, W., Sanz, L., Reinert, M., Nessau, S., Raida, M., & Töfer-Petersen E. (1995) Amino acid sequence of HSP-1, a major protein of stallion seminal plasma: effect of glycosylation on its heparin- and gelatin-binding capabilities. *Biochem J.* **310:** 615-622.

Calvete, J.J., Raida, M., Gentzel, M., Urbanke, C., Sanz, L. & Töpfer-Petersen, E. (1997) Isolation and characterization of heparin- and phosphorylcholine-binding proteins of boar and stallion seminal plasma. Primary structure of porcine pB1. *FEBS Lett.* **407:** 201-206.

Calvete, J.J., Raida, M., Sanz, L., Wempe, F., Scheit, K-H., Romer, A. & Topfer-Petersen, E. (1994) Localization and structural characterization of an oligosaccharide O-linked to bovine PDC-109. Quantitation of the glycoprotein in seminal plasma and on the surface of ejaculated and capacitated spermatozoa. *FEBS Lett.* **350:** 203-206

Chaiken, I., Rose, S. & Karlsson, R. (1992) Analysis of macromolecular interactions using immobilized ligands. *Anal. Biochem.* **201:** 197–210.

Chandonnet, L., Roberts, K.D., Chapdelaine, A. & Manjunath, P. (1990) Identification of heparin-binding proteins in bovine seminal plasma. *Mol Reprod Dev.* **26:** 313-318.

Chang, M.C. (1951) Fertilizing capacity of spermatrozoa deposited into the fallopian tubes. *Nature* **168:** 697-698.

Chattopadhyay, A. & Mukherjee, S. (1999a) Red edge excitation of a deeply embedded membrane probe: Implications in water penetration. *J. Phys. Chem. B* **103:** 8180-8185.

Chattopadhyay, A. & Mukherjee, S. (1999b) Depth-dependent solvent relaxation in membranes: wavelength-selective fluorescence as a membrane dipstick. *Langmuir* **15:** 2142-2148.

Chattopadhyay, A. (2003) Exploring membrane organization and dynamics by the wavelength-selective fluorescence approach. *Chem. Phys. Lipids.*

Chattopadhyay, A., Rawat, S.S., Kelkar, D,A., Ray, S & Chakrabarti, A. (2003) Organization and dynamics of tryptophan residues in erythroid spectrin: Novel structural features of denature spectrin revealed by the wavelength-selective fluorescence approach. *Protein Sci.* **12:** 2389-2403.

Cherry, R.J. (1981) Rotational diffusion of membrane proteins: measurements with bacteriorhodopsin, band-3 proteins and erythrocyte oligosaccharides. *Biochem. Soc. Symp.* **46:** 183-190.

Chipman, D.M., Grisaro, V. & Sharon, N. (1967) The binding of oligosaccharides containing *N*-acetylglucosamine and *N*-acetylmuramic acid to lysozyme. *J. Biol. Chem.* **242:** 4388-4394.

Clegg, R. M.,Loontiens, F. G. & Jovin, T. M. (1977) Binding of 4-methyl-umbelliferyl α-D-mannopyranoside to dimeric concanavalin A: fluorescence temperature-jump relaxation study. *Biochemistry* **16:** 167–175.

Clermont, Y., Oko, R. & Hermo, L. (1993) Cell biology of mammalian spermiogenesis. In Cell and molecular biology of the testis (Desjardans, C. & Ewing, J. Eds.), Oxford University Press, New York. pp. 332-376.

Constantine, K.L., Madrid, M., Bányai, L., Trexler, M., Patthy, L. & Linás M. (1992) Refined solution structure and ligand-binding properties of PDC-109 domain b. A collagen-binding type II domain. *J Mol Biol.* **223:** 281-98.

Constantine, K.L., Ramesh, V., Banyai, L., Trexler, M., Patthy, L. & Llinas, M. (1991) Sequence-specific ^{1}H NMR assignments and structural characterization of bovine seminal fluid protein PDC-109 domain b. *Biochemistry* **30:** 1663-72.

Cross, N.L. (1996) Human Seminal plasma prevents sperm from becoming acrosomally responsive to the agonist, progesterone: Cholesterol is the major inhibitor. *Bio. Reprod.* **54:** 138-145.

Danielle, J.F. & Davson, H. (1935) A contribution to the theory of permeability of thin films. *J. Cell. Comp. Physiol.* **5:** 495-508.

Davis B.K. (1982) Uterine fluid proteins bind sperm cholesterol during capacitation in the rabbit. *Experientia* **38:** 1063-1064.

Davis, B.K. (1981) Timing of fertilization in mammals: Sperm cholesterol/phospholipid ratio as a determinant of the capacitation interval. *Proc. Natl. Acad. Sci. USA* **78:** 7560-7564.

Davis, B.K., Byrne R. & Bedigian, K. (1980) Studies on the mechanism of cpacitation: albumin-mediated changes in plasma membrane lipids during in vitro incubation of rat sperm cells. *Proc. Natl. Acad. Sci. USA* **77:** 1546-1550.

de Krester D.M & Kerr J.B. (1994) The cytology of the testis. In physiology of reproduction (Knobil, E. & Neil, J. Eds.), Raven Press, New York. pp. 117-290.

Demchenko, A.P. (2002) The red-edge effects: 30 years of exploration. *Luminescence.* **17:** 19-42.

Desnoyers, L. & Manjunath, P. (1992) Major proteins of bovine seminal plasma exhibit novel interactions with phospholipids. *J. Biol. Chem.* **267:** 10149-10155.

Desnoyers, L. & Manjunath, P. (1993) Interaction of a novel class of phospholipids-binding proteins of bovine seminal fluid with different affinity matrices. *Arch. Biochem. Biophys.* **305:** 341-349.

Dravland, E. & Joshi, M.S. (1981) Sperm-coating antigens secreted by the epididymis and seminal vesicle of the rat. *Biol. Reprod.* **25:** 649-658.

Eads, J.C., Mahoney, N.M., Vorobiev,S., Bresnick, A.R., Wen, K.K., Rubenstein, P.A., Haarer, B.K. & Almo, S.C. (1998) Structure determination and characterization of Saccharomyces cerevisiae profilin. *Biochemistry* 37: 11171-11181.

Eftink, M. R. & Ghiron., C. A. (1981) Fluorescence quenching studies with protein. *Anal. Biochem.* **114:** 199-227.

Ehrenwald, E., Parks, J.E. & Foote, R.H. (1988a) Cholesterol efflux from bovine sperm: I. Induction of the acrosome reaction with lysophosphatidylcholine after reducing sperm cholesterol. *Gamete Res.* **20:** 145-157.

Ehrenwald, E., Parks, J.E. & Foote, R.H. (1988b) Cholesterol efflux from bovine sperm: II. Effect of reducing sperm cholesterol on penetration of Zona-free hamster and in vitro matured bovine ova. *Gamete Res.* **20:** 413-420.

Ehrenwald, E., Parks, J.E. & Foote, R.H. (1990) Bovine oviductal fluid components and their potentil role in sperm cholesterol efflux. *Mol. Reprod. Dev.* **25:** 195-204.

Ellena, J.F., Blazing, M.A. & McNamee, M.G. (1983) Lipid-protein interactions in reconstituted membranes containing acetylcholine receptor. *Biochemistry* **22:** 5523–5535.

Esch, F.S., Ling, N.C., Böhlen, P., Ying, S.Y. & Guillemin, R. (1983) Primary structure of PDC-109, a major protein constituent of bovine seminal plasma. *Biochem. Biophys. Res. Commun.* **113:** 861-867.

Esmann, M., Watts, A. & Marsh, D. (1985) Spin-label studies of lipid-protein interactions in (Na^+,K^+)-ATPase membranes from rectal glands of Squalus acanthias. *Biochemistry* **24:** 1386-1393.

Fawcett, D.W. (1975) The mammalian spermatozoon. *Dev. Biol.* **44:** 394-436.

Ferguson, M.A., Low, M.G., & Cross, G.A. (1985) Glycosyl-sn-1,2-dimyristylphosphatidylinositol is covalently linked to Trypanosoma brucei variant surface glycoprotein. *J Biol Chem.* **260:** 14547-14555.

Fleming, A.D. & Yanagimachi, R. (1981) Effects of various lipids on acrosome reaction and fertilizing capacity of guinea pig spermatozoa with special reference to the possible involvement of lysophospholipids in the acrosome reaction. *Gamete Res.* **4:** 253-273.

Gasset, M., Magdaleno, L. & Calvete, J.J. (2000) Biophysical study of the perturbation of model membrane structure caused by seminal plasma protein PDC-109. *Arch. Biochem. Biophys.* **374:** 241–247.

Gasset, M., Saiz, J. L., Sanz, L., Gentzel, M., Töpfer-Petersen, E. & Calvete. J.J. (1997) Conformational features and thermal stability of bovine seminal plasma protein PDC-109 oligomers and phosphorylcholine-bound complexes. *Eur. J. Biochem.* **250:** 735–744.

Gennis, R. (1989) Biomembranes: Molecular Structure and Function. Springer-Verlag, New York

Gerwig, G.L., Calvete, J.J., Töpfer-Petersen E & Vliegenthart, J.F. (1996) The structure of the O-linked carbohydrate chain of bovine seminal plasma protein PDC-109 revised by ^{1}H-NMR spectroscopy A correction. *FEBS Lett.* **387:** 99-100.

Go, K.J. & Wolf, D.P. (1985) Albumin-mediated changes in sperm sterol content during capacitation. *Biol. Reprod.* **32:** 145-153.

Go, K.J. &Wolf, D.P. (1983) The role of sterols in sperm capacitation. *Adv. Lipid Res.* **20:** 317-330.

Görrissen, H., Marsh, D., Rietveld, A. & de Kruijff, B. (1986) Apocytochrome *c* binding to negatively charged lipid dispersions studied by spin-label electron spin resonance. *Biochemistry* **25:** 2904 –2910.

Gorter, E. & Grendel, F. (1925) On biomolecular layers of lipid on the chromacytes of the blood. *J. Exp. Med.* **41:** 439-443.

Greube, A., Müller, K., Töpfer-Petersen, E., Herrmann, A. & Müller, P. (2001) Influence of the bovine seminal plasma protein PDC-109 on the physical state of membranes. *Biochemistry* **40:** 8326-8334.

Grinvald, A. & Steinberg., I. Z. (1976) The fluorescence decay of tryptophan residues in native and denatured proteins. *Biochim. Biophys. Acta.* **427:** 663-678.

Grinvald, A., & Steinberg, I. Z. (1974) On the analysis of fluorescence decay kinetics by the method of least-squares. *Anal Biochem.* **59:** 583-598.

Guidotti, G. (1972) Membrane proteins. *Annu. Rev. Biochem.* **41:** 731-752.

Gunstone, F.D., Harwood, J.L. & Padley, F.B. (1986) The lipid handbook. Chapman and Hall Ltd, New York. pp. 449-472.

Guraya, S.S. (1965) Histochemical studies on spermateleosis in sheep, goat and buffalo. *Cellule* **65:** 367-378.

Gwathmey, T.M., Ignotz, G.G. & Suarez, S.S. (2003) PDC-109 (BSP-A1/A2) promotes bull sperm binding to oviductal epithelium in vitro and may be involved in forming the oviductal sperm reservoir. *Biol. Reprod.* **69:** 809-815.

Handrow, R,R., Lenz, R.W. & Ax, R.L. (1982) Structural comparison among glycosaminoglycans to promote an acrosome reaction in bovine spermatozoa. *Biochem. Biophys. Res Commun.* **107:** 1326-1332.

Harper, M.J.K. (1994) The physiology of reproduction. In Gamete and zygote transport (Knobil, E., & Neill, J.D., Eds). Raven Press, New York. pp. 123–187.

Helenius, A. & Simons, K. (1975) Soulubilization of membranes by detergents. *Biochim. Biophys. Acta* **415:** 29-79.

Higgins, J. A. (1987) Separation and analysis of membrane lipid components. In Biological Membranes. A Practical Approach. (Findlay, J.B.C. & Evans, W.H. Eds.). IRL Press, Oxford.122.

Hoffmann, P., Sandhoff, K. & Marsh, D. (2000) Comparative dynamics and location of spin-labelled sphingomyelin and phosphatidylcholine in dimyristoyl phosphatidylcholine membranes studied by EPR spectroscopy. *Biochim. Biophys. Acta* **1468:** 359 –366.

Hoshi, K., Aita, T., Yanagida, K., Yoshimatzu, N. & Sato, A. (1990) Variation in the cholesterol/phospholipid ratio in human spermatozoa and its relationship with capacitation. *Hum. Reprod.* **5:** 71-74.

Ignotz, G., Lo, M.C., Perez, C.L., Gwathmey, T.M. & Suarez, S.S. (2001) Characterization of a fucose-binding protein from bull sperm and seminal plasma

that may be responsible for formation of oviductal sperm reservoir. *Biol. Reprod*. **64:** 1806-1811.

Jain, M.K. (1983) Nonrandom lateral organization in bilayers and biomembranes. In: Membrane fluidity in Biology (Aloia, R.C., Ed.). Academic press, New York. **Vol.1:** pp. 1-37

Jain, M.K. (1988) Introduction to biological membranes. Wiley, New York.

James, P.S., Wolfe, C.A., Ladha, S. & Jones, R. (1999) Lipid diffusion in the plasma membrane of ram and boar spermatozoa during maturation in the epididymis measured by fluorescence recovery after photobleaching. *Mol. Reprod. Dev.* **52:** 207-215.

Johnsson, B., Lofas, S. & Lindquist, G. (1991) Immobilization of proteins to a carboxymethyldextran-modified gold surface for biospecific interaction analysis in surface plasmon resonance sensors. *Anal. Biochem.* **198:** 268–277.

Jonas, A. & Krajnovich, D.J. (1977) Interaction of human and bovine A-1 apolipoproteins with L-alpha-dimyristoyl phosphatidylcholine and L-alpha-myristoyl lysophosphatidylcholine. *J Biol Chem.* **252:** 2194-2199.

Jost, P.C. & Griffith, O.H. (Eds.) (1982) Lipid-Protein Interactions. Wiley-Interscience, New York.

Kenoth, R. & Swamy, M.J. (2003) Steady-state and time-resolved fluorescence studies on *Trichosanthes cucumerina* seed lectin. *J. Photochem. Photobiol. B: Biol.* **413:** 131-138.

Killian, J.A., de Jong, A.M., Bijvelt, J., Verkleij, A.J. & de Kruijff, B. (1990) Induction of non-bilayer lipid structures by functional signal peptides. *EMBO J.* **9:** 815-819.

Knowles, P. F., Watts, A. & Marsh, D. (1979) Spin label studies of lipid immobilization in dimyristoylphosphatidylcholine substituted cytochrome oxidase. *Biochemistry* **18:** 4480–4487.

Knowles, P.F. & Marsh, D. (1991) Magnetic resonance of membranes. *Biochem. J.* **274:** 625-641.

Kouyama, T., Nishikawa, T., Tokuhisa, T. & Okumura, H. (2004) Crystal structure of the L intermediate of bacteriorhodopsin: evidence for vertical translocation of a water molecule during the proton pumping cycle. *J. Mol. Biol.* **335:** 531-546.

Laemmli, U. K. (1970) Cleavage of structural proteins during assembly of bacteriophage T4. *Nature* **227:** 680–685.

Lai, C., Brow, M.A., Nave, K.A., Noronha, A.B., Quarles, R.H., Bloom, F.E., Milner, R.J. & Sutcliffe, J.G. (1987) Two forms of 1B236/myelin-associated glycoprotein, a cell adhesion molecule for postnatal neural development, are produced by alternative splicing. *Proc. Natl. Acad. Sci. USA* **84:** 4337-4341.

Lai, J.S., Sarvas, M., Brammar, W.J., Neugebauer, K. & Wu, H.C. (1981) Bacillus licheniformis penicillinase synthesized in Escherichia coli contains covalently linked fatty acid and glyceride. *Proc Natl. Acad Sci USA* **78:** 3506-3510.

Lakowicz, J. R. (1999) Principles of Fluorescence Spectroscopy, 2nd Edition. Kluwer Academic Publishers, New York, pp. 238-265.

Lane, M.E., Thérien, I., Moreau, R. & Manjunath, P. (1999) Heparin and high-density lipoprotein mediate bovine sperm capacitation by different mechanisms. *Biol. Reprod.* **60:** 169-175.

Langlais, J., Kan, F.W.K., Granger, L., Raymond, L., Bleau, G. & Roberts K.D. (1988) Identification of sterol acceptors that stimulate cholesterol efflux from human spermatozoa during in vitro capacitation. *Gamete Res.* **20:** 185-201.

Leblond, E., Desnoyers, L. & Manjunath, P. (1993) Phosphorylcholine-binding proteins from the seminal fluids of different species share antigenic determinants with the major proteins of bovine seminal plasma. *Mol Reprod Dev.* **34:** 443-449

Lee, C.N., Handrow, R.R., Lenz, R.Q. & Ax, R.L. (1985) Interactions of seminal plasma and glycosaminoglycans on acrosome reactions in bovine spermatozoa in vitro. *Gamete Res.* **12:** 345-355.

Lefebvre, R., Chenoweth, P.J., Drost, M., LeClear, C.T., MacuCubbin, M., Dutton, J.T., Suarez, S.S. (1995) Characterization of the oviductal sperm reservoir in cattle. *Biol. Reprod.* **53:** 1066-1074.

Lehrer, S.S. (1971) Solute perturbation of protein fluorescence. The quenching of the tryptophyl fluorescence of model compounds and of lysozyme by iodide ion. *Biochemistry.* **10:** 3254-2363.

Liberda, J., Kraus, M., Ryslava, H., Vlaskova, M., Jonakova, V. & Ticha, M. (2001) D-fructose-binding proteins in bull seminal plasma. Isolation and characterization. *Folia Biol. (Praha)* **47:** 113-119.

Lowry, O. H., Rosebrough, N.J., Farr, L. & Randall. R.J. (1951) Protein measurement with the folin phenol reagent. *J. Biol. Chem.* **193:** 265–275.

Lux, S.E., Hirz, R., Shrager, R.I. & Gotto, A.M. (1972) The influence of lipid on the conformation of human plasma high density apolipoproteins. *J Biol Chem.* **247:** 2598-2606.

Manjunath, P. & Sairam, M.R. (1987) Purification and biochemical characterizationof three major acidic proteins (BSP-A1, BSP-A2 and BSP-A3) from bovine seminal plasma. *Biochem. J.* **241:** 685-692.

Manjunath, P. & Thérien, I. (2002) Role of seminal plasma phospholipid-binding proteins in sperm membrane lipid modification that occurs during capacitation. *J. Reprod. Immun.* **53:** 109-119.

Manjunath, P., Baillargeon, L., Marcel, Y.L., Seidah, N.G., Chretian, M. & Chapdelaine, A. (1988) Molecular Biology of Brain and Endocrine Peptidergic Systems (Chretian, M. and Mckerns, K.W., Eds.), Plenum Press, New York, pp. 259-273.

Manjunath, P., Chandonnet, L., Leblond, E. & Desnoyers L. (1994) Major proteins of bovine seminal vesicles bind to spermatozoa. *Biol. Reprod.* **50:** 27-37 [Published erratum appears in (1994) *Biol. Reprod.* **50:** 977.

Manjunath, P., Marcel, Y.L., Uma, J., Seidah, N.G., Chretien, M. & Chapdelaine, A. (1989) Apolipoprotein A-I binds to a family of bovine seminal plasma proteins. *J Biol Chem.* **264:** 16853-16857.

Manjunath, P., Nauc, V., Bergeron, A. & Menard, M. (2002) Major proteins of bovine seminal plasma bind to the low density lipoprotein fraction of hen's egg yolk. *Biol. Reprod.* **67:** 1250-1258.

Mann, T. & Lutwak-Mann, C. (1981) Male reproductive function and semen, Springer-Verlag, New York.

Marsh, D. & Horvath, L.I. (1998) Structure, dynamics and composition of the lipid-protein interface: perspectives from spin-labelling. *Biochim. Biophys. Acta* **1376:** 267-296.

Marsh, D. & Páli, T. (2004) The protein-lipid interface: perspectives from magnetic resonance and crystal structures. *Biochim Biophys Acta.* **1666:** 118-141.

Marsh, D. & Watts, A. (1982) Spin-labelling and lipid-protein interactions in membranes. In: Lipid-Protein Interactions. (Jost, P.C. & Griffith, O.H., Eds.). Wiley-Interscience, New York. **Vol. 2:** pp. 53-126.

Marsh, D. (1985) ESR spin label studies of lipid-protein interactions. In Progress in Protein-Lipid Interactions. (Watts, A. & de Pont, J. J. H. H. M., Eds.). Elsevier, Amsterdam. **Vol. 1:** pp. 143–172.

Marsh, D. (1990) CRC handbook of lipid bilayers. CRC press.

Marsh, D. (1993) The nature of the lipid-protein interface and the influence of protein structure on protein-lipid interactions. In: Protein-Lipid Interaction. New

comprehensive biochemistry [Watts, A., Ed.]. Elsevier, Amsterdam. **Vol. 25:** pp. 41-66.

Marsh, D. (1997) Stoichiometry of lipid-protein interaction and integral membrane protein structure. *Eur. Biophys. J.* **26:** 203–208.

Marsh, D. (2001) Applications of electron spin resonance for investigating peptide-lipid interactions, and correlation with thermodynamics. *Biochem. Soc. Trans.* **29:** 582–589.

Martinez, P. & Morros, A. (1996) Membrane lipid dynamics during human sperm capacitation. *Fronteir in Bioscience* **1:** 103-117.

McElhaney, R.N. (1986) Differential scanning calorimetric studies of lipid-protein interactions in model membrane systems. *Biochim Biophys Acta.* **864:** 361-421.

Mentre, P. (2001) Water in the cell. *Cell. Mol. Biol.* **47:** 709-970.

Miller, D.J., Winer, M.A. & Ax, R.L. (1990) Heparin-binding proteins from seminal plasma bind to bovine spermatozoa and modulate capacitation by heparin. *Biol. Reprod.* **42:** 899-915.

Moreau, R. & Manjunath, P. (1999) Characterization of lipid efflux particles generated by seminal phospholipid-binding proteins. *Biochim. Biophys. Acta* **1438:** 175-184.

Moreau, R. & Manjunath, P. (2000) Characterization of Cholesterol efflux induced by novel seminal phospholipid-binding proteins. *Biochim. Biophys. Acta.* **1487:** 24-32.

Moreau, R., Thérien, I., Lazure, C. & Manjunath, P. (1998) Type II domains of BSP-A1/-A2 proteins: binding properties, lipid efflux, and sperm capacitation potential. *Biochem. Biophys. Res. Commun.* **246:** 148-154.

Moubasher, A.E.D. & Wolf, D.P. (1986) The effect of exogenous cholesterol on human sperm funcition in vitro. *J. Androl.* **7:** 22 (abstract).

Mukherjee, Dc., Agrawak, A.K., Manjunath, R. & Mukherjee, A.B. (1983) Suppression of epididymal sperm antigenicity in the rabbit by uteroglobin and transglutaminase in vitro. *Science* **219:** 989-991.

Müller, P., Erlemann, K-R., Müller, K., Calvete, J.J., Töpfer- Petersen, E., Marienfeld, K. & Herrmann, A. (1998) Biophysical characterization of the interaction of bovine seminal plasma protein PDC-109 with phospholipid vesicles. *Eur. Biophys. J.* **27:** 33–41.

Müller, P., Greube, A., Topfer-Petersen, E. & Herrmann, A. (2002) Influence of the bovine seminal plasma protein PDC-109 on cholesterol in the presence of phospholipids. *Eur. Biophys. J.* **31:** 438–447.

Munske, G.R., Krakauer, H. & Magnuson, J.A. (1984) Calorimetric study of carbohydrate binding to concanavalin A. *Arch. Biochem. Biophys.* **233:** 582-587.

O'Shannesy, D. J., Brigham-Burke, M., Soneson, K.K., Hensley, P. & Brooks, I. (1993) Determination of rate and equilibrium binding constants for macromolecular interactions using surface plasmon resonance: use of nonlinear least-squares analysis methods. *Anal. Biochem.* **212:** 457–468.

Parks, J.E., Arion, J.W. & Foote, R.H. (1987) Lipids of plasma membrane and outer acrosomal membrane from bovine spermatozoa. *Bio. Reprod.* **37:** 1249-1258.

Parrish, J.J., Susko-Parrish, J.L. & First, N. (1989) Capacitation of bovine sperm by heparin: inbibitory effect of glucose and role of intracellular pH. *Biol. Reprod.* **41:** 683-699.

Phillips, D.M. (1975) Handbook of physiology. In Sect 7: Endocrinology (Hamilton, D.W, Greep, R.O., Eds). Am Physiol Soc, Washington DC. **Vol 5:** pp 405-420.

Pickford, A. R., Potts, J. R., Bright, J. R., Phan, I. & Campbell, I. D. (1997) Solution structure of a type 2 module from fibronectin: implications for the structure and function of the gelatin-binding domain. *Structure* **5:** 359 –370.

Premkumar, E. & Bhargava, P.M. (1972) Transcription and translation in bovine spermatozoa. *Nature New Biol.* **240:** 139-143.

Premkumar, E. & Bhargava, P.M. (1973) Isolation and characterization of newly synthesized RNA and protein in mature bovine spermatozoa and effect of inhibitors on these syntheses. *Ind. J. Biochem. Biophys.* **10:** 239-253.

Prince, R.C. (1987) Hopanoids: The world's Most Abundant Biomolecules? *TIBS* **12:** 455-456.

Ramakrishnan, M., Anbazhagan, V., Pratap, T.V., Marsh, D. & Swamy, M.J. (2001) Membrane insertion and lipid-protein interactions of bovine seminal plasma protein, PDC-109 investigated by spin label electron spin resonance spectroscopy. *Biophys. J.* **81:** 2215-2225.

Rao, J., Lin, Y., Bing, X. & Whitesides, G. M. (1999) Using surface plasmon resonance to study the binding of vancomycin and its dimer to self-assembled monolayers presenting D-Ala-D-Ala. *J. Am. Chem. Soc.* **121:** 2629–2630.

Revah, I., Gadella, B.M., Flesch, F.M., Colenbrander, B. & Suarez, S.S. (2000) Physiological state of bull sperm affects fucose- and mannose-binding properties. *Biol. Reprod.* **62:** 1010-1015.

Richardson, S.H., Hultin, H.O. & Fleisher, S. (1964) Interactions of mitochondrial structural protein with phospholipids. *Arch. Biochem. Biophys.* **105:** 254-260.

Robertson, J.D. (1957) New observations on the ultrastructure of the membranes of frog peripheral nerve fibers. *J. Biophys. Biochem. Cytol.* **3:** 1043-1047.

Robertson, J.D. (1959) The ultrastructure of cell membranes and their derivatives. *Biochem. Soc. Symp.* **72:** 3-43.

Rouser, G., Fleisher, S. & Yamamoto, A. (1970) Two dimensional thinlayer chromatographic separation of polar lipids and determination of phospholipids by phosphorus analysis of spots. *Lipids* **5:** 494–496.

Salois, D., Menard, M., Paquette, Y. & Manjunath, P. (1999) Complementary deoxyribonucleic acid cloning and tissue expression of BSP-A3 and BSP-30kDa: phosphatidylcholine and heparin-binding proteins of bovine seminal plasma. *Biol. Reprod.* **61:** 288-297.

Sankaram, M. B. & Marsh, D. (1993) Protein-lipid interactions with peripheral membrane proteins. In New Comprehensive Biochemistry. Protein-Lipid Interactions. (Watts, A., Ed.). Elsevier, Amsterdam. **Vol. 25:** pp. 127–162.

Sankaram, M. B., Brophy, P. J. & Marsh, D. (1989) Selectivity of interaction of phospholipids with bovine spinal cord myelin basic protein studied by spin-label electron spin resonance. *Biochemistry* **28:** 9692–9698.

Sato, N. & Oura, C. (1985) The fine structure of the neck region of cat spermatozoa. *Okajimas Folica Anat. Jpn.* **61:** 267-285.

Scheit, K-H., Kemme, M., Aumüller, G., Seitz, J., Hagendorff, G. & Zimmer, M. (1988) The major protein of bull seminal plasma: biosynthesis and biological function. *BioSci. Rep.* **8:** 589-608.

Schuck, P. (1997) Use of surface plasmon resonance to probe the equilibrium and dynamic aspects of interactions between biological macromolecules. *Annu. Rev. Biophys. Biomol. Struct.* **26:** 541–566.

Seidah, N.G., Manjunath, P., Rochemont, J., Sairam, M.R. & Cheretian, M. (1987) Complete amino acid sequence of BSP-A3 from bovine seminal plasma. Homology to PDC-109 and to the collagen-binding domain of fibronectin. *Biochem. J.* **243:** 195-203.

Shivaji, S., Scheit, K.H. & Bhargava, P.M. Proteins of seminal plasma. Wiley, New York, 1990.

Sigurskjold, B.W. & Bundle, D.R. (1992) Thermodynamics of oligosaccharide binding to a monoclonal antibody specific for a Salmonella O-antigen point to hydrophobic interactions in the binding site. *J. Biol. Chem.* **267:** 8371-8336.

Singer, S.J. & Nicolsen, G.L. (1972) The fluid mosaic model of the structure of cell membranes. *Science* **175:** 720-731.

Suarez, S.S. (1998) Minireview. The oviductal sperm reservoir in mammals. Mechanisms of formation. *Biol. Reprod.* **58:** 1105-1107.

Suarez, S.S. (2001) Carbohdrate-mediated formation of the oviducatal sperm reservoir in mammals. *Cells Tissues Organs* **168:** 105-112.

Sui, S.-F., Sun, Y.-T. & Mi, L.-Z. (1999) Calcium-dependent binding of rabbit C-reactive protein to supported lipid monolayers containing exposed phosphorylcholine group. *Biophys. J.* **76:** 333-341.

Sultan, N.A.M. & Swamy, M.J. (2005) Steady-state and time-resolved fluorescence studies on *Trichosanthes dioica* seed lectin. *J. Photochem. Photobiol. B: Biol.* **80:** 93-100.

Suzuki, F. (1990) Fertilization in Mammals. In Morphological aspects of sperm maturation: modification of the sperm plasma membrane during epididymal transport. (Bavister, B.D., Cummins, J., Roladan, E.R.S., Eds.). Serono Symposia, USA pp. 65-76.

Swamy, M. J. & Marsh, D. (1997) Spin-label studies on the anchoring and lipid-protein interactions of avidin with *N*-biotinylphosphatidylethanolamines in lipid bilayer membranes. *Biochemistry* **36:** 7403-7407.

Swamy, M. J., Ramakrishnan, M., Angerstein, B. & Marsh, D. (2000) Spin-label electron spin resonance studies on the mode of anchoring and vertical location of the *N*-acyl chain in *N*-acylphosphatidylethanolamines. *Biochemistry* **39:** 12476-12484.

Swamy, M.J. (2004) Interaction of bovine seminal plasma proteins with model membranes and sperm plasma membranes. *Current Science* **87:** 37-41.

Swamy, M.J., Marsh, D., Anbazhagan, V. & Ramakrishnan, M. (2002) Effect of cholesterol on the interaction of seminal plasma protein, PDC-109 with phosphatidylcholine membranes. *FEBS Lett.* **528:** 230-234.

Tanford, C. & Reynolds, J.A. (1976) Characterization of membrane proteins in detergent solutions. *Biochim. Biophys. Acta* **457:** 133-170.

Thérien, I., Bleau, G. & Manjunath, P. (1995) Phosphatidylcholine-binding proteins of bovine seminal plasma modulate capacitation of spermatozoa by heparin. *Biol Reprod.* **52:** 1372-1379.

Thérien, I., Moreau, R. & Manjunath, P. (1998) Major proteins of bovine seminal plasma and high-density lipoprotein induce cholesterol efflux from epididymal sperm. Biol. Reprod. **59:** 768-776.

Thérien, I., Moreau, R. & Manjunath, P. (1999) Bovine seminal plasma phospholipids-binding proteins stimulate phospholipids efflux from epididymal sperm. *Biol. Reprod.* **61:** 590-598.

Thérien, I., Soubeyrand, S. & Manjunath, P. (1997) Major proteins of bovine seminal plasma modulate sperm capacitation by high-density lipoprotein. *Biol. Reprod.* **57:** 1080-1088.

Thomas, C. J., Surolia, N. & Surolia, A. (1999) Surface plasmon resonance studies resolve the enigmatic endotoxin neutralizing activity of polymixin B. *J. Biol. Chem.* **274:** 29624–29627.

Thomas, C.J., Anbazhagan, V., Ramakrishnan, M., Sultan, N., Surolia, I. & Swamy, M.J. (2003) Mechanism of Membrane Binding by the Bovine Seminal Plasma Protein, PDC-109. A Surface Plasmon Resonance Study. Biophys. J. **84:** 3037-3044.

Torrecillas, A., Laynez, J., Menédez., Corbálan-García, S & Gomez-Fernández. (2004) Calorimetric study of the interaction of the C2 domains of classical protein kinaze C isoenzymes with Ca^{2+} and phospholipids. *Biochemistry* **43:** 11727-11739.

Vereb, G., Szollosi, J., Matko, J., Nagy, P., Farkas, T., Vigh, L., Matyus, L., Waldmann, T.A. & Damjanovich, S. (2003) Dynamic, yet structured: The cell membrane three decades after the Singer-Nicolson model. *PNAS* **100:** 8053-8058.

Villemure, M., Lazure, C. & Manjunath, P. (2003) Isolation and characterization of gelatin-binding proteins from goat seminal plasma. *Reprod. Biol. Endocrinol.* **1:** 39-48.

Visconti, P.E., Moore, G.D., Bailey, J.L., Leclerc, P., Connors, S.A. & Pan, D., Olds-Clarke, P. & Kopf, G.S. (1995) Cholesterol efflux-mediated signal transduction in mammalian sperm. β-cyclodextrins initiate transmembrane signaling leading to an increase in protein tyrosine phosphorylation and capacitation. *J. Biol. Chem.* **274:** 3235-2342.

Volanakis, J. E. & Wirtz, K. W. A. (1979) Interaction of C-reactive protein with artificial phosphatidylcholine bilayers. *Nature* **281:** 155–157.

Wah, D. A., Fernández-Tornero, C., Sanz, L., Romero, A. & Calvete, J. J. (2002) Sperm coating mechanism from the 1.8 Å crystal structure of PDC-109-phosphorylcholine complex. *Structure* **10:** 505–514.

Watson, P.F. (1981) In: Effects of Low Temperature on Biological Membranes (Morris, G.J. & Clarke, A., Eds.), Academic Press, London. pp. 189–218.

White, S. H. & Wimley, W. C. (1999) Membrane protein folding and stability: physical principles. *Annu. Rev. Biophys. Biomol. Struct.* **28:** 319–365.

Wieprecht, T., Beyermann, M. & Seelig, J. (1999) Binding of antibacterial magainin peptides to electrically neutral membranes: Thermodynamics and structure. *Biochemistry* **38**: 10377-10387.

Wilcox, C.A. & Olson, E.N. (1987). The majority of cellular fatty acid acylated proteins are localized to the cytoplasmic surface of the plasma membrane. *Biochemistry* **26:** 1029-1036.

Yanagimachi, R. (1994) Mammalian fertilization. In the physiology of Reproduction. (Knobil, E. & Neill, J. Eds.). Raven Press, New York. **2nd edition:** pp.189-317.

Yeagle, P.L. (1985) Cholesterol and the cell membrane. *Biochim. Biophys. Acta* **855:** 267-287.

Yeagle, P.L. (1991) Modulation of membrane function by cholesterol. *Biochimie* **73:** 1-9.

Zarintash, R.J. & Cross, N.L. (1996) Unesterified cholesterol content of human sperm regulates the response of the acrosome to the agonist, progesterone. *Biol. Reprod.* **55:** 19-24.

Curriculum vitae

V. Anbazhagan was born in the Pondicherry in 1978. After his schooling at Pondicherry, he joined St Joseph College of Arts and Science, Cuddalore, Tamil Nadu and obtain his B.Sc. degree in 1998. He received his M.Sc. degree in 2000 from Kanchi Mamunivar Centre for Post-Graduate Studies, Pondicherry. In August 2000 he joined the School of chemistry, University of Hyderabad, for the Ph. D. program. He was awarded JRF (2001) and SRF (2003) by Council for Scientific and Industrial Research, India. Besides lipid-protein interaction, his areas of research interests include synthesis and cell biology.

List of Publications

(= work pertinent to this thesis)*

*1. Ramakrishnan, M., **Anbazhagan, V.**, Pratap, T.V., Marsh, D. & Swamy, M.J. (2001) Membrane insertion and lipid-protein interactions of bovine seminal plasma protein PDC-109 investigated by spin-label electron spin resonance spectroscopy. *Biophys. J.* **81:** 2215-2225.

*2. Swamy, M.J., Marsh, D., **Anbazhagan, V.** & Ramakrishnan, M. (2002) Effect of cholesterol on the interaction of seminal plasma protein, PDC-109. *FEBS Lett.* **538:** 230-234.

*3. Thomas, C.J., **Anbazhagan, V.**, Ramakrishnan, M., Sultan, N., Surolia, I. & Swamy, M.J. (2003) Mechanism of membrane binding by the bovine seminal plasma protein, PDC-109: A surface plasmon resonance study. *Biophys. J.* **84:** 3037-3044.

*4. **Anbazhagan, V.** & Swamy, M.J. (2005) Thermodynamics of the binding of phosphorylcholine and lysophosphatidylcholine to PDC-109, a major protein of the bovine seminal plasma. *FEBS Lett.* **159:** 2933-2938.

*5. **Anbazhagan, V.**, Paul, A. & Swamy, M.J. (2005) Fluorescence investigations on the interaction of PDC-109, a multifunctional protein from bovine seminal plasma, with phosphorylcholine and lipid membranes. (*to be communicated*).

*6. **Anbazhagan, V.** & Swamy, M.J. (2005) Isothermal titration calorimetric studies on the interaction of PDC-109, the major protein from bovine seminal plasma, with phospholipid membranes and micelles. (*to be communicated*).

7. **Anbazhagan, V.**, Damai, R.S. & Swamy, M.J. (2005) Energetics of heparin binding to bovine seminal plasma protein, PDC-109. (*Manuscript under preparation*).

8. Damai, R.S., **Anbazhagan, V.** & Swamy, M.J. (2005) Interaction of bovine seminal plasma protein, PDC-109 with phospholipid membranes. A ^{31}P-NMR study. (*Manuscript under preparation*).

Presentation and Workshops

1. **Anbazhagan, V.** & Swamy, M.J. Binding of phosphorylcholine and L (-) fucose by the major protein from bovine seminal plasma, PDC-109. *XVII International Symposium on Glycoconjugates.* January 12-16, 2003. Indian Institute of Science, Bangalore, India.

2. **Anbazhagan, V.** & Swamy, M.J. Fluorescence investigation on PDC-109, the choline phospholipids binding protein from bovine seminal plasma. *The Second Indian Symposium of Protein Society. Protein Structure and Function.* October, 28-30, 2004. Indian Institute of Technology Bombay, Mumbai, India.

3. Damai, R.S., **Anbazhagan, V.** & Swamy, M.J. Modulation of the structure of DMPC membranes by PDC-109, the major protein from bovine seminal plasma. A ^{31}P-NMR study. *The Second Indian Symposium of Protein Society. Protein Structure and Function.* October, 28-30, 2004. Indian Institute of Technology Bombay, Mumbai, India.

4. Swamy, M.J., **Anbazhagan, V.** & Damai, R.S. Biophysical investigation on the binding of PDC-109, a multifunctional protein from bovine seminal plasma, with phospholipids and soluble ligands. *National Symposium on 'Recent Trends in Molecular and Medical Biophysics'.* January 22-25, 2005. University of Pune, Pune, India.

5. **Workshop attended:** *Workshop on Pharmacoinformatics in Drug Design.* April 14-16, 2005. National Institute of Pharmaceutical Education and Research (NIPER), Punjab, India.

A Synopsis of the Thesis Entitled

Biophysical Investigations on the Interaction of the Major Bovine Seminal Plasma Protein, PDC-109 with Model Membranes

by

V. Anbazhagan

School of Chemistry
University of Hyderabad
Hyderabad – 500 046
INDIA

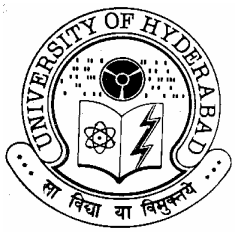

Thesis Supervisor: **Prof. Musti J. Swamy**
School of Chemistry
University of Hyderabad
Hyderabad 500 046
Email: mjssc@uohyd.ernet.in
Tel: +91-40-2301-1071
Fax: +91-40-2301-2460

SYNOPSIS

Chapter 1 provides an introduction to the subject of biomembranes and its components. The major focus of the thesis is on the interaction of the bovine seminal plasma protein, PDC-109 with model membranes. Therefore, the effect of protein on the lipid phase properties and the effect of lipid on the protein structure and function are discussed briefly. Additionally, models of biological membranes are also briefly discussed. Since the thesis deals with a protein from seminal plasma, the general features of the sperm cell and its constituents are reviewed. Further, the role of acidic seminal plasma proteins and other constituents of seminal plasma are discussed in the context of sperm cell capacitation and acrosome reaction.

PDC-109 is a **P**rotein containing *N*-terminal aspartic acid (**D**) and *C*-terminal cysteine (**C**), and has **109** amino acids in its primary structure. It is the major protein of bovine seminal plasma, and its *in vivo* concentration is 15-25mg/ml. Approximately 9.3×10^6 molecules of PDC-109 bind to each sperm cell surface upon ejaculation [Scheit et al., 1988; Calvete et al., 1994]. The 109 amino acid sequence of this protein is composed of two tandemly repeating fibronectin type II domains, preceded by a 23-residue *N*-terminal segment. The sperm cell membrane contains a variety of lipids [Parks et al., 1987] and the lipid specificity experiments with the BSP proteins showed that PDC-109 (BSP-A1/A2) specifically recognized phospholipids containing the phosphorylcholine head group, such as phosphatidycholine (PC), sphingomyelin (SM), lyso-PC, PC plasmalogen, platelet activating factor (PAF), and lyso-PAF [Desnoyers and Manjunath, 1992]. Upon binding to spermatozoa PDC-109 induces the efflux of cholesterol and choline phospholipids (also referred to as

cholesterol efflux), which is a critical step in sperm capacitation, which in turn is a prerequisite to fertilization [Manjunath and Therien, 2002]. Although sperm capacitation is a physiologically significant process, the mechanism underlying it still remains an enigma. In order to understand the mechanism of cholesterol efflux mediated by PDC-109, it is essential to carry out systematic studies on its interactions with lipid membranes. Although there have been a few reports describing biophysical studies on the interaction of PDC-109 with the soluble head group of phosphatidylcholine, phosphorylcholine (PrC) and choline phospholipids and their mixtures with other lipids [Müller et al., 1998; Gasset et al., 1997, 2000], the molecular details of how PDC-109 interacts with lipid membranes are largely unclear. Therefore, systematic studies on the interaction of PDC-109 with phospholipid membranes, especially those made up of phosphatidylcholine and its mixtures with cholesterol, have been taken up. The results obtained are presented in the subsequent chapters of the thesis.

Chapter 2, presents results of electron spin resonance (ESR) studies on the interaction of PDC-109 with membranes made up of phosphatidylcholine and phosphatidylcholine/cholesterol mixtures bearing probe amounts of different spin-labeled phospholipids and steroid probes [Ramakrishnan et al., 2001; Swamy et al., 2002, Swamy 2004]. Particularly, by using spin-labeled phospholipids bearing the nitroxide probe at different positions of the *sn*-2 acyl chain of phophatidylcholine as well as spin labeled phospholipids with different head groups, the following aspects of the interaction were studied: **i**) the influence of the protein on the lipid chain mobility and on the membrane chain-melting phase transition, **ii**) the penetration of the protein into the membrane interior and its direct interaction with the lipid acyl

chains, and **iii**) the specificity of interaction of PDC-109 with phospholipids having different polar head groups. These studies showed that in addition to spin-labeled phosphatidylcholine and sphingomyelin, PDC-109 also recognizes phosphatidylserine and phosphatidylglycerol spin labels as well as a cholesterol analogue, androstanol spin label with considerable affinity, whereas very weak interaction was observed with spin-labeled phosphatidylethanolamine. It has also been demonstrated that, upon binding PDC-109 penetrates into the hydrophobic interior of the membrane. The effect of cholesterol on the interaction of PDC-109 with model membranes made up of dimyristoylphosphatidylcholine was also investigated by spin-label ESR spectroscopy. The results obtained indicate that the interaction of PDC-109 with different phospholipids is increased considerably by the presence of cholesterol.

In ***chapter 3***, the kinetics and mechanism of the interaction of PDC-109 with phospholipid membranes were investigated by the surface plasmon resonance technique [Thomas et al., 2003]. Binding of PDC-109 to different phospholipid membranes containing 20% cholesterol (wt/wt) indicated that binding occurs by a single step mechanism. The association rate constant (k_1) for the binding of PDC-109 to DMPC membranes containing cholesterol was estimated as 5.7×10^5 M^{-1} s^{-1} at 20^oC, while the values of k_1 estimated at the same temperature for the binding to membranes of negatively charged phospholipids such as dimyristoylphosphatidylglycerol (DMPG) and dimyristoylphosphatidic acid (DMPA) containing 20% cholesterol (wt/wt) were at least three orders of magnitude lower. The dissociation rate constant (k_{-1}) for the DMPC/PDC-109 system was found to be 2.7×10^{-2} s^{-1} whereas the k_{-1} values obtained with DMPG and DMPA was about three to four times higher. From the kinetic data, the association constant for the binding of

PDC-109 to DMPC was estimated as 2.1×10^7 M^{-1}. Binding of PDC-109 to dimyristoylphosphatidylethanolamine (DMPE), which is also zwitterionic, was found to be very weak, clearly indicating that the charge on the lipid headgroup is not the determining factor for the binding. The association constants for different phospholipids investigated decrease in the order: DMPC > DMPG > DMPA > DMPE. Thus, the higher affinity of PDC-109 for choline phospholipids is reflected in a faster association rate constant and a slower dissociation rate constant for DMPC as compared to the other phospholipids. Analysis of the activation parameters indicated that the interaction of PDC-109 with DMPC membranes is favored by a strong entropic contribution, whereas negative entropic contribution is primarily responsible for the rather weak interaction of this protein with DMPA and DMPG.

In ***Chapter 4***, the binding of phosphorylcholine (PrC) and lysophosphatidyl-choline (Lyso-PC) to PDC-109 was investigated by monitoring the ligand-induced changes in the absorption spectrum of PDC-109 [Anbazhagan and Swamy, 2005]. At 20^oC, the association constants (K_a), for PrC and Lyso-PC were obtained as 81.4 M^{-1} and 2.02×10^4 M^{-1}, respectively, indicating that the binding of Lyso-PC to PDC-109 is 250 fold stronger than that of PrC. These studies show that while the choline moiety of phosphatidylcholine is specifically recognized by PDC-109, binding of PrC is quite weak and that the overall affinity of association of phosphatidylcholines strongly increases with the presence of the glycerol backbone and with each of the fatty acyl chains by two to three orders of magnitude. From the temperature dependence of the K_a values, enthalpy of binding (ΔH^o) and entropy of binding (ΔS^o), were obtained as -79.7 $kJ.mol^{-1}$ and -237.1 $J.mol^{-1}.K^{-1}$, for PrC and -73.0 $kJ.mol^{-1}$ and -167.3 $J.mol^{-1}.K^{-1}$, for Lyso-PC, respectively. These results demonstrate that although

the binding of these two ligands is driven by enthalpic forces, smaller negative entropy of binding associated with Lyso-PC results in its significantly stronger binding.

In ***Chapter 5***, the exposure and accessibility of the tryptophan residues of PDC-109 and the effect of binding of phospholipid bilayer, micelles and phosphorylcholine on them were probed by quenching studies employing two neutral quenchers (acrylamide and succinimide), an anionic quencher (I^-) and a cationic quencher (Cs^+). Quenching was highest with acrylamide and succinimide with the latter, which is bulkier yielding slightly lower quenching values, whereas the extent of quenching obtained with the ionic quenchers, I^- and Cs^+ was significantly lower. The degree of quenching of the protein intrinsic fluorescence by acrylamide, succinimide, I^- and Cs^+ at a quencher concentration of 0.5 M was 92%, 77%, 35% and 45%, respectively, which decreased to 81%, 34 %, 22% and 16%, respectively, when PDC-109 was bound to DMPC vesicles, indicating that partial penetration of the protein into the hydrophobic interior of the lipid membrane results in the shielding of tryptophan residues from the quenchers. Stern-Volmer plots obtained for acrylamide quenching in different conditions, such as binding to DMPC membrane, Lyso-PC and PrC yielded an upward curvature, indicating that the quenching mechanism involves both dynamic and static components. The Stern-Volmer plots with I^- and Cs^+ yielded biphasic quenching profiles, indicating that the Trp residues in PDC-109 fall into at least two groups that differ considerably in their environment. Further the percent quenching obtained for I^- and Cs^+, suggest that charged residues could be present in the close proximity to some of the Trp resides. Time-resolved fluorescence experiments yielded bi-exponential decay curves with different lifetimes for native

PDC-109 and in the presence of DMPC vesicles, Lyso-PC and PrC. Results obtained from red-edge excitation shift (REES) experiments suggest that upon binding to choline phospholipid membranes, some of the Trp residues of PDC-109 get embedded in the hydrophobic interior of the membrane.

In ***Chapter 6*** the interaction of PDC-109 with phospholipid bilayers and micelles is investigated by isothermal titration calorimetry (ITC), which is a highly sensitive and powerful tool for investigating interaction of specific molecules with other molecules or molecular assemblies, such as membranes. These studies yielded valuable information on the energetics and mechanism of PDC-109 binding to lipid bilayers and micelles. Binding of PDC-109 to dimyristolyphosphatidylcholine and dipalmitoylphosphatidylcholine (DPPC), could be analyzed in terms of a single type of binding sites on the protein for the choline phospholipids. The stoichiometry of binding for the PDC-109/DMPC interaction was determined as 7.4 lipids per protein monomer at 20oC, but increased at lower temperatures. At 20^{o}C, the binding constant, K_a, and thermodynamic parameters, ΔG^o, ΔH^o and ΔS^o for this interaction were found to be $(4.39 \pm 0.04) \times 10^5$ M^{-1}, -7.58 kcal.mol^{-1}, 4.05 ± 0.05 kcal.mol^{-1}, and 39.6 cal.mol^{-1}.K^{-1}, respectively. Qualitatively similar results were obtained for the interaction of PDC-109 with DPPC membranes. These observations indicate that binding of PDC-109 to choline phospholipids is entropically favored with negative contribution from enthalpy of binding.

Binding data for the interaction of PDC-109 with Lyso-PC micelles could not be satisfactorily analyzed with one type of binding sites; it was necessary to invoke the two sets of binding sites on the protein – a low-affinity one (with a K_a of 6.9×10^3 M^{-1}) and two high-affinity sites (with a K_a of 9.79×10^5 M^{-1}). At 20^{o}C, binding to

both these sites is exothermic with ΔH values of -17.56 ± 0.33 kcal.mol^{-1} and -2.58 ± 0.44 kcal.mol^{-1}, for the low and high affinity sites, respectively. K_a values for Lyso-PC binding to the low affinity sites increase with temperature whereas those for the high affinity sites decrease with increase in temperature. The thermodynamic parameters indicate that Lyso-PC binding to the high affinity sites is favored by both entropic and enthalpic contributions, with the entropic contribution being larger, whereas binding of Lyso-PC to the low-affinity sites is enthalpically driven, with a negative entropic contribution.

Chapter 7 gives a general discussion of all the results presented in chapters 2 to 6 and the conclusions drawn on the interaction of PDC-109 with phospholipids membranes, micelles and soluble ligands in terms understanding the mechanism involved in phospholipid and cholesterol efflux, a necessary event before the spermatozoa undergo capacitation.

References:

Anbazhagan, V., and Swamy, M.J. (2005) Thermodynamics of phosphorylcholine and lysophosphatidylcholine binding to major protein of bovine seminal plasma, PDC-109. *FEBS Lett.* **579:** 2933-2938.

Calvete, J.J., Raida, M., Sanz, L., Wempe, F., Scheit, K-H., Romero, A. and Topfer-Petersen E. (1994) Localization and structural characterization of an oligosaccharide *O*-linked to bovine PDC-109. Quantitation of the glycoprotein in seminal plasma and on the surface of ejaculated and capacitated spermatozoa. *FEBS Lett.* **350:** 203-206.

Desnoyers, L. and Manjunath, P. (1992) Major proteins of bovine seminal plasma exhibit novel interactions with phospholipids. *J. Biol. Chem.* **267:** 10149-10155.

Manjunath, P. and Therien, I. (2002) Role of seminal plasma phospholipid-binding proteins in sperm membrane lipid modification that occurs during capacitation. *J. Reprod. Immun.* **53:** 109-119.

Parks J.E., Arion, J.W. and Foote, R.H. (1987) Lipids of plasma membrane and outer acrosomal membrane from bovine spermatozoa. *Biol. Reprod.* **37:** 1249-1258.

Ramakrishnan, M., Anbazhagan, V., Pratap, T.V., Marsh, D. and Swamy, M.J. (2001) Membrane insertion and lipid-protein interactions of bovine seminal plasma protein,

PDC-109 investigated by spin label electron spin resonance spectroscopy. *Biophys. J.* **81:** 2215-2225.

Scheit, K-H., Kemme, M., Aumuller, G., Seitz, J., Hagendorff, G. and Zimmer, M. (1988) The major protein of bull seminal plasma: biosynthesis and biological function. *BioSci. Rep.* **8:** 589-608.

Swamy, M.J. (2004) Interaction of bovine seminal plasma proteins with model membranes and sperm plasma membranes. *Curr. Sci.* **87:** 203-211.

Swamy, M.J., Marsh, D., Anbazhagan, V. and Ramakrishnan, M. (2002) Effect of cholesterol on the interaction of seminal plasma protein, PDC-109 with phosphatidylcholine membranes. *FEBS Lett.* **528:** 230-234.

Thomas, C.J., Anbazhagan, V., Ramakrishnan, M., Sultan, N., Surolia, I. and Swamy, M.J. (2003) Mechanism of Membrane Binding by the Bovine Seminal Plasma Protein, PDC-109. A Surface Plasmon Resonance Study. *Biophys. J.* **84:** 3037-3044.